The Pennsylvania State University

The Graduate School

Department of Chemistry

THE ROLE OF SMALL ORGANIC MOLECULES IN ATMOSPHERIC CHEMISTRY AND PARTICLE FORMATION

A Dissertation in

Chemistry

by

Erin Goken

Submitted in Partial Fulfillment
of the Requirements
for the Degree of

Doctor of Philosophy

December 2010

The dissertation of Erin Goken was reviewed and approved* by the following:

A. Welford Castleman, Jr.
Evan Pugh Professor of Chemistry and Physics
Eberly Distinguished Chair in Science
Dissertation Advisor
Chair of Committee

James B. Anderson
Evan Pugh Professor of Chemistry and Physics

John Badding
Professor of Chemistry

James H. Adair
Professor of Materials Science and Engineering

Barbara J. Garrison
Shapiro Professor of Chemistry
Head of the Department of Chemistry

*Signatures are on file in the Graduate School

ABSTRACT

Flow tube experiments were performed on two small organic molecules in order to determine the roles these chemicals play in the atmosphere, specifically solvation and particle growth. Research presented in this dissertation was performed using a fast-flow reactor at variable temperatures and pressures to mimic atmospheric conditions. This dissertation gives an introduction to the field of atmospheric chemistry and specifically water. The experimental method employed is described in detail, and the results of flow-tube studies of formic acid-water mixed clusters and methanol-water mixed clusters are compared. While methanol undergoes a switching reaction with water clusters, formic acid clearly causes growth of the water clusters. It is concluded that formic acid enhances the growth of water clusters. This hypothesis is examined further by theoretical calculations on small, neutral formic acid-water clusters as well as calculations on protonated clusters in the size range of 21 molecules. It was determined that formic acid strongly interacts with the hydrogen bonding network of the water clusters, altering the stability and ability to grow. In addition a theory for the stability of the magic water-21 cluster is presented. Bromoform and its anionic degradation products are examined; the solvation of the degradation products is shown as a function of temperature and relative pressure of bromoform and water. The solvation is more dependent on water than the ionic core of the cluster. The solvated ions are hypothesized to not be the dominate means of migration of halogen ions from the troposphere to the stratosphere. In addition, some interesting results of the cationic reaction of bromoform with water at room temperature are presented.

TABLE OF CONTENTS

LIST OF FIGURES

LIST OF TABLES

ACKNOWLEDGEMENTS

There are so many people to which I am grateful upon the completion of my dissertation. Thank you to Will for everything; I have learned so much about science and more importantly about myself by working in your group. I want to thank Connie Smith for putting up with me throughout the years. I would like to thank my collaborators Dr. Adri van Duin, Dr. Mike Russo, and Kaushik Joshi for all of their help with calculations and work with formic acid. Thank you to my committee: Dr. Adair, Dr. Anderson, Dr. Badding, and Dr. Weiss. Thank you also to my research group, both past and present.

I would not have been able to finish my degree without the help and support of my family and friends. Thank you to my parents who always wanted me to have the best education but mostly to be happy in life. Thank you to my siblings for inspiring me and pushing me to work hard. Thank you to the rest of my family for all of their love and support. Thanks to my friends here at Penn State and everywhere else who managed to keep me sane over the last five years. Rob, you know how much I appreciate all of your love and support (and patience!) but I want to thank you again. Finally, I dedicate my dissertation to my father who never thought he was smart and was always so proud of all of his kids—I learned so much from you about how to work hard and to be a good and kind person and most of all to laugh at life.

Chapter 1

Introduction

1.1 Background

Water is a chemical substance that is vital to the existence of life. All living organisms require some degree of liquid water during their life cycles. Humans require clean water for both drinking and for washing, as washing clothes and bodies with clean water is the best way to prevent the spread of diseases. Countries with little or poor quality drinking water have a lower quality of life than those with better access to clean water. Water has had a dramatic affect on the history of humans; for example, the first highly developed human civilizations rose up around major river valleys. Extreme droughts have contributed to natural disasters like the Dust Bowl in 1930s. In contrast, excessive levels of water from storms cause other natural disasters including floods and mudslides.

The significant impact that water has on human civilization as well as its relative abundance on our planet has led to extensive scientific investigation of the substance. Water has been shown to demonstrate many unique properties that are not found in any other molecules. For example, water is one chemical that exists in all three of its states—solid, liquid, and gas—in nature. The shape of the molecule is bent, with the lone pairs on the oxygen molecule pushing the two hydrogen atoms down; this shape as well as the electron distribution of the molecule makes it polar. This polarity contributes to the high surface tension of water, as well as many other unique properties including capillary action. Water is called the universal solvent because of its polarity and ability to form hydrogen bonds, and it plays an important role in industrial chemical processes.

The atmosphere of Earth has many layers and each possesses unique characteristics [*Finlayson-Pitts and Pitts*, 2000]. There are five main layers: the exosphere, thermosphere, mesosphere, stratosphere, and troposphere, four of which are profiled in Figure **1.1**. The layer of the atmosphere that lies the farthest from the surface of the planet is the exosphere. The exosphere consists mainly of light atoms like hydrogen and helium. The thermosphere lies below the exosphere. It extends from 85 km above the surface of Earth to about 690 km above the surface. This is the layer where space stations orbit our planet and where the Aurora Borealis phenomenon occurs. Below the thermosphere lies the mesosphere. This layer, 50 km to 85 km above the surface of the planet, contains the coldest temperatures of our atmosphere. This is also the layer where meteors burn up on entry to the atmosphere. The stratosphere lies just below the mesosphere, from 20 km to 50 km above Earth's surface. This layer contains the ozone layer and roughly 90% of the ozone in our atmosphere exists in this layer. The layer of the atmosphere where humans live and where weather occurs is called the troposphere. This layer extends from the surface of the Earth to about 20 km. The water cycle paints a general picture of the pathways involved in transport throughout the lower levels of the atmosphere, as water forms clouds, rain, and snow.

The separation of one layer from another is mainly based on differences in temperature, pressure, and a chemical profile [*Finlayson-Pitts and Pitts*, 2000]. The pressure decreases with height from the surface of the Earth. The temperature of the troposphere decreases with increasing altitude as it is heated mainly through surface radiation. The stratosphere is characterized by an increase in temperature with increasing altitude. Temperatures in the mesosphere drop as altitude is increased; the temperatures in the thermosphere increase with altitude from the surface of the Earth because solar radiation has a greater affect on the thermal characteristics of this layer. The layers of the atmosphere all have distinct temperature profiles as well as physical properties including light scattering and absorption which affect the chemistry of

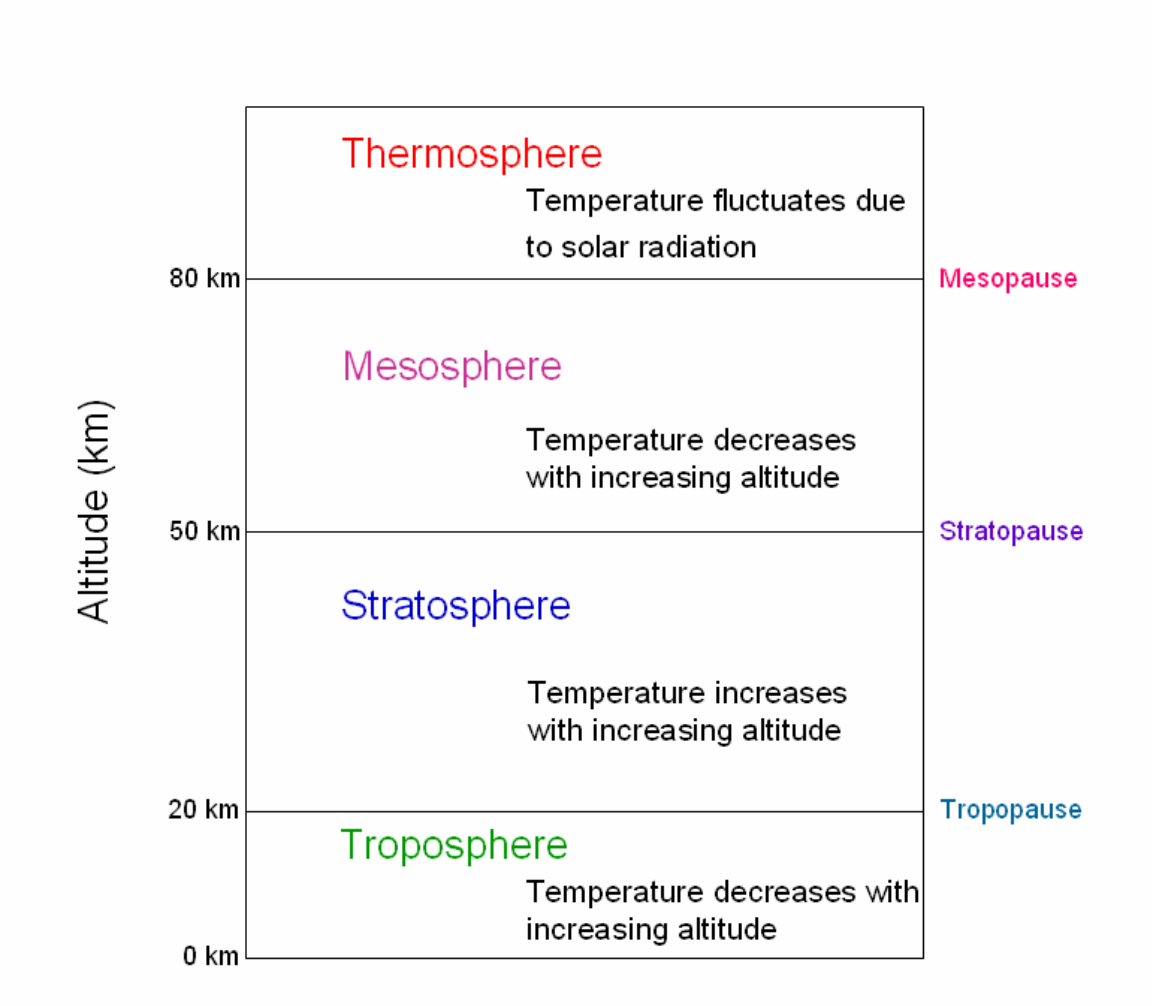

Figure **1.1**: The layers of the atmosphere along with their altitudes and temperature profiles are shown. On the right, the intermediate layers which exist between the main layers are shown; these layers exhibit a pause in the change of the temperature profiles as indicated by their names.

each layer. There are also border layers which exist between the layers where the temperature remains constant: the tropopause lies between the troposphere and stratosphere, the stratopause lies between the stratosphere and the mesosphere, the mesopause lies between the mesosphere and the thermosphere, etc. Water is present predominately in the tropospheric and, to a lesser extent, in the stratospheric layers of the atmosphere, it is important to discover how other chemicals—including pollutants and aerosol particles—interact with water under atmospheric conditions.

Atmospheric chemistry, which seeks to understand and quantify the chemical species and pathways involved in the Earth's atmosphere, is a critically important field. The first reported evidence for new particle formation came in 1897 [*Aitken*]. Even now, current techniques for studying direct measurements of the atmosphere are limited in terms of mobility, economic feasibility, and chemical selectivity. Only recently has instrumentation been developed that can study particles in the atmosphere in the 1 nm to 10 nm size regime [*McMurray*, 2000; *Mirme et al.*, 2007; *Tammet*, 2004]. Particles of this size range are vital to the understanding of the gas–to-particle transition phase of particle growth in the atmosphere. However, even with recent developments in instrumentation, direct measurements of the atmosphere are still unable to study the initial stages of nucleation and particle growth [*Kulmala et al.*, 2007a,b]. Flow tube studies may be used to model systems for the initial stages in order to gain insight into the chemical make-up of nucleation embryos and how they form. A better understanding of how particles nucleate and grow in the atmosphere is important to further our knowledge of how they affect human health, the water cycle, and potential climate change [*IPCC*, 2007; *Lohmann and Feichter*, 2005; *Stieb et al.*, 2002].

Organic molecules are of particular interest in the atmosphere as they are released from biogenic sources, sea salt aerosols, and pollution from industrial processes. The organic molecules present in the atmosphere range from larger aromatic organic molecules, volatile

organic chemicals (VOCs), and small to medium chain organic acids [*Finlayson-Pitts and Pitts*, 2000]. For the most part, the role of small- to medium-chain organic acids in the atmosphere remains a mystery; however, research into this area of atmospheric chemistry has increased in recent years. Small organic molecules have been shown to contribute up to 84% of the molar volume of nucleated particles in field studies [*Smith et al.*, 2008]. Most previous studies of atmospheric chemical processes have centered on the formation of acid rain, specifically how sulfuric acid and/or nitric acid interact with water; however, recent calculations on the structures of atmospherically important chemicals have shown that the addition of small organic acids can enhance the uptake of sulfuric acid by water [*Nadykto and Yu*, 2006].

1.2 Dissertation organization

The main focus of this dissertation is to present flow tube studies of atmospherically relevant organic molecules and their reactions with ionic water clusters ranging from 2-30 molecules as well as to provide insight into the structural effects of such reactions. Flow tube studies have been shown to be a useful method of determining how reactant gases interact with water under carefully controlled conditions which can mimic atmospheric conditions at various levels of the atmosphere [*Castleman, Holland, and Keese*, 1978; *Gilligan and Castleman*, 2001; *Goken and Castleman*, 2010]. Our studies focus primarily on reactions that could occur under the conditions of the troposphere and the stratosphere, the two layers closest to the surface of the planet that together make up over 80% of the mass of the atmosphere.

Chapter 2 of this dissertation outlines the experimental method used to form and characterize reactions of water clusters using a flow tube instrumental apparatus. The instrument is broken down into three distinct regions and discussed in detail. Additionally, a brief introduction to the theoretical calculation methods used in the study of the structure of the

clusters is provided. Detailed descriptions of the methodologies for these calculations are discussed in Chapter 4.

Chapter 3 focuses on the reaction of formic acid with water clusters. Varied concentrations of formic acid were added to the flow tube, and the mixed formic acid-water cluster products were examined. In addition, these flow tube results are compared to the well-studied system of methanol-water mixed clusters to provide insight into the reaction mechanisms by which formic acid is solvated and incorporated into water clusters which can lead to particle growth.

Chapter 4 addresses the effects that the addition of formic acid molecules to a pure water cluster has on the structure and stability of the hydrogen bonding network of the cluster. Small neutral clusters are studied using Density Functional Theory (DFT), and large, protonated water clusters are examined using a type of Molecular Dynamics (MD) calculations called Reactive Force Field (ReaxFF).

Chapter 5 shows how bromoform, a small organic molecule released from sea salt aerosols, breaks down and how the derivative molecules interact with water. This chapter deals with particle growth and stability through solvation.

Chapter 6 provides conclusions on the work presented in this dissertation as well as ideas for future studies.

An Appendix discusses findings of cationic formation of bromine-containing hydrocarbon species at room temperature under typical flow-tube conditions.

1.3 References:

Aitken. J.A. (1897), On some nuclei of cloudy condensation, *Trans. Roy. Soc.* XXXIX, 1897.

Castleman, A.W. Jr., P. Holland, and R. Keesee (1978), The properties of ion clusters and their relationship to heteromolecular nucleation, *J. Chem. Phys., 68*, 1760-1764, doi:10.1063/1.435946.

Finlayson-Pitts, B. and J. Pitts, Jr. (2000), *Chemistry of the Upper and Lower Atmosphere,* Academic Press, New York.

Gilligan, J. and A.W. Castleman, Jr. (2001), Acid Dissolution by Aqueous Surfaces and Ice: Insights from a Study of Water Cluster Ions, *J. Phys. Chem. A.*, *105*, 5601-5605, doi:10.1021/jp003480p.

Goken, E.G. and A.W. Castleman, Jr. (2010) Reactions of formic acid with protonated water clusters: Implications of cluster growth in the atmosphere, *J. Geophys. Res.-Atmos.* (in press).

IPCC (2007) The Scientific Basis. A report of Working Group I of the Intergovernmental Panel on Climate Change. In: S. Solomon, D. Qin, M. Manning, Z. Chen, M. Marquis. K.B. Averyt, M. Tignor, H.L. Miller (Eds.), Climate Change 2007: The Physical Science Basis. Contribution of Working Group I to the Fourth Assessment Report of the Intergovernmental Panel on Climate Change. Cambridge University Press, Cambridge, United Kingdom and New York, NY, USA.

Kulmala, M. et al. (2007a), The condensation particle counter battery (CPCB): a new tool to investigate the activation properties of nanoparticles, *J. Aerosol Sci.*, *38*, 89-304.

Kulmala, M. et al. (2007b), Toward direct measurement of atmosphereic nucleation, *Science*, *318*, 89-92, doi: 10.1126/science.1144124.

Lohmann, U. and J. Feichter (2005), Global indirect aerosol effects: a review, *Atmos. Chem. Phys.*, *5*, 715-737.

McMurry, P.H. (2000) A review of atmospheric aerosol measurements, *Atmos. Environ.*, *34*, 1959-1999.

Mirme, A. et al. (2007) A wide-range multi-channel air ion spectrometer, *Boreal Environ. Res.*, *12*, 247-264.

Smith, J., M. Dunn, T. VanReken, K. Iida, M. Stolzenburg, P. McMurry, and L. Huey (2008), Chemical composition of atmospheric nanoparticles formed from nucleation in Tecamac, Mexico: Evidence for an important role for organic species in nanoparticles growth, *Geophys. Res. Lett.*, *35*, L04808, doi:10.1029/2007GL032523.

Steib, D.M., S. Judek, and P.H. McMurry (1991), Meta-analysis of time-series studies of air pollution and mortality: effects of gases and particles and their influence of cause of death, age and season, *J. Air Manage. Assoc.*, *52*, 470-484.

Tammet, H. (2004), Balance scanning mobility analyzer BSMA. In: Kasahara, M., and M. Kulmala (Eds.), Nucleation and Atmospheric Aerosols 2004, 16th International Conference, Kyoto, pp. 294-297.

Chapter 2

Experimental methods

2.1 Introduction

In this chapter the experimental apparatus setup and the conditions used to obtain water cluster spectra are provided. The experimental methods shown here were used to obtain the results given in Chapters 3, 4, and 5, as well as Appendix A. The intent of this chapter is to provide experimentalists with a guide for using the instrumentation presented within this dissertation. In addition, this chapter contains background on the theoretical calculations which are used to support the experimental findings.

2.2 Instrumental apparatus

The instrument employed in our laboratory consists of three major parts: a high-pressure ion source, a flow tube, and a quadrupole mass spectrometer. The apparatus is depicted in Figure **2.1** and is described in detail in each subsection. This fast-flow reactor produces small ionic clusters that range in size from 2-30 molecules. The technique described in this dissertation has been used in the past to study the stability and reactivity of water clusters, acid solvation with water, and other ion-molecule reactions [*Gilligan*, 2000; *Jones*, 2008; *MacTaylor*, 1998; *Mereand*, 1996; *Passarella*, 1988; *Shul*, 1987; *Upshulte*, 1986; *Yang*, 1991; *Zhang*, 1994].

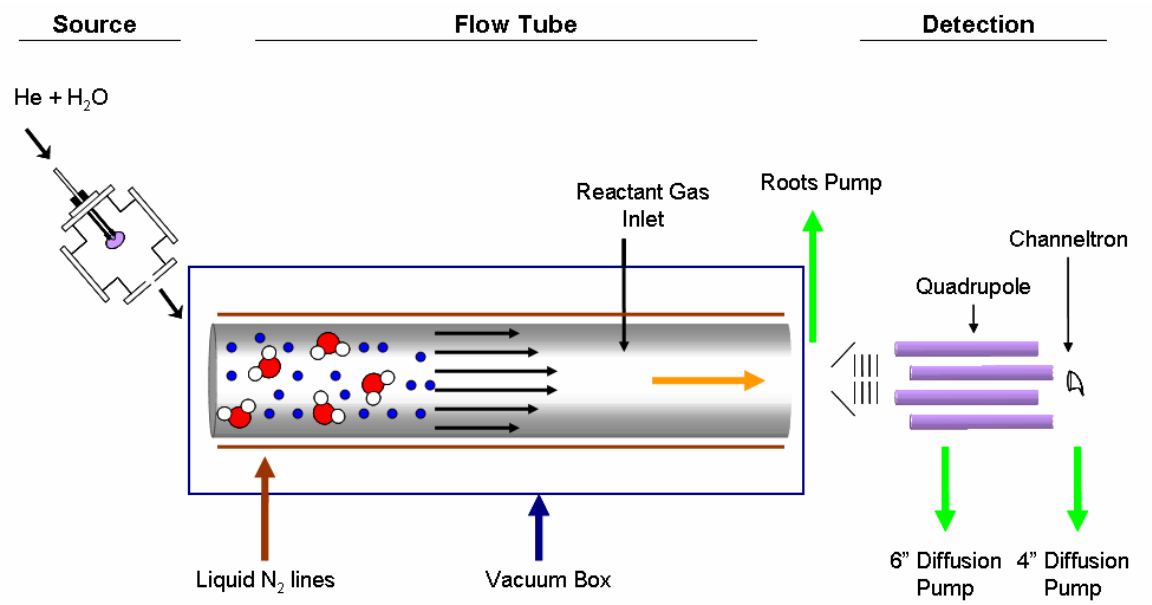

Figure **2.1**: Schematic representation of the experimental apparatus.

2.2.1 Ion Source

Ionic water clusters are generated by passing a small amount of water seeded in helium carrier gas over two platinum wires (32 gauge), which have an applied potential on each that can range from -900 volts to +900 volts. The ion source is a homebuilt or poorman's source that is depicted in Figure **2.2**. In the experiments reported herein, the voltages used were +380 volts and -460 volts. These specific voltages were determined by observing how the ion signal changed with various applied voltages, and these produced the most intense as well as the best resolved ion signal. Voltages that are too high can cause arcing within the source which disrupts the ion signal, affecting the resolution. Voltages that are too low produce insufficient ionization to result in adequate signal.

The applied voltages cause a corona discharge between the two wires in the source, creating a plasma that mimics ion formation caused by sunlight in the atmosphere. This plasma gives off both positive and negative ions which allows study of either cationic or anionic water clusters as is most appropriate to the system under investigation.

2.2.2 Flow Tube

The flow tube (304 stainless steel tubing; 4.0" I.D., 0.125" thick, and 44" long) is separated from the high pressure source by use of a 2-3 mm inner diameter (I.D.) copper diaphragm; this permits the flow tube to remain at approximately 0.3 Torr in pressure. Cluster ions are carried into the flow tube in helium carrier gas at a typical flow rate of 7000 standard cubic centimeters per minute (sccm). This high flow of carrier gas allows for the thermalization of the ionic clusters through ~10^5 collisions with the helium gas.

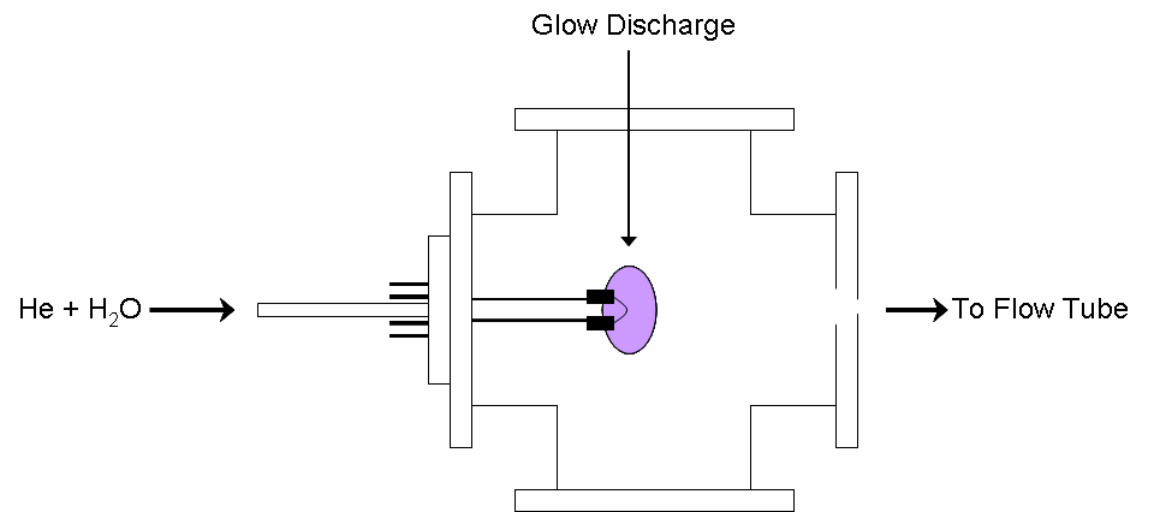

Figure **2.2**: Schematic diagram of the high-pressure ion source used in experiments.

Approximately 30 cm downstream from the source, a selected concentration of a reactant gas is leaked into the flow tube. The reactant gases, which in the case of this dissertation are formic acid and bromoform, are contained in a specially designed glass bubbler which is shown in Figure **2.3**. This glassware was designed with Swagelock fittings, one Teflon control valve to allow for the flow of helium over a liquid, and a second Teflon control valve to release the reactant gas into a four-liter stainless steel chamber shown in Figure **2.4**. Different concentration dilutions of the reactant gas and additional helium gas are prepared in this mixing chamber; they are then leaked into the flow tube at a predetermined flow rate that is controlled using a 200 sccm range MKS flow meter attached to the reactant gas inlet.

The reactant gas inlet (RGI) used for the studies reported in this dissertation is a heated finger inlet. The inlet is located 30 cm away from the orifice, and is inserted into the center of the flow tube. The ideal shape and positioning of this inlet has been described elsewhere [*Wincel et al.*, 1996]. A diagram of the RGI is shown in Figure **2.5**. The cluster ions and the neutral reactant gas are allowed to react for several milliseconds (~71 cm distance in the flow tube) before a small portion is sampled through a 1 mm orifice. A Stokes-Penwalt Roots blower, housed in a closet at the front of the lab, is used to pump away the majority of the volume of carrier gas and ions from the flow tube. The Roots blower is separated from the fast-flow reactor by a manual gate valve that allows for the throttling of the pumping capacity. In addition, when the instrument is not in use, the flow tube can be isolated from the roots blower by an electropneumatic gate valve.

One special feature of this fast-flow reactor is our ability to perform studies over a wide temperature range (133-400 K). This temperature range can mimic differing conditions as they would occur at various regions and levels of the atmosphere. Low temperatures are maintained with a precision of $\pm$1K by passing liquid nitrogen through a series of copper tubes that line the outside of the flow tube. In order to reach temperatures lower than 240 K a steel box was

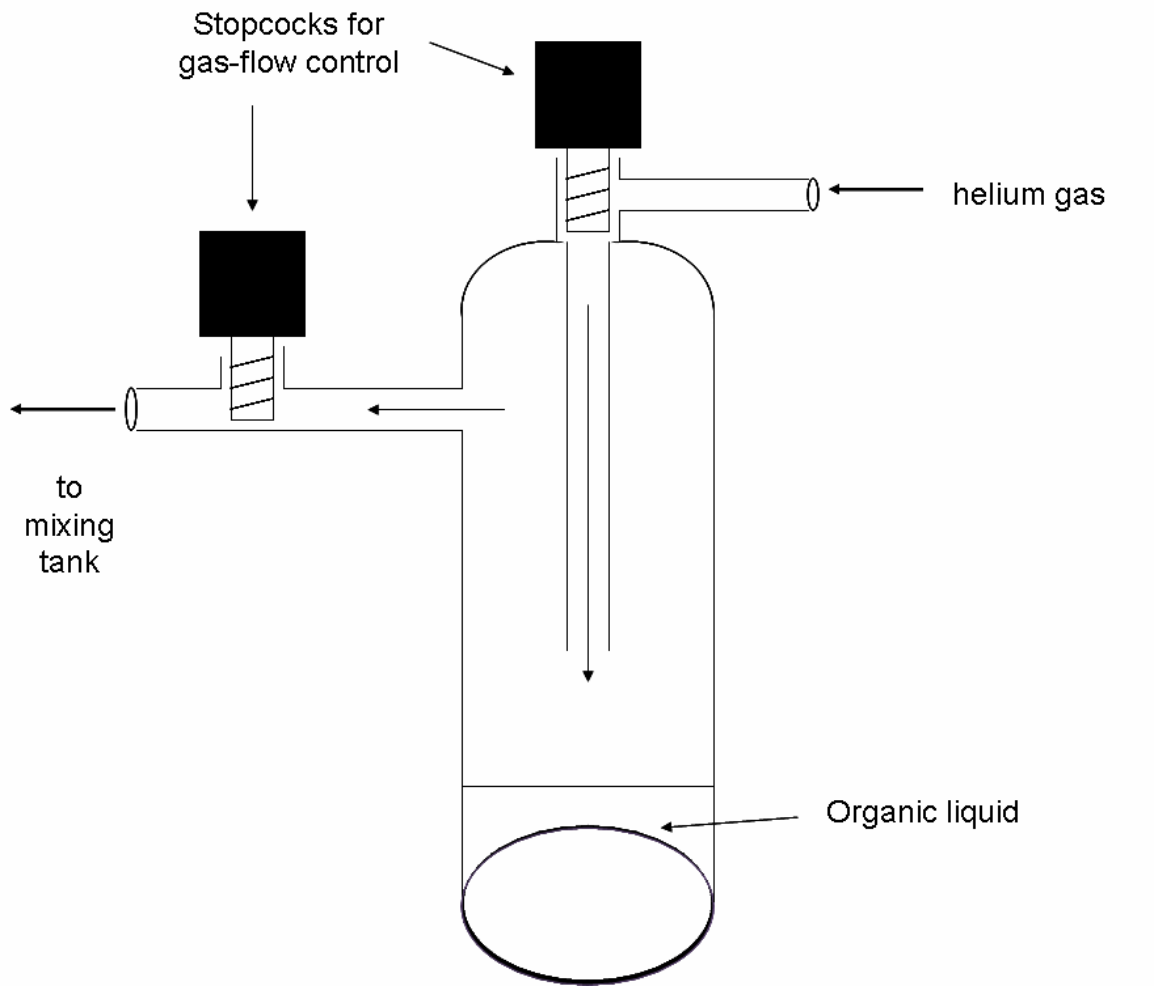

Figure **2.3**: Glass bubbler used to seed the reactant gas in helium.

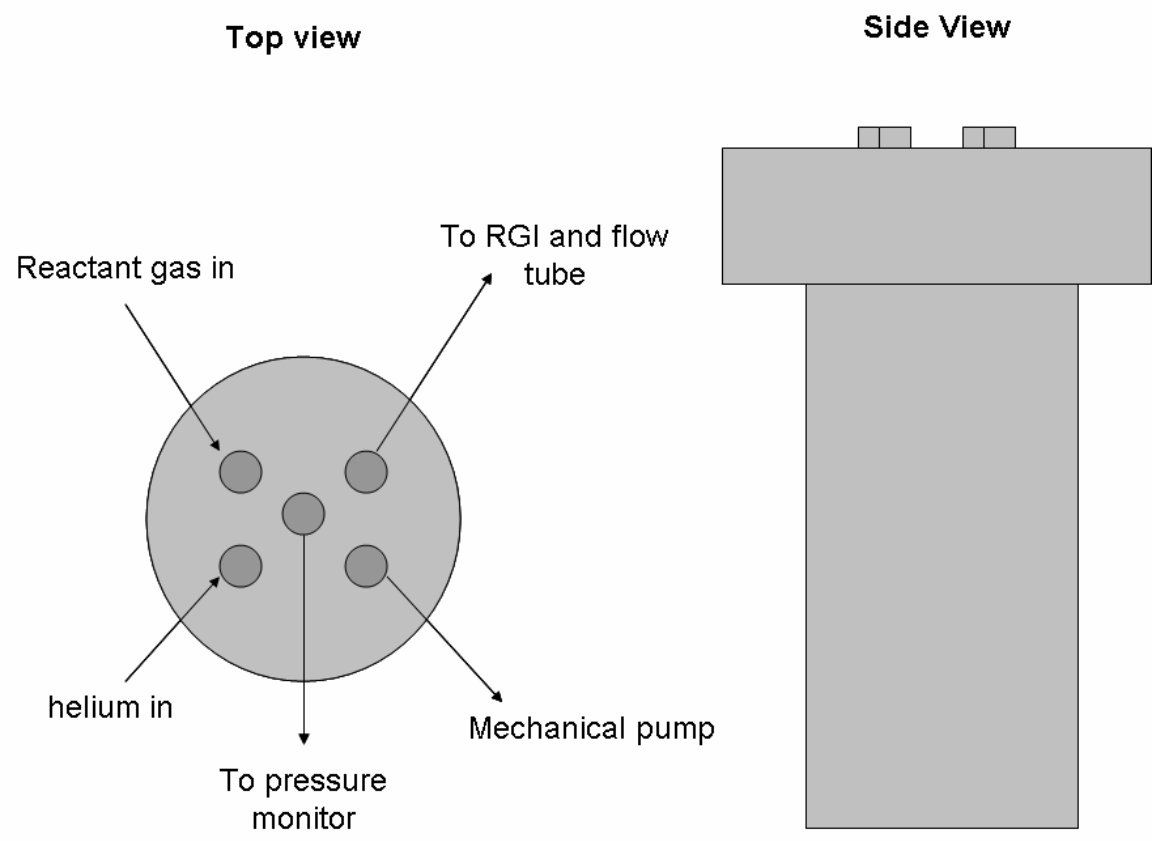

Figure **2.4**: Schematic of the 4 liter mixing tank used to make reactant gas dilutions.

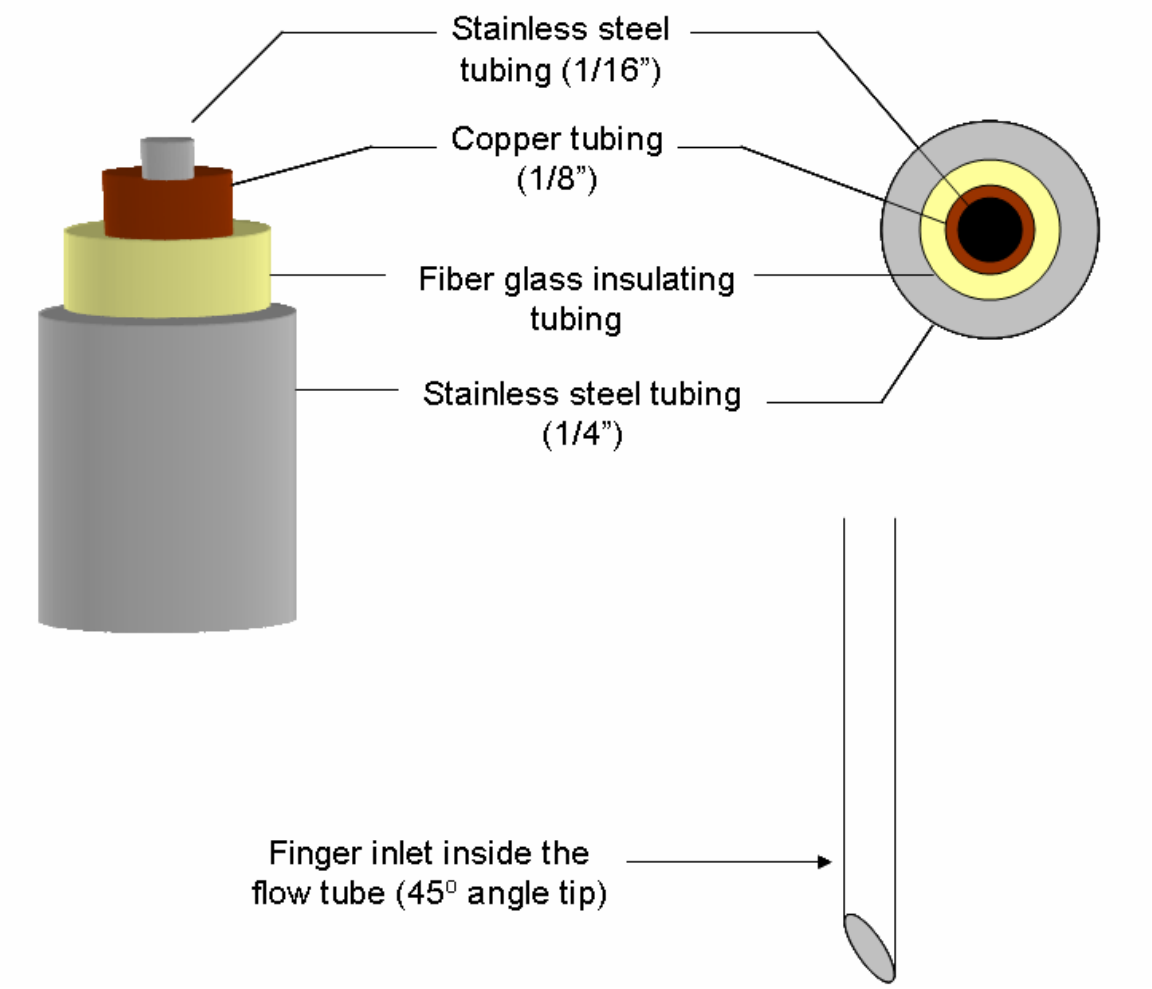

Figure **2.5**: Schematic diagram of the heated RGI and the finger inlet that is inserted into the flow tube.

constructed around the flow tube that can be pumped to a pressure of -50 kPa using a mechanical pump. The vacuum around the flow tube reduces the formation of condensation, as condensation can insulate the flow tube and prevent cooling of the temperature within the flow tube below the freezing point of water. Temperatures above room temperature can be maintained by connecting a Variac heater to copper wires that also run the length of the flow tube. For high temperature experiments it is best if the vacuum box is kept open to atmosphere by opening a needle valve that is connected to stainless steel tubing that runs into the vacuum box on one side, and stainless steel tubing that is open to the room on the other side.

2.2.3 Detection Region

The reactant ions and product ions pass through the sampling orifice to the detection region. A series of four lenses are used to guide the ions into the mass analyzer, an Extranuclear quadrupole mass filter with a range of ~20 amu to ~800 amu. The ionic clusters are then detected using a DeTech Inc. channeltron electron multiplier. The quadrupole chamber is pumped by a six inch Alcatel diffusion pump while the detection chamber that houses the electron multiplier is pumped by a four inch Edwards diffusion pump. Under normal operating conditions the pressures in the quadrupole chamber and detection chamber are ~3 x 10^{-5} Torr and ~3 x 10^{-6} Torr, respectively. Under conditions where the flow tube is not in use, the pressures drop to 1 x 10^{-6} and 5 x 10^{-7} Torr, respectively. Also, while the instrument is not in use and the flow tube has been isolated from the roots blower, an electropneumatic gate valve can be opened to allow the diffusion pumps to pump out the flow tube region to further remove any remaining reactant gases.

The detector can be used to detect ion signal for either cationic or anionic clusters. The voltages applied to the front and back plates of the electron multiplier are adjusted and controlled using a home-built control box for the cations and a separate control box for the anions as shown

in Figures **2.6** and **2.7**, respectively. The cation box splits the voltage in such a way that the front plate of the electron multiplier holds most of the applied voltage (typically ~ -3000 Volts), and the back plate is a virtual ground. The signal that is detected is then sent to a pulse counter and converted to a spectrum on the computer by a DAC program chip. The anion box can be used to apply a smaller voltage (~ +2000 Volts) to the front plate of the detector and a much larger positive voltage (~ +5000 Volts) to the back plate of the detector. The charge of the applied voltage must be changed on the power supply by means of control knob with two settings, positive and negative. The two control boxes are designed in such a way that the voltage splitting between the front plate and the back plate of the detector takes place within the box; this means the total voltage can be set on the power supply which is connected to the control boxes.

2.3 Theoretical Calculations

The flow tube experiments described in this dissertation elucidate the chemical details of the ion-molecule reactions that are performed. In order to gain a better understanding of the structure of the clusters being studied, further investigation is necessary. Two types of theoretical calculations have been performed, giving us structural detail of pure water clusters as well as mixed water cluster systems. The findings of these calculations are presented in detail in Chapter 4, and only a brief background introduction is given here.

2.3.1 Density Functional Theory

Density Functional Theory (DFT) is a versatile method used in computational chemistry. It is a quantum mechanical theory used to gain insight into the electronic structure of atoms, molecules, and condensed phases to relate these results to experimental data as is the case for this

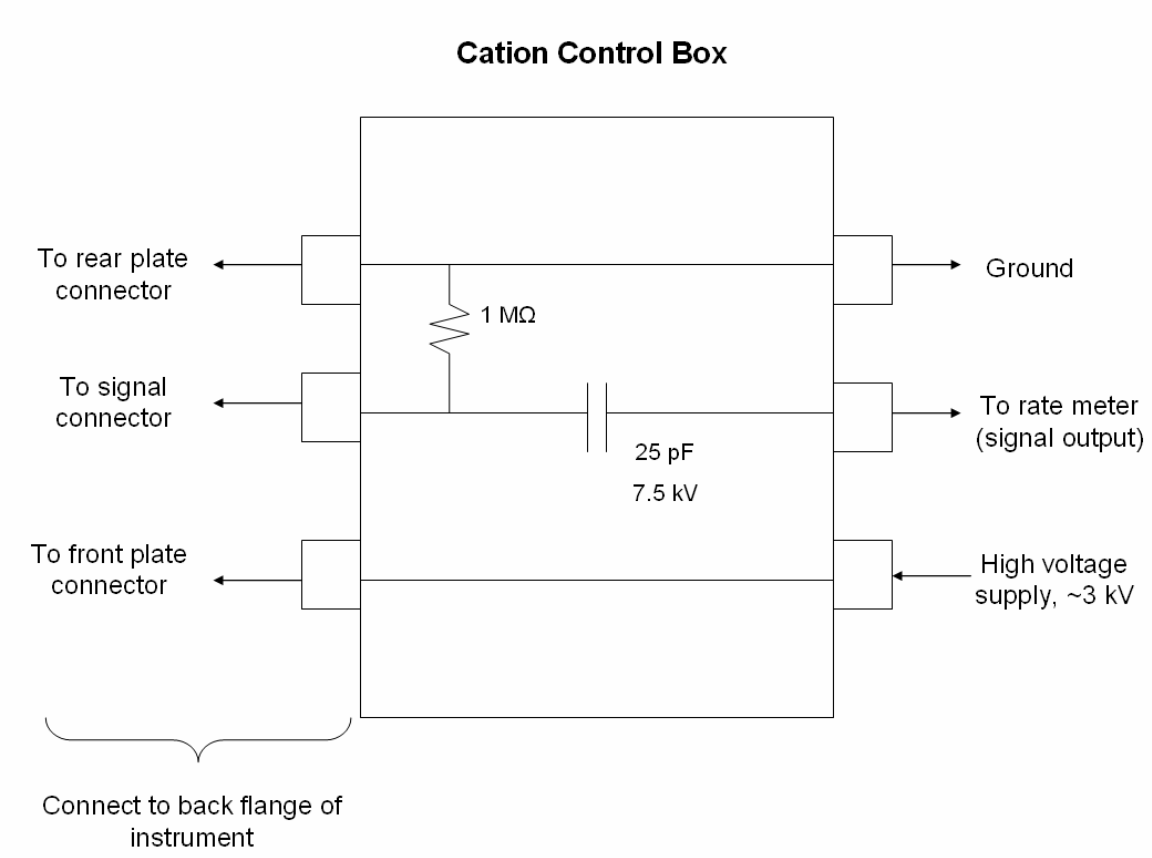

Figure **2.6**: Schematic of the cation detector control box. The schematic shows the necessary capacitors and resistors for the typical detection voltage input.

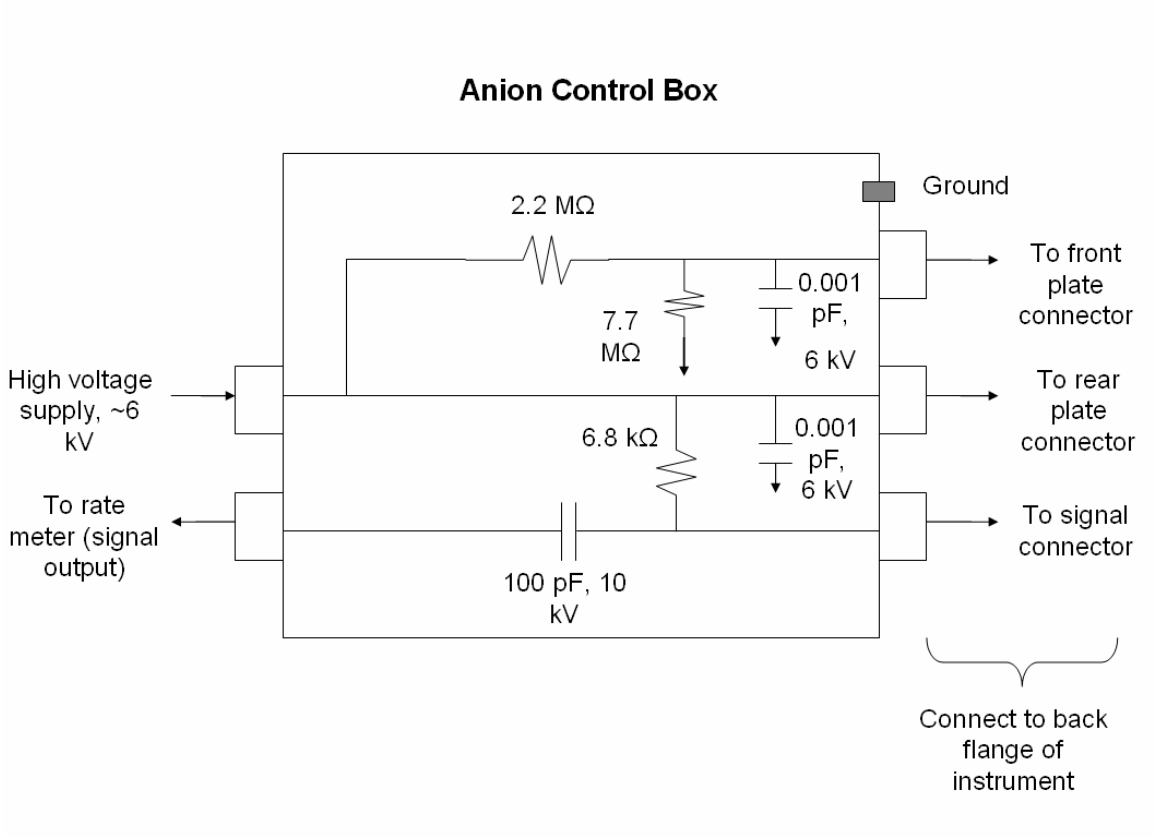

Figure **2.7**: Schematic diagram of the anion detection control box. Resistor and capacitors are shown for the typical running voltage input. In addition, the 7.7 MΩ resistor and the two 0.001 pF capacitors are denoted with a downward arrow that indicates they are connected to the ground shown in the upper right-hand corner of the diagram.

dissertation. DFT has been used for solid state physics calculations since the 1970s; it became more widely accepted for use in quantum chemistry in the 1990s after the approximations in the theory were improved. The benefits of DFT include being much faster, and therefore computationally less expensive, than calculations based on wavefunctions, such as Hartree-Fock. However, DFT has limitations in its ability to deal with van der Waals forces. Additional specifications for the DFT calculations performed for this dissertation will be discussed in Chapter 4.

2.3.2 Reactive Force Field Calculations (ReaxFF)

Reactive Force Field (ReaxFF) calculations were performed to corroborate the small neutral cluster calculations performed using DFT with our experimental data on larger sized protonated clusters. ReaxFF is a force field that can be used in molecular dynamics (MD) simulations that employs a continuous bond order/bond distance relation. This ability enables ReaxFF to dissociate bonds and to form new bond during the simulation [*van Duin et al.*, 2001], as opposed to the traditional force fields e.g. [*Allinger et al.*, 1989; *Cornell et al.*, 1995; *Jorgensen et al.*, 1983], which usually employ a rigid bond definition. ReaxFF is several magnitudes faster than quantum mechanical (QM) methods, enabling applications to large systems and dynamic simulations. The ReaxFF MD calculations were performed by our collaborators in the Mechanical and Nuclear Engineering Department at The Pennsylvania State University: Kaushik Joshi, Dr. Mike Russo, and Dr. Adri van Duin. Details of how the force field was optimized are contained in Chapter 4 of this dissertation.

2.4 References

Allinger, N.L, Y.H. Yuh and J.-H. Lii, (1989*),* Molecular mechanics. The MM3 force field for hydrocarbons. 1, *J. Am. Chem. Soc,. 111*, 8551-8566, doi:10.1021/ja00205a001.

Cornell, W.D., P. Cieplak, C.I. Bayly, I.R. Gould, K.M. Merz, D.M. Ferguson, D.C. Spellmeyer, T. Fox, J.W. Caldwell and P.A. Kollman (1995), A Second Generation Force Field for the Simulation of Proteins, Nucleic Acids, and Organic Molecules, *J. Am. Chem. Soc*., *117*, 5179-5197, doi:10.1021/ja00124a002.

Gilligan, J. (2000), The Role of Solvation of Ion-Molecule Reactions: Elucidating Mechanisms of Heterogeneous Atmospheric Chemistry and the Reactivity of Metal-Ligand Complexes, Ph.D. thesis, 96 pp., The Pennsylvania State University, University Park, PA, USA.

Jones, C.E. (2008), Clusters: Addressing Material and Environmental Issues, Chapter 5, Ph. D. Thesis, 92 pp., The Pennsylvania State University, University Park, PA, USA.

Jorgensen, W.L, J. Chandrasekhar, J.D. Madura, R.W. Impey and M.L. Klein (1983), Comparison of Simple Potential Functions for Simulating Liquid Water, *J. Chem. Phys.*, *79*, 926, doi:10.1063/1.445869.

MacTaylor, R.S. (1998), Molecular Activation by Surface Coordination: Insight into Heterogeneous Atmospheric Chemistry through Cluster-Ion Molecule Reactions, 182 pp., Ph. D. Thesis, The Pennsylvania State University, University Park, PA, USA.

Mereand, E. (1996), Studies of Cluster Ion-Molecule Reactions of Atmospherically Relevant Species, Ph. D. Thesis, 246 pp., The Pennsylvania State University, University Park, , PA, USA.

Passarella, R. (1988), The Kinetics of Ion-Molecule Reactions, Ph. D. Thesis, 191 pp., The Pennsylvania State University, University Park, PA, USA.

Shul, R.J. (1987), A Kinetic Study of Gas Phase Ion-Molecule Reactions with a Selected Ion Flow Tube, Ph. D. Thesis, 246 pp., The Pennsylvania State University, University Park, University Park, PA, USA.

Upshulte, B.L. (1986), Thermodynamics, Kinetic, and Chemiluminescence of Cluster Ion Reactions, and Diagnostics of Flow Tube Techniques, Ph. D. Thesis, 248 pp., University of Colorado, Boulder, CO, USA.

van Duin, A.C.T., S. Dasgupta, F. Lorant, and W.A. Goddard III (2001) ReaxFF: A Reactive Force Field for Hydrocarbons, *J. Phys. Chem. A*, *105*, 9396-9409, doi:10.1021/jp004368u.

Wincel, H., E. Mereand, A.W. Castleman, Jr. (1996), Gas-Phase Reactions of DNO_3 with $X^-_0(D_2O)_n$, X = O, OD, O_2, DO_2, and O_3, *J. Phys. Chem., 100*, 7488-7493.

Yang, X. (1991), Kinetics of Reactions of Gas Phase Cluster Ions, Ph. D. Thesis, 265 pp., The Pennsylvania State University, University Park, PA, USA.

Zhang, X. (1994), Influence of Solvation on Ion-Molecule Reactions, Ph. D. Thesis, 118 pp., The Pennsylvania State University, University Park, PA, USA.

Chapter 3

Reactions of formic acid with protonated water clusters: Implications of cluster growth in the atmosphere

3.1 Introduction

Many reactions that occur in the Earth's atmosphere, and in particular nucleation phenomena, remain poorly understood due to the inability to study the processes directly. There are several mechanisms by which nucleation occurs in the atmosphere as outlined in various reviews [*Holmes*, 2007; *Kulmala and Kerminen*, 2008]. A nucleation process that is influenced by the presence of an ion, atom, or foreign molecule of different chemical composition from the bulk nucleating phase is considered heteromolecular nucleation [*Castleman et al.*, 1978]. Because heteromolecular reactions are affected by additional interactions relative to homogeneous nucleation, it is likely that atmospheric particle formation involves two or more different chemical species, an acid molecule with a water molecule as one example [*Finlayson-Pitts and Pitts*, 2000]. The significance of ion-mediated (ion-induced) nucleation has been actively debated in the literature [*Kulmala et al.*, 2007; *Iida et al.*, 2006], and has been supported based on studies of the sulfuric acid dimer and trimer by Hanson and Lovejoy [2006]. Yu et al. propose that ion-mediated nucleation could be significant on a global scale based on simulation model studies [2000; 2008]. In addition, studies by Boy et al. showed that ion-induced nucleation of sulfuric acid and water can contribute up to 15% of new particles in the 3-10 nm size range [2008].

The key to understanding nucleation processes is being able to study the particle formation events with chemical detail. However, most current instrumental techniques are

largely confined to studying particles of 3 nm in size or larger, meaning details on the initial stages of particle growth are not well investigated [*Kulmala et al.*, 2004]. However, there are a few recent advances that permit sub-3 nm particle measurement including the balanced scanning mobility analyzer (BMSA) and air ion spectrometer (AIS) [*Kulmala and Kerminen*, 2008 and *Kulmala et al.*, 2007]. Also, current studies of particle growth in the atmosphere are focused on sulfuric acid and/or ammonia complexes, and are only just recently starting to examine the effects of organic acids [*Zhang et al.*, 2004, *Zhao et al.*, 2009]. A viable means of studying these phenomena is the use of clusters as model systems, especially since recent experimental results revealed that cluster ions, or ions smaller than 1.5 nm in size, are always present in the atmosphere [*Kulmala and Tammet*, 2007]. Neutral clusters are also observed where nucleation occurs [*Kulmala et al.,* 2007]. Clusters are aggregates of atoms and/or molecules of a determined size distribution that can be used to study the properties of materials that exist in the size regime between atomic scale and bulk scale chemistry. Water clusters in particular can and have been used to mimic the surface of clouds and ice surfaces in the upper atmosphere and to model the reactions that occur on these surfaces [*Zhang et al.*, 1994]. The findings of previous flow-tube studies have also led to a determination of the number of water molecules necessary to solvate single acid molecules, providing detailed chemical information for interactions on a molecular scale [*Gilligan and Castleman*, 2001]. These experiments show that clusters can also be used to gain some insight into the initial stages of nucleation in the atmosphere.

Formic acid is a weak acid that is present in the atmosphere with sources ranging from vegetation [*Jolley Herlihy et al.*, 1987] and burning biomass to urban pollution [*Schultz Tokos et al.*, 1992] and ant colonies [*Keene and Galloway*, 1986]. According to studies by Jacob, formic acid can survive in the upper troposphere for 1-2 weeks [1986]. Formic acid and acetic acid have been shown to contribute to acidity in precipitation and to enhance the uptake and stability, and thus the acidic effect, of strong acids like sulfuric and nitric acid in their reactions with water in

the atmosphere [*Nadykto and Yu*, 2007]. These conclusions are further supported by more recent calculations on organic molecules binding with sulfuric acid and ammonia [*Zhang et al.,* 2004; *Zhao et al.*, 2009]. Experiments have shown that nucleated particles contain more organics than nitrates with one recent study showing over 80% organic molecules when compared to nitrates (6%) and sulfates (10%) [*Smith et al.*, 2008].

Aloisio et al. showed that the addition of formic acid shortened the water to water hydrogen bond lengths in clusters relative to the bond lengths in pure water clusters of the same number of molecules [2002]. The authors termed this a "cooperative bonding effect" which enhanced the bonding of a water molecule, enabling water to bond more strongly to adjacent water molecules in a cluster complex. It was postulated that such hydrated acid complexes could grow more easily on a molecular level than pure water clusters. Stimulated by calculations of formic acid binding to very small, neutral water clusters that showed that the weak acid molecule significantly affected water cluster bonding and structure, we developed flow-tube experiments to investigate formic acid reactions with protonated water clusters.

In this chapter, the findings of ion-molecule reactions of protonated water clusters with formic acid studied under well-defined thermal conditions are presented with the reaction products clearly identified. The reaction leads to the formation of mixed-cluster ions of the form $H^+(H_2O)_n(HCOOH)_m$. There is a particular focus on clathrate-like structures, which are a predominant form for the $H^+(H_2O)_{21}$ cluster of the protonated water cluster ion series. The formic acid-water results are compared with both pure water and methanol-water clusters which have been previously studied by our group [*Zhang and Castleman*, 1994].

3.2 Experimental Methods

The experimental set-up includes a home-built apparatus described in detail in Chapter 2 of this dissertation that consists of a fast-flow reactor coupled with a high-pressure ion source that produces small, protonated water clusters [$H^+(H_2O)_n$, n = 2-30]. This apparatus can be used to investigate reactions for thermal collision conditions over a wide temperature range (133-400 K) that can simulate various atmospheric conditions. As this technique has been described in detail earlier, it will only be described briefly here [*Ferguson*, 1988; *Gilligan*, 2000]. Water clusters are generated by discharge ionization of an H_2O/helium mixture and are carried into the flow tube by a continuous flow of 7000 sccm (standard cubic centimeters per minute) of helium buffer gas maintained at a pre-selected, monitored pressure (c.a. 0.3 Torr). A selected concentration of reactant gas is introduced approximately 30 cm downstream from the source through a reactant gas inlet (RGI). The water cluster ions and neutral reactant gas are allowed to interact for several milliseconds before a small fraction of reactant and product ions are sampled through a nose cone, filtered by a quadrupole mass spectrometer, and detected by a channeltron electron multiplier. To study reactions at low temperatures, the flow tube is kept at a specific temperature by flowing liquid nitrogen/nitrogen gas through copper cooling coils that are wrapped lengthwise along the flow-tube. These temperatures are held constant and are precise to $\pm$1K.

The flow-tube apparatus has been used to test the solvation of acid molecules on water cluster distributions. It is possible to add any chemical species with an appreciable vapor pressure into the flow-tube by mixing it with a helium flow to ensure low concentrations relative to the water which enters at the source. The cluster formation process that occurs in our flow tube is considered thermalized; this means that very small amounts of water are mixed with large amounts of helium causing clusters to undergo ~10^5 collisions throughout their lifetime within the instrument. In short, our clusters are constantly being built up and broken down throughout the

experiment giving us a steady-state distribution of stable clusters. This pure distribution is then compared with the reacted product distribution. The reacted distribution is then used to determine a mechanism of reaction rather than a cluster growth rate. In this way our group has previously studied atmospherically relevant species including HBr, HCl, NO_x, O_3, etc. [e.g. *Castleman et al.*, 1978; *Zhang et al.*, 1994; *Gilligan and Castleman*, 2001].

In the experiments reported herein, helium gas was mixed with formic acid vapor to obtain diluted concentrations of acid. The resulting mixture was then leaked into the flow tube to react with water clusters under both room temperature and cold temperature conditions. The flow rate of formic acid, and thus the relative concentration, was controlled using an MKS brand flow meter. The same methodology was followed for methanol mixtures.

Steps were taken to ensure the precision of the experimental measurements. For example, the flow rates of the reactant gas mixtures were not varied sequentially (ie. 25 sccm to 50 sccm etc.) to reduce the likelihood of any reaction being the result of a built up concentration of reactant gas within the flow tube. Additionally, spectra were obtained under conditions of pure water between each reaction of water and the reactant gas. As an example, the experiments were run with 125.5 sccm, then pure water spectra were obtained for 1-3 spectra, then 12.5 sccm of reactant gas, 1-3 pure water spectra, 100 sccm of reactant gas, etc.

3.3 Results and Discussion

Water cluster studies in our group have generally centered around the 'magic' cluster with the formula $H^+(H_2O)_{21}$. Many structures have been proposed for the $H^+(H_2O)_{21}$ cluster [*Miyazaki et al.*, 2004; *Nagashima et al.*, 1986; *Shin et al.*, 2004; *Shinohara et al.*, 1985; *Wei et al.*, 1991]. All of the structures proposed agree that there are dangling hydrogen bonds off the main body of the cluster, while they disagree on the position of the H^+ being either inside the

cluster or residing on the surface. The present chapter focuses on the cluster structure involving the dangling hydrogens and not the location of the solvated proton. Under our typical experimental conditions this magic cluster forms at temperatures below 153 K and is highly stable when compared to other clusters in a spectrum. Figure **3.1** shows water cluster distributions at two different temperatures, where it can be seen that water cluster distributions under thermal conditions are sensitive to the temperature of the flow tube. At higher temperatures, smaller clusters dominate, while larger cluster sizes form more easily at lower temperatures.

Relative intensities of clusters are often compared to determine if a cluster is 'magic' if it stands out based on mass spectral abundance or displays an abrupt discontinuity in an otherwise smoothly varying distribution. Intensity ratios are defined as

$$R = \frac{I[n]}{I[n+1]} \qquad (3.1)$$

and are not appreciably sensitive to temperature change. Figure **3.2** shows the intensity ratio plots for the water cluster spectra shown in Figure **3.1**. Though the distributions shown in Figure **3.1** are slightly different, both show a distinct peak in intensity ratio at n=21, indicating a magic cluster that is particularly prominent. This is also true, to a lesser extent, for n=28. Ion-molecule reactions occur when neutral formic acid vapor seeded in helium is introduced to the flow tube through the RGI. The products observed from this reaction are of the form $H^+(H_2O)_n(HCOOH)_m$. The mass distributions of reactions at four different concentrations compared to the pure water distribution are shown in Figure **3.3**. The distribution for pure water is the bottom-most spectrum, with formic acid flow rates of 12.5, 25, 50 and 125 sccm appearing in successive order. Table **3.1** shows an estimated comparison of these flow rates based on the temperature and pressure within the flow tube to parts per billion volume (ppbv) which are the units that atmospheric concentrations of formic acid are reported. The table shows a reported value for

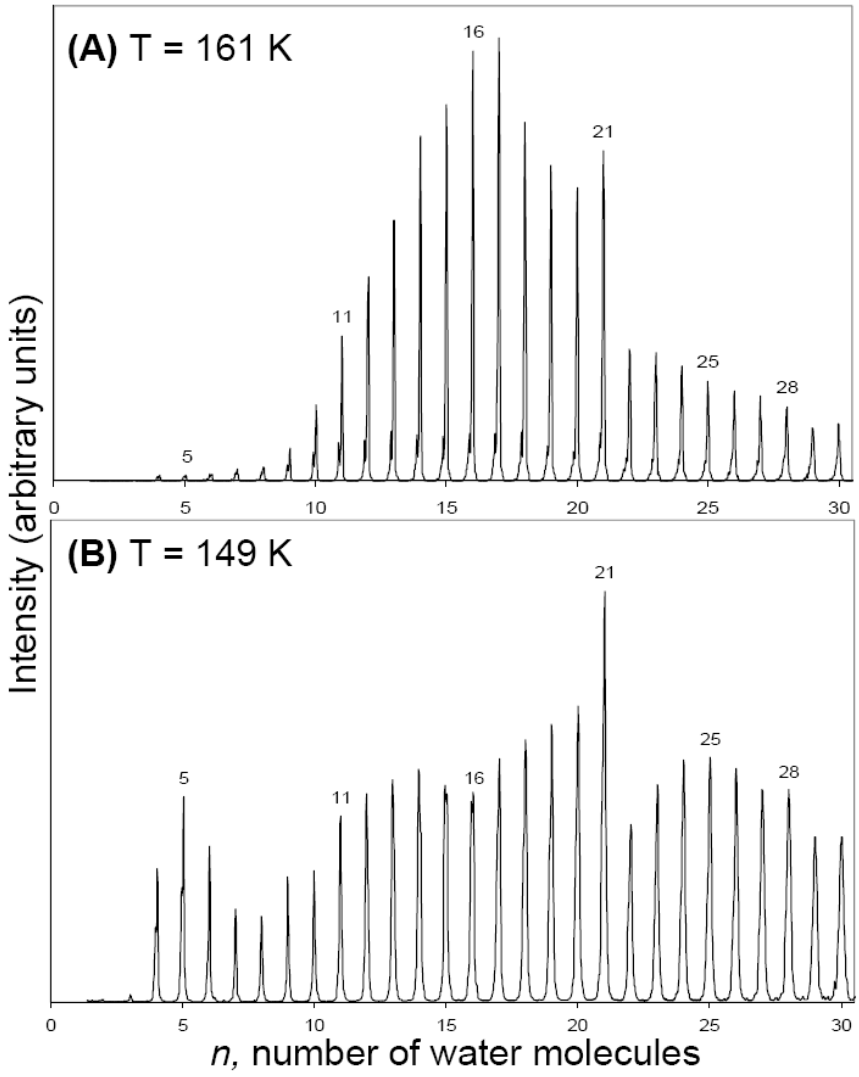

Figure **3.1**: Mass spectra of $H^+(H_2O)_n$ at (A) T=161 K and at (B) T=149 K.

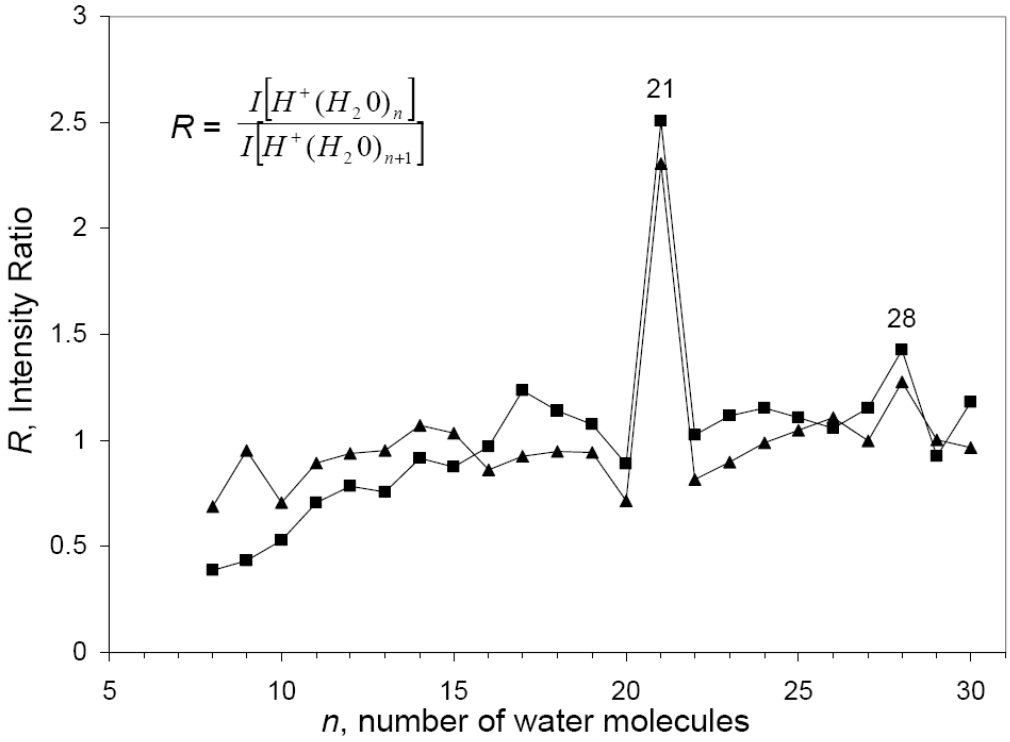

Figure **3.2**: Intensity ratio R=I[$H^+(H_2O)_n$]/I[$H^+(H_2O)_{n+1}$] for distributions of water clusters at T= 161 K (■) and 149 K (▲).

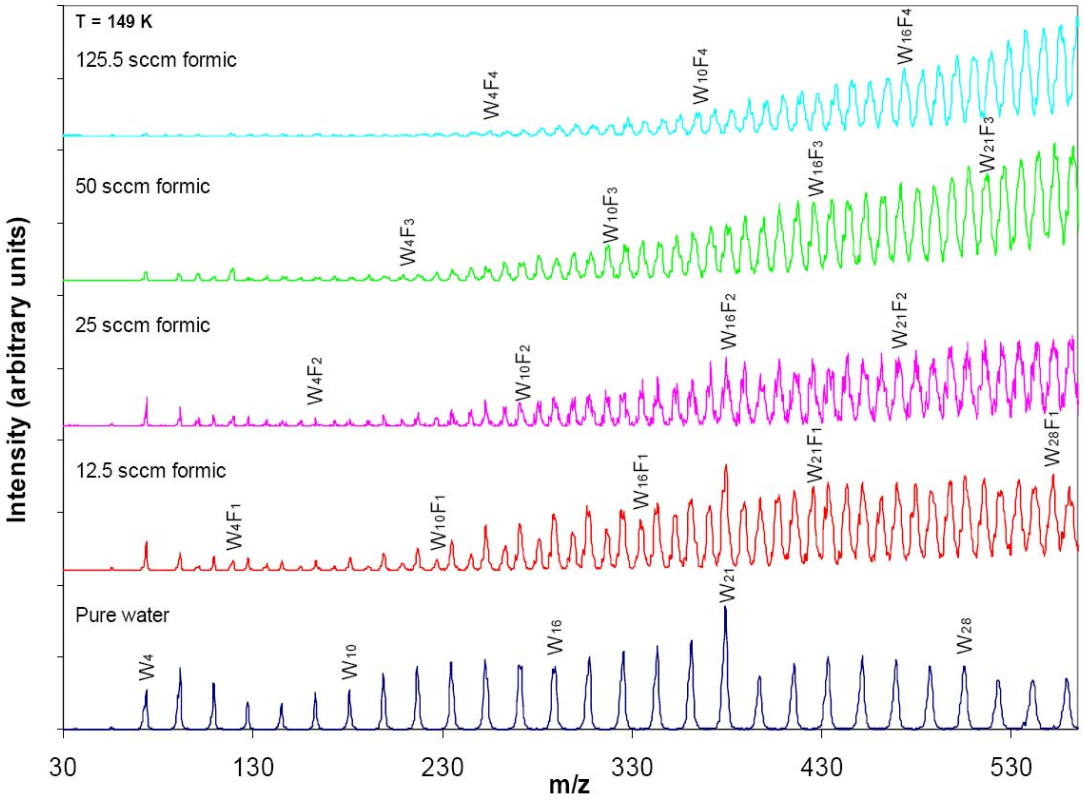

Figure **3.3**: Mass spectra of $H^+(H_2O)_n(HCOOH)_m$ obtained at varying concentrations at 149 K. $W_nF_m = H^+(H_2O)_n\,(HCOOH)_m$.

Table 3.1: Formic acid pressures studied. *Value obtained from Lawrence et al. [1994], Schultz Tokos et al. [1992], and Talbot et al. [1995]

Concentrations in Standard Cubic Centimeters per Minute (sccm)	12.5	25	50	125.5	Literature range of values*
ppbv	19.2	38.4	76.8	192.8	7.3 ± 2.5 to 46

formic acid of 7.3 $\pm$ 2.5 ppbv, but it has been reported at values up to 46 ppbv [*Lawrence et al.* 1994; *Schultz Tokos et al.* 1992; *Talbot et al*. 1995]. At 12.5 sccm, pure water clusters remain relatively abundant in the mass spectrum and mixed clusters containing a single formic acid molecule begin to be observed. The water 21-mer is also still present at this low flow rate, corresponding to 19.2 ppbv. However, as the flow rate is increased, pure water clusters occur less abundantly and the addition of multiple formic acids is observed. Further, the mass distribution shifts to more intense higher-mass clusters with each increase of formic acid flow rate. This shift is indicative of a particle growth mechanism taking place.

To better explain the growth pattern observed in formic acid-mixed clusters the formic acid reaction was compared to another small organic molecule: methanol. In addition to the pure water spectrum, Figure **3.4** shows three concentrations of methanol at 25, 50 and 100 sccm which were reacted with water clusters. It is clear that the methanol-water mixed clusters do not undergo an appreciable shift to higher mass clusters while retaining the general distribution shape present with pure water. Methanol has been shown to be compatible with the water hydrogen bonding network, with one methanol molecule easily taking the place of one water molecule without appreciably disrupting the hydrogen bonding network [*Suhara et al.*, 2007; *Zhang and Castleman,* 1994]. As the methanol-water mixed clusters do not show a shift in the mass spectra toward larger sized clusters, there is a clear difference between the methanol reaction with water and that of formic acid and water.

Upon closer inspection of the 25 sccm flow rate spectrum in Figure **3.5**, it can be seen that the shape of the distribution matches that of the general shape of a heteromolecular nucleation event presented by Castleman and Tang and shown on the left side of the figure [1972]. In this picture of a nucleation event, one can see that the original distribution will continue to exist but that another distribution that experiences rapid growth in both mass and intensity also appears within the experimental spectrum. This basic shape of the experimental

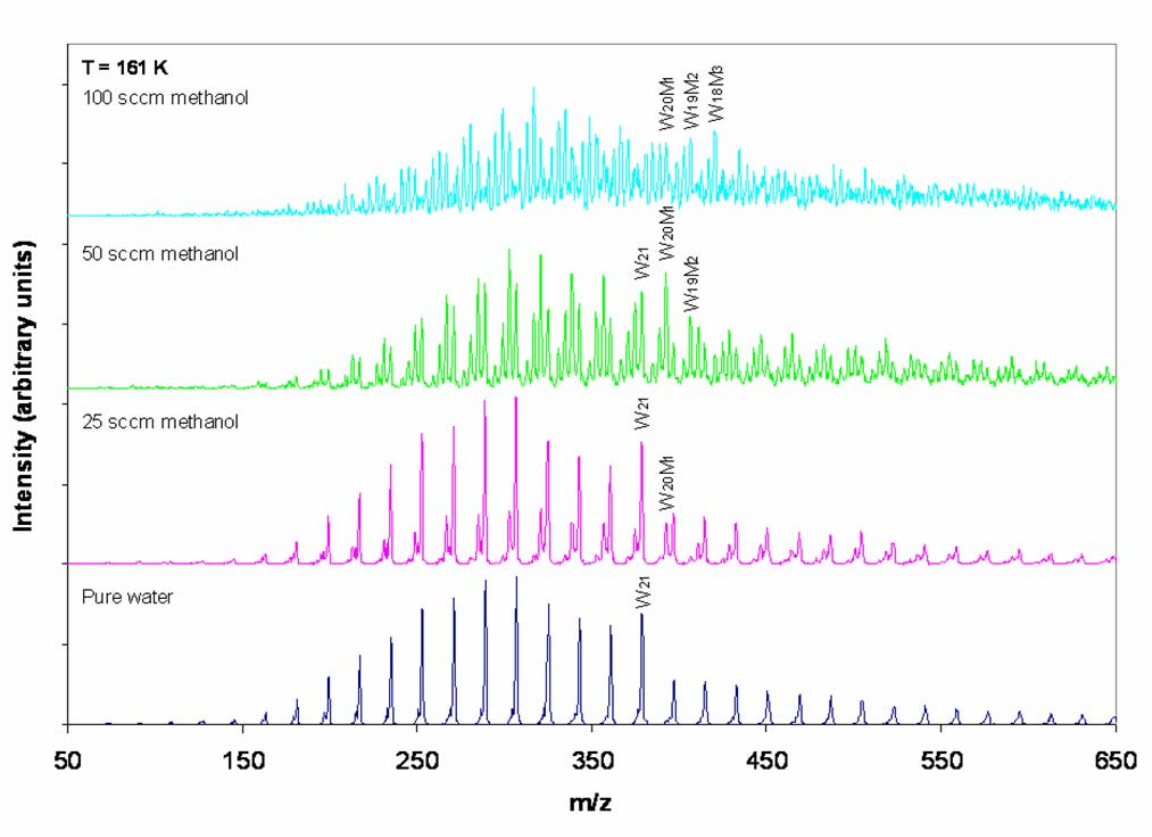

Figure **3.4**: Mass spectra of $H^+(H_2O)_n$ $(CH_3OH)_m$ obtained at varying concentrations at 161 K. $W_nM_m = H^+(H_2O)_n$ $(CH_3OH)_m$. The colors correspond to the matching concentrations in Figure 3. Especially in the 100 sccm spectra, the peaks that have been identified may not appear prominent at first glace; however they are prominent upon close inspection of their respective molecular distributions.

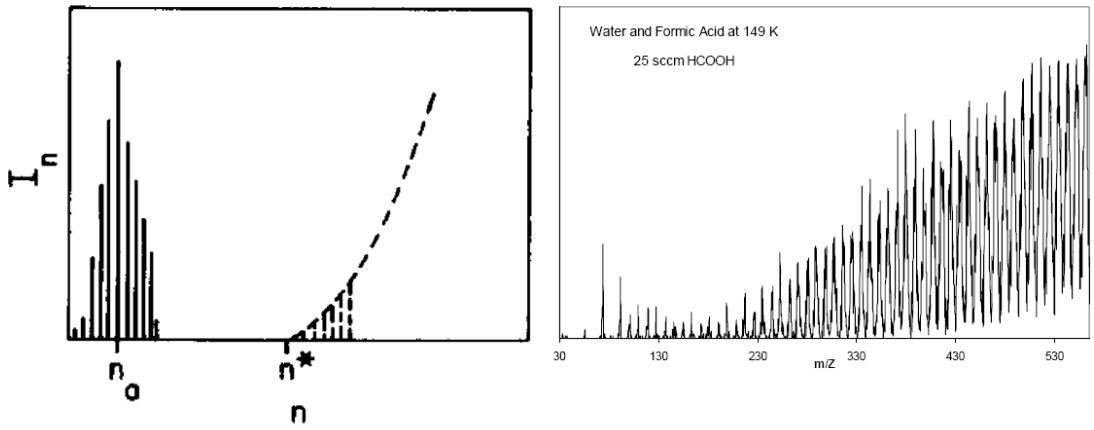

Figure **3.5**: Comparison of the $H^+(H_2O)_n$ $(HCOOH)_m$ spectra at 149 K with 25 sccm of formic acid to a sketch of the shape of a heteromolecular nucleation event spectra taken from Castleman and Tang, 1972. (Reprinted with permission from Castleman, A. Jr., and I. Tang (1972), Role of Small Clusters in Nucleation about Ions, *J. Chem. Phys.*, *57*, 3629-3638, doi:10.1063/1.1678819. Copyright 1972, American Institute of Physics.)

data is mirrored by the 25 sccm spectrum of the formic acid-water mixed clusters as shown specifically in Figure **3.5**. It is also present in Figure **3.3** for the 50 and 125.5 sccm data sets, though the high intensities of the larger clusters dominate the spectra making the initial distribution more difficult to see. Based on the cooperative bonding effect seen in small clusters by Aloisio et al. [2002], it is possible that adding formic acid to larger water clusters would result in a similar effect, shortening the water-water hydrogen bonds. Such a structural change in larger clusters might contribute to an increased growth rate of larger clusters and possibly nucleation as discussed by Mizuse et al. in their work involving the hydrogen-bonding structure of large protonated pure water clusters [2007].

Because cluster distributions are dependent on experimental conditions including temperature, another method must be employed to determine if a magic cluster exists. To do this, the intensity ratios of the formic acid-water mixed clusters were compared to those of both pure water and of methanol-water mixed clusters. Figure **3.6** shows the intensity ratio chart for methanol-water mixed clusters for the experiments performed. Previous studies in our group showed that clusters with a total molecule number of 21, corresponding to the magic water-21 cluster, have a higher relative intensity in the spectra. This is true of clusters of the form $H^+(H_2O)_n(CH_3OH)_m$ where m = 1-4 and $n+m$ =21 [*Zhang and Castleman*, 1994]. In each case, the $n+m$ =21 peak stands out significantly which was based on the formation of a stable 3D clathrate-like structure [*Zhang and Castleman*, 1994]. Inspection of the intensity ratios for formic acid-water mixed clusters does not reveal any such magic peak. As seen in Figure **3.7** for clusters of $H^+(H_2O)_n(HCOOH)_m$ where m=1-4, the 21 molecule peak does not stand out for any case.

Given the results from previous studies of water clusters in our laboratory, protonated water clusters may possibly undergo three different reaction channels when reacted with neutral molecules. Methanol may undergo a switching mechanism, where one methanol molecule replaces one water in the cluster structure; this is evidenced by the retention of the magic cluster

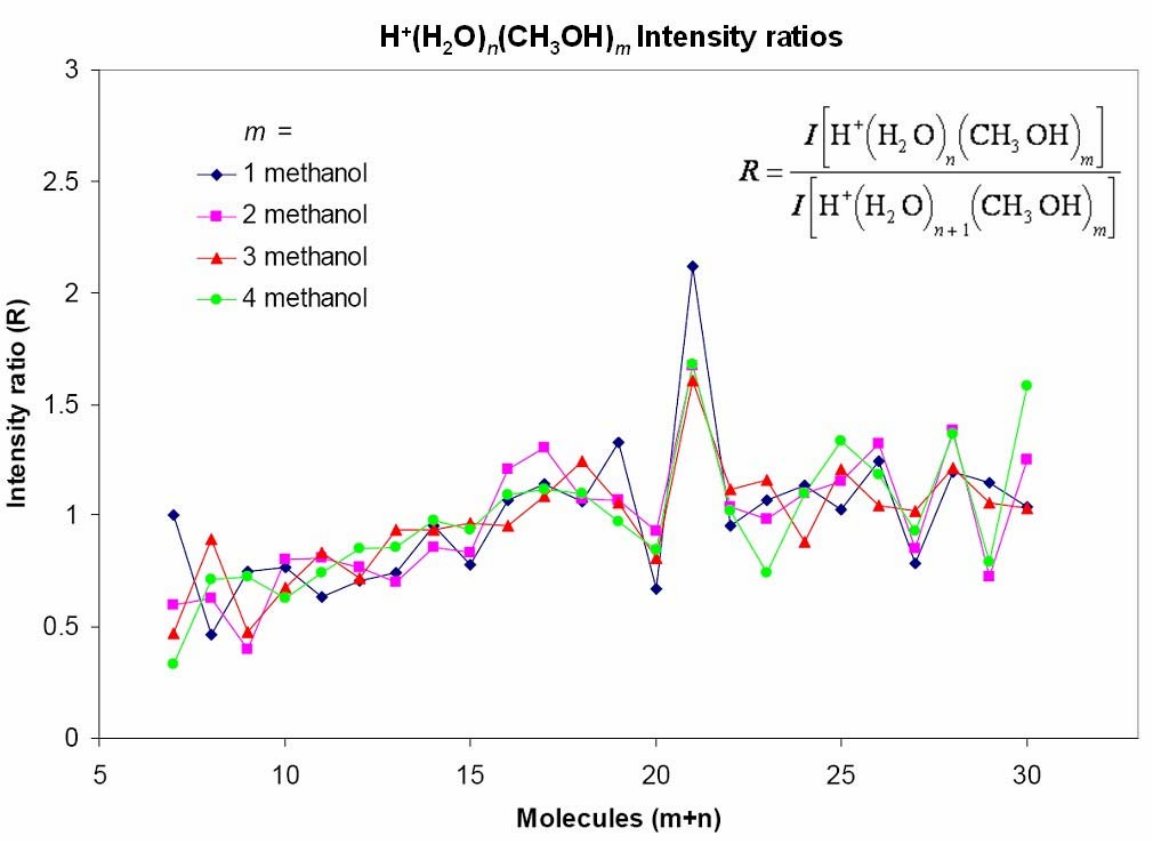

Figure **3.6**: Intensity ratio for pure water-methanol cluster distributions $R=I[H^+(H_2O)_n(CH_3OH)_m]/I[H^+(H_2O)_{n+1}(CH_3OH)_m]$ at 161 K and a flow rate of 50 sccm.

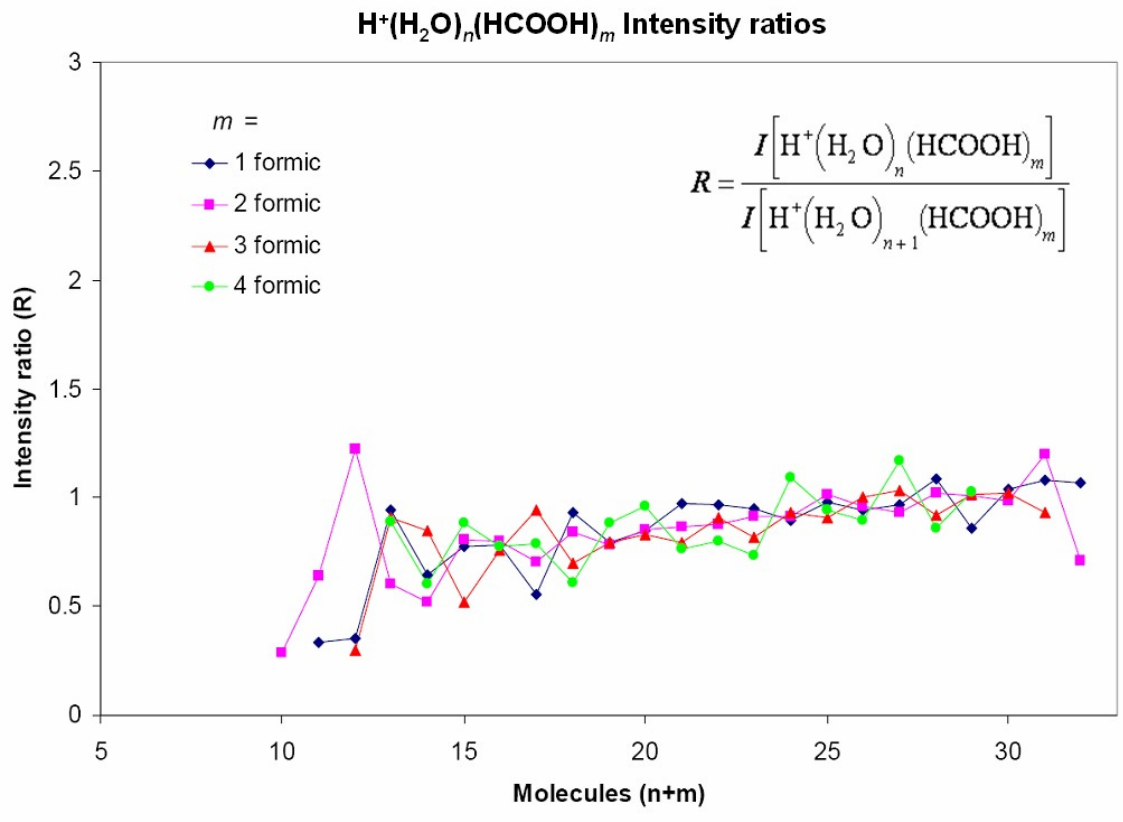

Figure **3.7**: Intensity ratio for pure water-formic acid cluster distributions R=I[H+(H2O)n(CHOOH)m]/I[H+(H2O)n+1(CHOOH)m] at 149 K and a flow rate of 150 sccm.

characteristics observed in the intensity ratio plots [*Zhang and Castleman*, 1994] which show that multiple methanol molecules may replace any of the ten dangling hydrogens present in the pure water-21 cluster. These conclusions by Zhang and Castleman based on mass spectrometry results were recently confirmed with IR data and theoretical calculations [1994; *Suhara et al.*, 2007]. It is important to note that the data presented and discussed here only involves up to four methanol or formic acid molecules reacting with a water cluster. At first glance, formic acid intensity plots do not seem to support a switching mechanism since the peak intensity of the 21 molecule cluster does not stand out as it does for the pure water 21 cluster. A second possible mechanism is an association channel where a molecule links to a protonated water molecule through intermolecular forces. It is concluded that this is also not the case for the $H^+(H_2O)_n(HCOOH)_m$ clusters because the intensity ratio of the $H^+(H_2O)_{21}(HCOOH)$ cluster should be the same as that for $H^+(H_2O)_{21}$, which is not observed. The third possible mechanism is proton transfer which is ruled out because no protonated formic acid clusters of the form $H^+(HCOOH)_n$ are observed in the spectra as would be the case if the protonated water clusters transferred the proton to a formic acid cluster. There is also evidence that water clusters prefer the H_3O^+ ion core over an $MeOH_2^+$ in methanol-water mixed clusters though methanol has a slightly higher proton affinity than water [*Suhara et al.*, 2007]; this same evidence can be applied to the formic acid system to say that it is unlikely for the mixed clusters to undergo proton transfer, as the proton affinities of formic acid, methanol, and water are all comparable.

Since the intensity ratio plots rule out switching, association, and proton transfer reactions in the case of formic acid-water mixed clusters, a different explanation must be considered. In fact, while it is likely that a single formic acid molecule replaces one water molecule in the clathrate structure, some factor of the reaction affects the stability of the magic water 21 cluster structure. When a methanol molecule replaces a water molecule in the cluster cage structure, the –OH is able to substitute for the water within the hydrogen bonding network,

leaving the $–CH_3$ end dangling off the cluster. The nonpolar methyl group would be able to replace the "dangling" hydrogen without further interacting with the cluster structure [*Suhara et al.*, 2007; *Zhang and Castleman*, 1994]. The fact that the methyl group does not further interact with the water cluster is what determines the maximum number of methanol molecules that interact and permits the mixed cluster to retain its magic characteristics [*Suhara et al.*, 2007]. However, a formic acid molecule possesses a polar carbonyl group which would protrude from the cluster if the –OH group replaced a water molecule. This polar group could be close enough to the surface of the cluster cage to form further hydrogen bonds with the surrounding water molecules in the hydrogen bonding network. The accommodation of an extra hydrogen-bonding interaction with the formic acid located within the existing hydrogen bonding network would alter the structure and shape of the cluster, affecting its stability. Based on the cooperative bonding effect demonstrated by Aloisio et al., it is likely that the formic acid shortens and strengthens the hydrogen bonds between the waters [2002]. The altered structure that results could be more conducive to nucleated growth which would explain the spectral results of increased growth rates for larger clusters. This nucleation could also be enhanced by addition of multiple formic acid molecules to the water cluster structure as seen at higher formic acid flow rates.

The findings presented in this chapter show that formic acid initiates a nucleation mechanism when reacted with pure water clusters in a flow-tube; that is, formic acid increases the ability of water to bond or interact with other water molecules. The data support the conclusions of Aloisio et al. of a cooperative bonding effect on a larger scale than their group pursued [2002]. We were also able to obtain detailed chemical information on these small clusters which could serve as pre-nucleation embryos. It is important to note that recent calculations and experiments have indicated that pure formic acid clusters do not grow by nucleation [*Baptista et al.*, 2008], while the results presented in this chapter pertain to formic acid molecules enhancing the

nucleation and growth of mixed water clusters. Further structural calculations, specifically on small and larger ionic clusters and their structural changes in the presence of formic acid which are discussed in Chapter 4, will lead to a more detailed and quantitative understanding of this phenomenon.

3.4 Conclusions

In conclusion, this chapter provides clear evidence that formic acid molecules lead to significant changes in the structure of protonated water clusters. The formic acid molecule is able to form multiple hydrogen bonds within the hydrogen bonding network of the cluster structure, thus disrupting the original structure. This possible structural change corresponds to the shortening of the water-water hydrogen bonds observed by Aloisio et al. in small neutral water clusters with a single formic acid [2002]. They concluded that this cooperative bonding effect made water more likely to bond to other water molecules, which is supported by our data on ionic clusters made up of 4 to 30 molecules. An increased intensity of larger clusters is seen, and with increasing concentrations at 12.5, 25, 50 and 125.5 sccm of formic acid, the distribution shifts so that few or no small clusters are observed while larger clusters show a dramatic increase in intensity. The cluster distributions also show a distinct and important lack of the $H^+(H_2O)_{21}$ magic cluster, further supporting a disruption of the clathrate-like structure. Further, the formic acid-water mixed clusters are distinctly different than methanol-water mixed cluster distributions which retain a magic cluster containing 21 molecules, with each methanol replacing a single water in the cluster hydrogen bonding network. Formic acid and methanol mixed cluster systems were compared directly using intensity ratios to determine the presence of this magic peak. The 21 molecule cluster stands out significantly in the methanol-water mixed clusters while the

formic acid-water mixed clusters display no magic peaks. These findings suggest that formic acid can likely interact with water molecules to form pre-nucleation clusters in the atmosphere.

3.5 References

Aloisio, S., P. Hintze, and V. Vaida (2002), The Hydration of Formic Acid, *J. Phys. Chem.*, *106*, 363-370, doi:10.1021/jp0121901.

Baptista, L., D. Andrade, A. Rocha, M. Rocco, H. Boechat-Roberty, E. da Silveira, E. da Silva, and G. Arbilla (2008), Theoretical Investigation on the Stability of Ionic Formic Acid Clusters, *J. Phys. Chem.*, *112*, 13382-12292, doi:10.1021/jp807792s.

Boy, M., J. Kazil, E. Lovejoy, A. Guenther, and M. Kulmala (2008), Relevance of ion-induced nucleation of sulfuric acid and water in the lower troposphere over the boreal forest at northern latitudes, *J. Atmos. Res.*, *90*, 151-158, doi:10.1016/j.atmosres.2008.01.002.

Castleman, A.W. Jr., and I. Tang (1972), Role of Small Clusters in Nucleation about Ions, *J. Chem. Phys.*, *57*, 3629-3638, doi:10.1063/1.1678819.

Castleman, A.W. Jr., P. Holland, and R. Keesee (1978), The properties of ion clusters and their relationship to heteromolecular nucleation, *J. Chem. Phys., 68*, 1760-1764, doi:10.1063/1.435946.

Ferguson, E. (1988), Flow tube studies of ion-molecule reactions, *Adv. At. Mol. Phys., 25*, 61-81.

Finlayson-Pitts, B. and J. Pitts, Jr. (2000), *Chemistry of the Upper and Lower Atmosphere,* Academic Press, New York.

Gilligan, J. (2000), The Role of Solvation of Ion-Molecule Reactions: Elucidating Mechanisms of Heterogeneous Atmospheric Chemistry and the Reactivity of Metal-Ligand Complexes, Ph.D. thesis, 96 pp., The Pennsylvania State University, State College, PA, USA.

Gilligan, J. and A.W. Castleman, Jr. (2001), Acid Dissolution by Aqueous Surfaces and Ice: Insights from a Study of Water Cluster Ions, *J. Phys. Chem. A.*, *105*, 5601-5605, doi:10.1021/jp003480p.

Hanson, D. and E. Lovejoy (2006), Measurement of the Thermodynamics of the Hydrated Dimer and Trimer of Sufuric Acid, *J. Phys. Chem. A Let., 110,* 9525-9528, doi:10.1021/jp062844w.

Holmes, N. S. (2007), A review of particle formation events and growth in the atmosphere in the various environments and discussion of mechanistic implications, *Atmos. Environ.*, *41*, 2183-2201, doi: 10.1016/j.atmosenv.2006.10.058.

Iida, K., M. Stolzenburg, P. McMurry, M. Smith, J. Smith, F. Eisele and P Keady (2006), Contribution of ion-induced nucleation to new particle formation: Methodology and it's application to atmospheric observations in Boulder, Colorado, *J. Geophys. Res.*, *111*, D23201, doi:10.1029/2006JD007167.

Jacob, D. (1986), Chemistry of OH in Remote Clouds and Its Role in the Production of Formic Acid and Peroxymonosulfate, *J. Geophys. Res.*, *91*(D9), 9807-9826, doi:10.1029/JD091iD09p09807.

Jolley Herlihy, L., J. Galloway, and A. Mills (1987), Bacterial Utilization of Formic Acid and Acetic Acid in Rainwater, *Atmos. Environ.*, *21*, 2397-2402, doi:101016/0004-6981(87)90374-X.

Keene, W. and J. Galloway (1986), Considerations Regarding Sources for Formic and Acetic Acids in the Troposphere, *J. Geophys. Res.*, *91*(D13), 14466-14474, doi:10.1029/JD091iD13p14466.

Kulmala, M., and V.-M. Kerminen (2008), On the formation and growth of atmospheric nanoparticles, *Atmos. Res.*, *90*, 132-150, doi:10.1016/j.atmosres.2008.01.005.

Kulmala, M., and H. Tammet (2007), Finnish-Estonian air ion and aerosol workshops, *Boreal Environ. Res.*, *12*(3), 237-245.

Kulmala, M., H. Vehkamaki, T. Petaja, M. Dal Maso, A. Lauri, V.-M. Kerminen, W. Birmili, and P. McMurry (2004), Formation and growth rates of ultrafine atmospheric particles: a review of observations, *J. Aerosol Sci.*, *35*, 143-176, doi:10.1016/j.jaerosci.2003.10.003.

Kulmala, M. et al. (2007), Toward Direct Measurement of Atmospheric Nucleation, *Science*, *318*, 89-92, doi:10.1126/science.1144124.

Lawrence, J.E. and P. Koutrakis (1994), Measurement of Atmospheric Formic and Acetic Acids: Methods Evaluation and Results from Field Studies, *Environ. Sci. and Tech.*, *28*, (5), 957-964.

Miyazaki, M., A. Fujii, T. Ebata, and N. Mikami (2004), Infrared Spectroscopic Evidence for Protonated Water Clusters Forming Nanoscale Cages, *Science*, *304*, 1134-1137, doi:10.1126/science.1096037.

Mizuse, K., A. Fujii, and N. Mikami (2007), Long range influence of an excess proton on the architecture of the hydrogen bond network in large-sized water clusters, *J. Chem. Phys.*, *126*, 231101, doi:10.1063/1.2750669.

Nadykto, A., F. Yu (2007), Strong hydrogen bonding between atmospheric nucleation precursors and common organics, *Chem. Phys. Let.*, *435*, 14-18, doi:10.1016/j.cplett.2006.12.050.

Nagashima, U., H. Shinohara, N. Nishi, and H. Tanaka (1986), Enhanced stability of ion-clathrate structures for magic number water clusters, *J. Chem. Phys.*, *84*, 209-214, doi:10.1063/1.450172.

Schultz Tokos, J., S. Tanaka, T. Morikami, H. Shigetani, and Y. Hashimoto (1992), Gaseous Formic and Acetic Acids in the Atmosphere of Yokohama, Japan, *J. Atmos. Chem.*, *14*, 85-94, doi:10.1007/BR00115225.

Shin, J.-W., N. Hammer, E. Diken, M. Johnson, R. Walters, T. Jaeger, M. Duncan, R. Christie, and K. Jordan (2004), Infrared signature of structures associated with the $H^+(H_2O)_n$, n=6-27, clusters, *Science*, *304*, 1137-1140, doi:10.1002/chin.200431007.

Shinohara, H., U. Nagashima, H. Tanaka, and N. Nishi (1985), Magic numbers for water-ammonia binary clusters: Enhanced stability of ion clathrate structures, *J. Chem. Phys.*, *83*, 4183-4192, doi:10.1063/1.449083.

Smith, J., M. Dunn, T. VanReken, K. Iida, M. Stolzenburg, P. McMurry, and L. Huey (2008), Chemical composition of atmospheric nanoparticles formed from nucleation in Tecamac, Mexico: Evidence for an important role for organic species in nanoparticles growth, *Geophys. Res. Lett.*, *35*, L04808, doi:10.1029/2007GL032523.

Suhara, K., A. Fujii, K. Mizuse, N. Mikami, and J. Kuo (2007), Compatibility between methanol and water in the three-dimensional cage formation of large-sized protonated methanol-water mixed clusters, *J. Chem. Phys.*, *126*, 194306, doi:10.1063/1.2734969.

Talbot, R.W., B.W. Mosher, B.G. Heikes, D.J. Jacob, J.W. Munger, B.C. Daube, W.C. Keene, J.R. Maben, and R.S. Artz (1995) Carboxylic acids in the rural continental atmosphere over the eastern United States during the Shenandoah Cloud and Photochemistry Experiment, *J. Geophys. Res.*, *100*, (D5), 9335-9345.

Wei, S., Z. Shi, and A.W. Castleman, Jr. (1991), Mixed cluster ions as a structure probe: Experimental evidence for clathrate structure of $(H_2O)_{20}H^+$ and $(H_2O)_{21}H^+$, *J. Chem. Phys.*, *94*, 3268-3270, doi:10.1063/1.459796.

Yu, F., and R. Turco (2000), Ultrafine aerosol formation via ion-mediated nucleation, *Geophys. Res. Lett.*, *27*, 883-886, doi:10.1029/1999GL011151.

Yu, F., Z. Wang, G. Luo, and R. Turco (2008), Ion-mediated nucleation as an important global source of tropospheric aerosols, *Atmos. Chem. Phys.*, *8*, 2537-2554.

Zhang, R., I. Suh, J. Zhao, D. Zhang, E. Fortner, X. Tie, L. Molina, and M. Molina (2004), Atmospheric New Particle Formation Enhanced by Organic Acids, *Science*, *304*, 1487-1490, doi:10.1126/science.1095139.

Zhang, X. and A.W. Castleman, Jr. (1994), Evidence for the formation of clathrate structures of protonated water-methanol clusters at thermal energy, *J. Chem. Phys.*, *101*, 1157-1164, doi:10.1063/1.467809.

Zhang, X., E. Mereand, and A.W. Castleman, Jr. (1994), Reactions of Water Cluster Ions with Nitric Acid, *J. Phys. Chem.*, *98*, 3554-3557, doi:10.1021/j100064a044.

Zhao, J., A. Khalizov, R. Zhang, and R. McGraw (2009) Hydrogen-Bonding Interaction in Molecular Complexes and Clusters of Aerosol Nucleation Precursors, *J. Phys. Chem. A, 113*, 680-689, doi:10.1021/jp806693r.

Chapter 4

The effect of formic acid addition on water cluster stability and structure

4.1 Introduction

Water clusters have been studied using a wide range of methods, both experimental e.g. [*Gilligan and Castleman*, 2001; *Nagashima et al.*, 1986; *Searcy and Fenn*, 1974] and computational e.g. [*Miyazaki et al.*, 2004; *Shin et al.*, 2004]. Studies of water clusters are used to examine the fundamentals of intermolecular interactions such as hydrogen bonding and cluster structure as well as such phenomena relevant to atmospheric chemistry as solvation and nucleation. Small water clusters are important because they can provide information on the gas-to-particle transition, which is of particular interest in atmospheric chemistry. Flow-tube studies of water cluster distributions at well controlled temperatures and their reactions with atmospherically relevant chemical species recently have been shown to serve as a complementary method to direct atmospheric measurement to identify chemicals in the atmosphere that may contribute to nucleation and particle growth [*Goken and Castleman*, 2010].

Under various experimental conditions—including expansion of ionized water vapor [*Searcy and Fenn*, 1974], near-threshold vacuum-UV photoionization [*Nagashima et al.*, 1986], and thermal flow tube conditions at cold temperatures [*Castleman et al.*, 1978; *Gilligan and Castleman*, 2001; *Goken and Castleman*, 2010; *Zhang et al.*, 1994]—the water 21 cluster stands out as having "magic" characteristics. Magic clusters can be defined as standing out based on mass spectral abundance or displaying an abrupt discontinuity in an otherwise smoothly varying distribution. A more accurate means of determining if a cluster has magic character is to make an intensity ratio plot using Equation 3.1 which is described in more detail in Chapter 3. A large

peak in the intensity ratio plot indicates a magic cluster. The structure of the magic water 21 cluster and what causes its magic character has long been disputed. The debate about whether the excess proton resides on the surface of the cluster or within the cage is ongoing and will not be discussed in this work.

Many explanations have been developed to account for the magic stability of the water 21 magic cluster. Miyazaki et al. observed the IR spectra of water clusters ranging from 4 to 27 molecules; the authors observed that the acceptor-acceptor-donor (AAD), where the water molecule is accepting hydrogen-bonding character from two other molecules while donating to only one, stretch was the most prominent at the 21 molecule cluster, which they concluded indicated that the transition from 2-D chains to a 3-D cage structure was complete [2004]. Shin et al. observed the OH stretching frequencies of clusters ranging from 6 to 27 molecules [2004]. Their experiments showed that a doublet stretching feature present for clusters larger than 11 molecules shifted to only a single peak at the 21 molecule cluster, indicating only one type of OH stretch was present and all dangling OH bonds were equivalent [*Shin et al.*, 2004]. Both of these theories focus on the structure of the clusters and how that relates to the magic character of water 21.

The magic character of the water 21 cluster makes it an ideal species to study the reaction of molecules with water using a flow tube apparatus. The reacted cluster species can be compared to pure water distributions to provide information about possible reaction mechanisms and products under certain conditions. Chapter 3 of this dissertation describes the three likely reaction channels that are used in water cluster ion-molecule studies—association, proton transfer, and switching—in detail. The flow-tube studies of formic acid-water mixed clusters and methanol-water mixed clusters that were described in the previous chapter were performed because of interest generated from calculations presented by Aloisio et al. that examined the changes in the hydrogen bonding network of small, neutral water clusters upon the addition of

formic acid [2002]. In this chapter, similar DFT calculations have been performed and compared to those presented by Aloisio et. al. [2002]; the calculations presented here have been expanded to include small, neutral methanol-water clusters.

In order to further examine the differences between the formic acid-water mixed clusters and the methanol-water mixed clusters and to determine if incorporation of formic acid into the cluster causes a structural change on a larger size scale, numerical modeling of protonated water clusters was performed using the ReaxFF reactive force-field model. The ReaxFF force field method allows us to model moderately large systems (up to 4000 atoms on a single processor, $>10^6$ atoms on a parallel environment) at low computational cost while still retaining near quantum mechanical (QM) accuracy. ReaxFF is a bond-order dependent reactive force field and is capable of modeling the breaking and formation of bonds during molecular dynamics simulation. The parameters used within this force field are developed by fitting against experimental and QM calculations. The ReaxFF reactive force field was initially developed for hydrocarbons [*van Duin et al.*, 2001; *van Duin*, 2003] and has been extended for many other organic and inorganic systems e.g. [*Chenoweth, van Duin, and Goddard*, 2008; *Chenoweth et al.*, 2008; *Cheung et al.*, 2005; *Jarvi et al.*, 2008; *Nielson et al.*, 2005; *Ojwang et al.*, 2008].

4.2 Experimental Methods

4.2.1 Flow tube studies

The experimental data employed in this chapter for comparing theory and experiment is described in Chapter 3 of this dissertation. A brief review of how these data were obtained is described here. A flow of helium was passed over water to obtain a mixture of water vapor seeded in the helium flow. This water mixture was passed over a wire that had a voltage applied

to it, ionizing the water. The ionized water mixture was then passed into the flow tube where it underwent ~10^5 collisions with a high pressure of helium carrier gas. About 30 cm from the source, a reactant mixture of either formic acid or methanol seeded in helium was leaked into the flow tube at a specified flow rate from an MKS flow meter. The reactant gas and the water clusters interacted within the flow tube for an additional distance. A sample of the clusters then passed through a nose-cone orifice, 1mm in diameter, and was sampled through a quadrupole mass analyzer. The clusters were detected using a channeltron detector.

4.2.2 Computational Methods

4.2.2.1 Density Functional Theory

Aloisio et al. performed QM calculations on small pure water clusters (1-4 molecules) as well as clusters with the same number of molecules that had one formic acid molecule replacing one water molecule within the cluster structure [2002]. The authors performed an extensive study of the various basis sets involved in geometrical optimization in DFT. In this chapter we present calculations performed using the GAUSSIAN 03 suite of programs [*Gaussian 03, Revision C.02*, 2004] using the B3LYP/6-311++G (d,p) basis set, which was the highest level of theory Aloisio et al. presented for their geometry calculations [2002]. In addition, only the most stable cage structures calculated by Aloisio et al. were used in the present chapter [2002]. The nomenclature of the calculated clusters is consistent with the naming of the cage structures presented in Aloisio et al. and has been expanded to describe the methanol-water clusters [2002].

It is true that DFT calculations, including the B3LYP/6-311++G (d,p) basis set, do not perfectly describe the interactions and bonding involved in van der Waals clusters. However, these calculations are much less computationally expensive than other methods including coupled

cluster methods which might better describe the weak interactions. In addition, we wanted to compare our calculations to those already reported in the literature, which is why this particular method and basis set were chosen. The calculations for larger water clusters were performed using the ReaxFF method, described below.

4.2.2.2 ReaxFF Force Field Method

The ReaxFF system is based on a balance of energies:

$$E_{system} = E_{bond} + E_{val} + E_{tors} + E_{over} + E_{under} + E_{lp} + E_{H\text{-}bond} + E_{vdWaals} + E_{coulomb} \quad (4.1)$$

The partial contributions in Equation (4.1) include bond energies (E_{bond}), valence angle energies (E_{val}), torsion angle energies (E_{tors}), energy to penalize over-coordination of atoms (E_{over}), energy to stabilize under-coordination of atoms (E_{under}), lone pair energies (E_{lp}), hydrogen bond energies ($E_{H\text{-}bond}$) and terms to account for non-bonded Coulomb ($E_{coulomb}$) and van der Waals ($E_{vdWaals}$) interaction energies. All of the energy contributions, excluding the last two terms of Equation 4.1, depend on the bond order. This bond order dependence allows for the smooth transitions between bond breaking and formation during the dynamic modeling. A more detailed description of each individual energy term and the ReaxFF method can be found in Refs [*Chenoweth, van Duin, and Goddard*, 2008; *van Duin et al.*, 2001; *van Duin et al.*, 2003].

4.2.2.3 ReaxFF Force Field Parameterization

For this chapter, our collaborators from Dr. Adri van Duin's research group re-optimized the ReaxFF potential to incorporate the effect of formic acid on the cooperative hydrogen bonding of water molecules. The initial force field parameters of H/O/C interaction have been extensively optimized using the quantum data describing reactive and non-reactive interactions

relevant to water. This includes equations of state for water dimers, proton transfer barriers and crystal ice. A full description of the water force field is described elsewhere [*A.C.T. van Duin, V. Bryantsev, J. Su and W.A. Goddard*, manuscript in progress]. For the work described in this chapter, additional complexes between formic acid and water molecules (HCOOH-$(H_2O)_n$ where n=1-2) were included in the optimization. These data points were taken from Aloisio et al [2002]. The training set was further extended with QM data describing the energy barrier for the protonation of formic acid in the presence of a single water molecule. A single-parameter-based parabolic extrapolation method was used to optimize the force field parameters against the QM data present in the training set [*van Duin et al.*, 2001].

4.2.2.4 Molecular Dynamics Method

All the MD simulations in this study are performed on protonated clusters. A MD-NVT based anneal simulation method was used to obtain the most stable configuration of each cluster. Each anneal cycle consists of heating the cluster from 0 K to T_{max} in 4ps, equilibrating the cluster at T_{max} for 2ps, cooling down the cluster from T_{max} to 0 K in 4ps and finally equilibrating the cluster again at 0 K for 2ps where T_{max} is maximum temperature. Each structure is subjected to 82 such anneal cycles to find the most stable cluster configuration. For water clusters ($H^+(H_2O)_n$) and formic acid-water mixed clusters ($H^+(H_2O)_n$ (HCOOH)), a maximum temperature of 160 K was used. For methanol clusters ($H^+(H_2O)_n$ (CH_3OH)) the maximum temperature used was 110 K. A lower value of maximum temperature was selected for methanol clusters because at higher temperatures, methanol has the tendency to evaporate from the water cluster due to its weaker binding characteristics.

4.3 Results and Discussion

Pure water distributions at cold temperatures, below ~153 K, display a magic peak at the 21 molecule cluster. Comparing previous experimental studies of methanol in our group and experiments and calculations in the literature, it is shown that methanol reacts with water through a switching reaction mechanism [*Suhara et al.*, 2007; *Zhang and Castleman*, 1994]. Methanol can replace a water molecule in the cluster structure and still retain the magic cluster characteristics, as evidenced by flow tube studies and confirmed by more recent IR studies [*Suhara et al.*, 2007; *Zhang and Castleman*, 1994]. This can be seen in Figure **3.4** (Chapter 3) where methanol-water mixed clusters retain the general distribution shape seen in pure water. The formic acid-water mixed clusters shown in Figure **3.3** (Chapter 3) do not retain a similar distribution shape to the pure water clusters, though it is believed that the formic acid also replaces water molecules within the cluster structure through a switching reaction. Figure 3.5 (Chapter 3) shows that the shape of the formic acid spectrum closely resembles the theoretical spectrum with a double-humped shape that is expected in the case of nucleation [*Goken and Castleman*, 2010].

In order to prove that there is no magic cluster character in the formic acid-water mixed clusters case, intensity ratio plots were compared to those of pure water and of methanol-water mixed clusters. As opposed to methanol-water clusters and pure water clusters which display a distinct magic peak at the 21-molecule cluster, the formic acid case clearly does not show a peak at the 21-molecule cluster, nor anywhere else in the intensity ratio plot for the size region examined. This plot indicates that there is no magic cluster observed within our range of mass detection. This lack of an intense peak rules out an association reaction, which would show a magic peak at $H^+(H_2O)_{21}(HCOOH)$. Proton transfer from the water clusters to formic acid would result in pure formic acid cationic clusters, which do not appear in the spectrum.

As stated in Chapter 3, we hypothesize that the formic acid molecules replace a water molecule within the hydrogen bonding network of the water cluster as is the case with methanol. Methanol is composed of a polar –OH group which is able to hydrogen bond within the cluster network and a nonpolar $–CH_3$ group which can easily replace a dangling hydrogen [*Suhara et al.*, 2007]. Because there are ten dangling hydrogen bonds, it is believed that up to ten methanol molecules can replace waters in the cluster without seriously disrupting the stable magic cluster structure. However, in the case of a formic acid, there is an ability to form more than one hydrogen bond with the cluster for each individual formic acid molecule. This additional hydrogen bonding capability is believed to disrupt the hydrogen bonding network. We have hypothesized that this disruption is sufficient to alter the 21 molecule cluster and cause it to lose its magic character [*Goken and Castleman*, 2010].

4.3.1 DFT Geometry Calculations

DFT geometry optimization calculations presented in this chapter were performed on small pure water, formic acid-water, and methanol-water mixed clusters. These calculations were done for the neutral case for two reasons. First, Aloisio et al. used the GAUSSIAN 98 suite of programs, and since the present approach utilizes the GAUSSIAN 03 suite of programs [2002; *Gaussian 03, Revision C.02*, 2004], it was critical to ensure that our calculations were comparable to those presented in the prior literature. Secondly, simulations on the mixed methanol-water cluster system were necessary to compare our experiments to the conclusions of Aloiso et al. and to determine if methanol has a significant impact on the water-water hydrogen bonds in the small neutral clusters [2002]. As seen in Table **4.1**, we calculated the bond lengths and angles for the monomers of water, formic acid, and methanol. For water and formic acid our calculated values are compared to those reported in Aloisio et al. [2002]. From Table **4.1** it is clear that our

Table **4.1**: Geometry optimization of monomers as compared to data from Aloisio et al. [2002]. All bond lengths are reported in Å and angles in degrees.

Molecule	Coordinate	6-311++G(d,p)*	Aloisio et al.
H_2O	O-H	0.962	0.962
	H-O-H	105.1	105.0
Formic Acid (Z)	O-H	0.971	0.971
	C=O	1.199	1.199
	C-H	1.098	1.098
	C-O	1.346	1.346
	H-O-C	107.9	108
	O-C=O	125.1	125.2
	H-C=O	125.3	125.2
	H-C-O	109.6	Not reported
Formic Acid (E)	O-H	0.966	0.966
	C=O	1.192	1.192
	C-H	1.105	1.105
	C-O	1.353	1.353
	H-O-C	110.0	110.0
	O-C=O	122.5	122.6
	H-C=O	124.0	123.9
	H-C-O	113.5	Not reported
Methanol	O-H	0.961	
	C-O	1.423	
	C-H	1.090	
		1.097	
		1.097	
	H-O-C	108.9	
	O-C-H	106.8	
		112.1	
		112.1	

calculations are consistent with those previously reported for water and formic acid. In Table **4.2**, we directly compared our calculations of pure water clusters up to four molecules and formic acid-water mixed clusters up to four molecules with the literature results. Our calculated structures are shown in Figure **4.1**. The figures are named to correspond to the naming of the cage clusters presented by Aloisio et al. FAZ1 indicates a formic acid with one water molecules that forms a closed ring/cage structure. FAZ11 indicates a formic acid with two water molecules that forms a closed cage structure. FAZ111 indicates a formic acid with three water molecules that forms a closed cage structure. R(1) refers to the hydrogen bond between the –OH group of the formic acid and a water molecule. R(2) refers to the hydrogen bond length between the carbonyl group of formic acid and a water molecule. The bond lengths from the literature and those calculated here are within a few hundredths of an Ångstrom. The calculated bond angles of the formic acid are the same for virtually every case. Although bond lengths vary between our calculations and those reported by Aloisio et al., the variations between different simulated clusters are equal [2002]. For example, the water-4 bond lengths vary by less than 0.001 Å, as seen in Table 4.4. Table 4.4 shows the calculated water-water hydrogen bond lengths, R(W), for the pure water clusters, formic acid-water mixed clusters, and the methanol-water mixed clusters. Therefore we concluded that our calculations were sufficient to compare methanol-water mixed clusters with those composed of formic acid and water.

The bond distances of the methanol-water cage clusters of a size up to four molecules are shown in Table **4.3**. Figure **4.2** shows the calculated structures obtained. The naming of the clusters corresponds to that described above for formic acid. In this case, however, R(1) refers to the hydrogen bond length between the H side of the –OH group of the methanol and a water molecule, and R(2) refers to the hydrogen bond length between the O side of the –OH group of the methanol and a water molecule. The bond distances show that replacing a water molecule with a methanol in the four molecule cluster causes a shortening of the water-water hydrogen

Table **4.2**: Formic acid bond lengths (in Å) for HCOOH-$(H_2O)_n$ (n = 1-3). FAZ1, FAZ11, and FAZ111 indicate various conformations of formic acid-water complexes, as shown in Figure 4.1 and also in Aloisio et al. [2002]. The present work uses the B3LYP/6-311G++(d,p) basis set as described in Table 4.1.

	C=O		O-H		C-H		C-O		R(1)		R(2)	
	Present work	Aloisio et al	Present work	Aloisio et al	Present work	Aloisio et al	Present work	Aloisio et al	Present work	Aloisio et al	Present work	Aloisio et al
FAZ1	.211	1.211	0.989	0.989	1.098	1.098	1.328	1.328	1.788	1.790	2.076	2.056
FAZ11	.215	1.216	1.003	1.003	1.098	1.098	1.316	1.316	1.662	1.662	1.844	1.841
FAZ111	.215	1.215	1.006	1.006	1.098	1.099	1.313	1.313	1.638	1.637	1.808	1.808

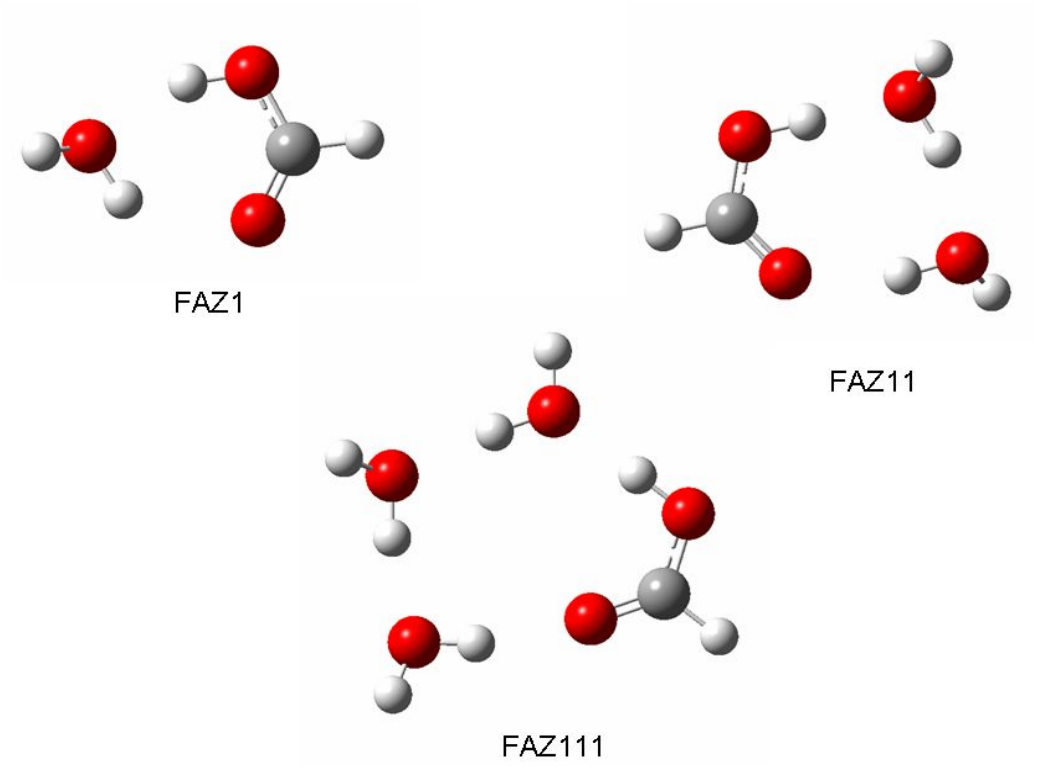

Figure **4.1**: Formic acid-water cage clusters calculated using B3LYP/6-311++G(d,p). The naming scheme corresponds to that in Aloisio et al. for ease of comparison.

Table **4.3**: Methanol bond lengths (in Å) and angles (in degrees) for CH_3OH-$(H_2O)_n$ (n = 1-3), calculated in the present work using the B3LYP/6-311G++(d,p) basis set.

	O-H	C-O	C-H	R(1)	R(2)
MeOH1	0.962	1.432	1.089	1.896	
			1.095		
			1.095		
MeOH11	0.974	1.425	1.091	1.861	1.913
			1.096		
			1.096		
MeOH111	0.980	1.424	1.091	1.749	1.802
			1.096		
			1.096		

Table **4.4**: Water-water hydrogen bond lengths (in Å) for waters in formic acid clusters, methanol clusters, and pure water clusters. Values are given for both the present work using the B3LYP/6-311G++(d,p) basis set and those reported by Aloisio et al. [2002].

	R(w)	
	Present Work	Aloisio et al
W2	1.954	1.932
W3	1.920	1.894
	1.923	1.897
	1.926	1.919
FAZ11	1.757	1.758
MeOH11	1.917	
W4	1.798	1.775
	1.799	1.777
	1.799	1.778
	1.800	1.779
FAZ111	1.737	1.738
	1.714	1.714
MeOH111	1.748	Not reported
	1.790	

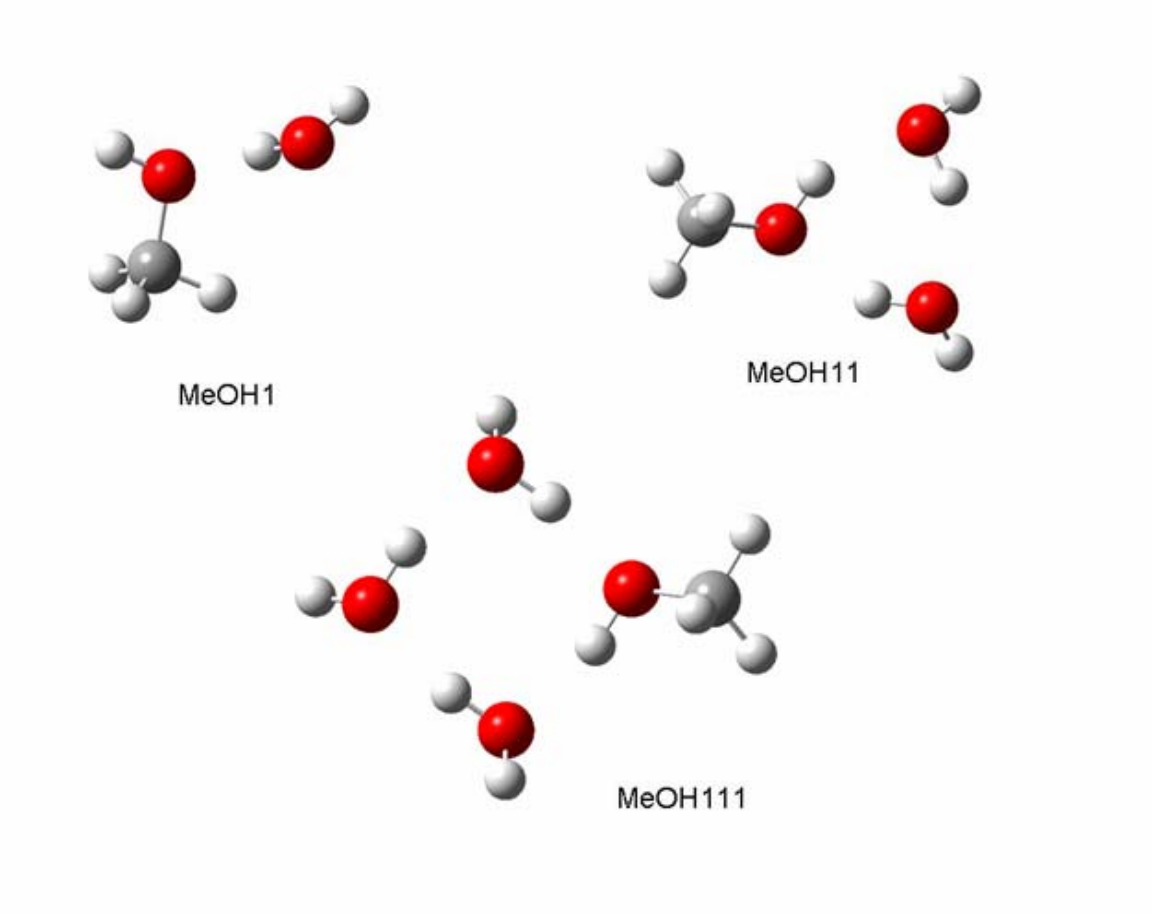

Figure **4.2**: Neutral cage structures of methanol-water mixed clusters calculated using B3LYP/6-311++G(d,p).

bond length. However, this shortening of the bond length does not occur to the extent seen when one water is replaced with a formic acid. From this result, we conclude that methanol does not disrupt the hydrogen bonding network of a water cluster to the same extent as does formic acid. Table **4.5** and Figure **4.3** show the O-H bond lengths and H-O-H bond angles of the water molecules contained in the 4 molecule clusters. For the pure water 4 cluster, all of the O-H bonds contained in the hydrogen bonding network of the cluster are consistent; in addition the O-H bonds that represent the dangling hydrogen bonds are also consistent. A slight stretching of the bonds within the hydrogen bonding network is seen, corresponding to a slight shortening of the O-H bonds that are not within the network. The lengthening of the bonds within the hydrogen bonding network corresponds to an increase in the size of the H-O-H bond angle, which is shown to be consistent across all four water molecules.

Table **4.5** and Figure **4.4** show that the methanol-water 4 molecule cluster has similar characteristics with all of the O-H bond lengths within the cluster cage being similar and the O-H bond lengths not comprising the cage being similar to each other. The H-O-H bond angles for the methanol-water cluster are significantly smaller than those for the pure water cluster and are closer to the bond angle of a pure water monomer. The key point is that all three H-O-H bond angles are similar for this cluster.

When the bond lengths and bond angles are examined for the formic acid-water 4 molecule cluster however, the O-H bond lengths on the water hydrogen bonded to the carbonyl group are noticeably different from the other two water molecules as shown in Figure **4.5**. Corresponding to this difference in bond lengths the H-O-H bond angles are different, with one water molecule being similar to the waters in a pure cluster and two resembling those observed in the methanol cluster.

Taking these numbers into account, the four waters in the pure water cluster appear to be equivalent in their ability to form new hydrogen bonds and add to the hydrogen bonding network.

Table **4.5**: Water bond distances (in Å) and angles (in degrees) for the 4-molecule clusters, 3-molecule clusters, 2-molecule clusters, and a water monomer.

Cluster	Water molecule	Involved in H-bond network	Dangling –OH bond	H-O-H Angle
W4	Wa	0.979	0.959	107.8
	Wb	0.979	0.959	107.8
	Wc	0.979	0.959	107.8
	Wd	0.979	0.959	107.8
FAZ111	Wa	0.977	0.961	107.2
	Wb	0.982	0.962	106.5
	Wc	0.988	0.962	106.6
MeOH111	Wa	0.983	0.961	106.3
	Wb	0.983	0.961	106.5
	Wc	0.986	0.961	106.3
W3	Wa	0.973	0.960	107.7
	Wb	0.972	0.960	107.8
	Wc	0.973	0.960	107.7
FAZ11	Wa	0.978	0.961	106.7
	Wb	0.984	0.962	107.1
MeOH11	Wa	0.976	0.961	106.7
	Wb	0.979	0.961	106.7
W2	Wa	0.969	0.961	105.3
	Wb	---	0.962	106.3
FAZ1	Wa	0.972	0.962	107.3
MeOH1	Wa	0.972	0.961	105.2
W1		---	0.962	105.1

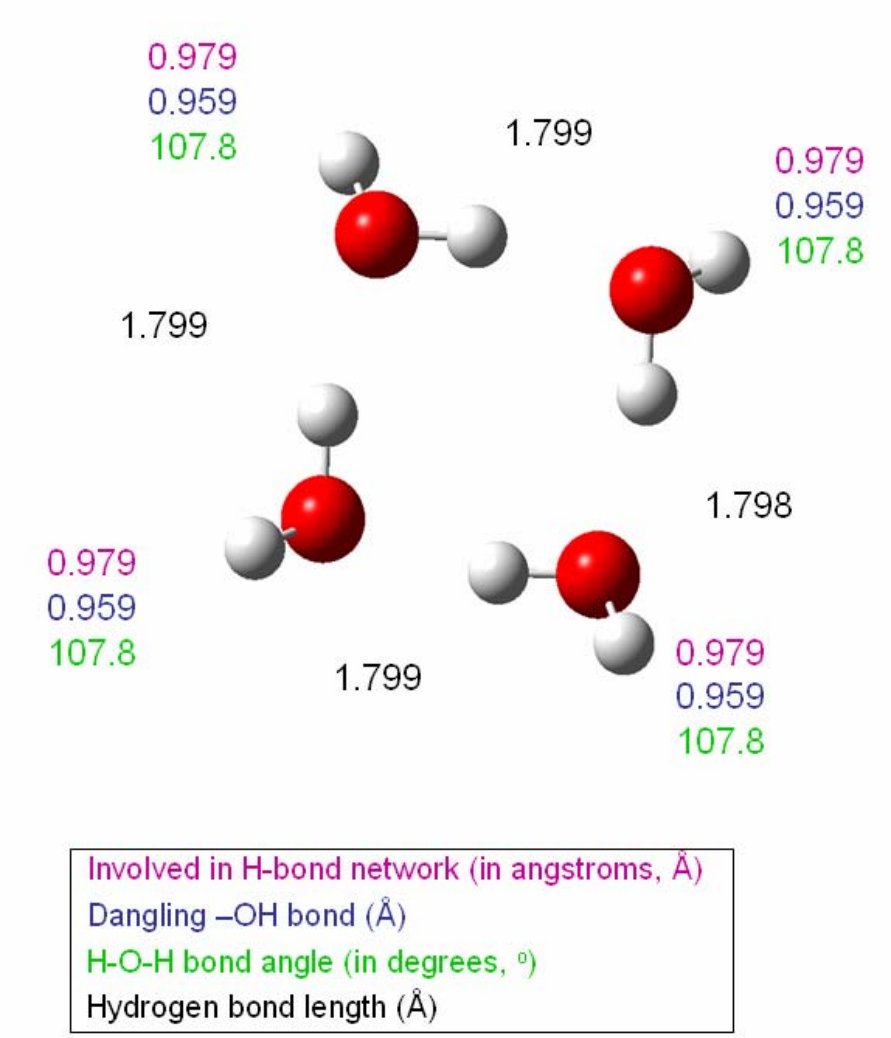

Figure **4.3**: Bond lengths and angles for the neutral $(H_2O)_4$ cluster.

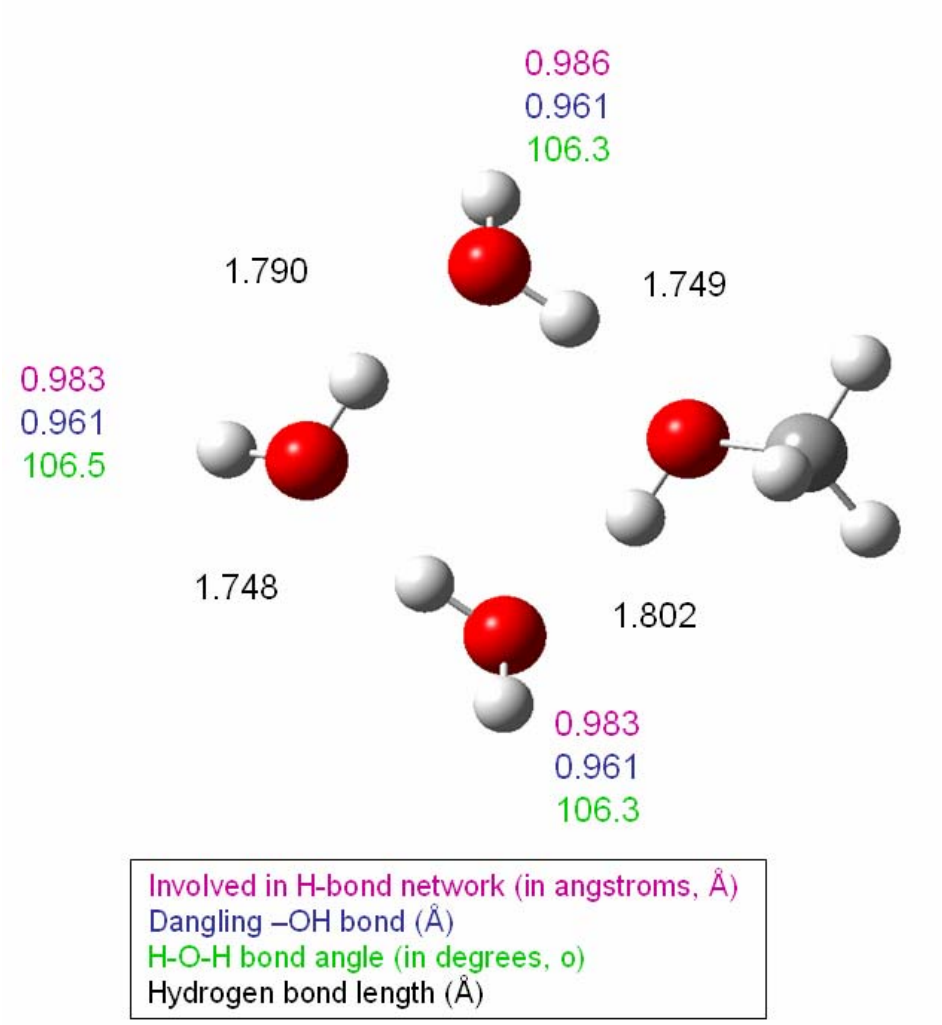

Figure **4.4**: Bond lengths and angles for the neutral $(H_2O)_3CH_3OH$ cluster.

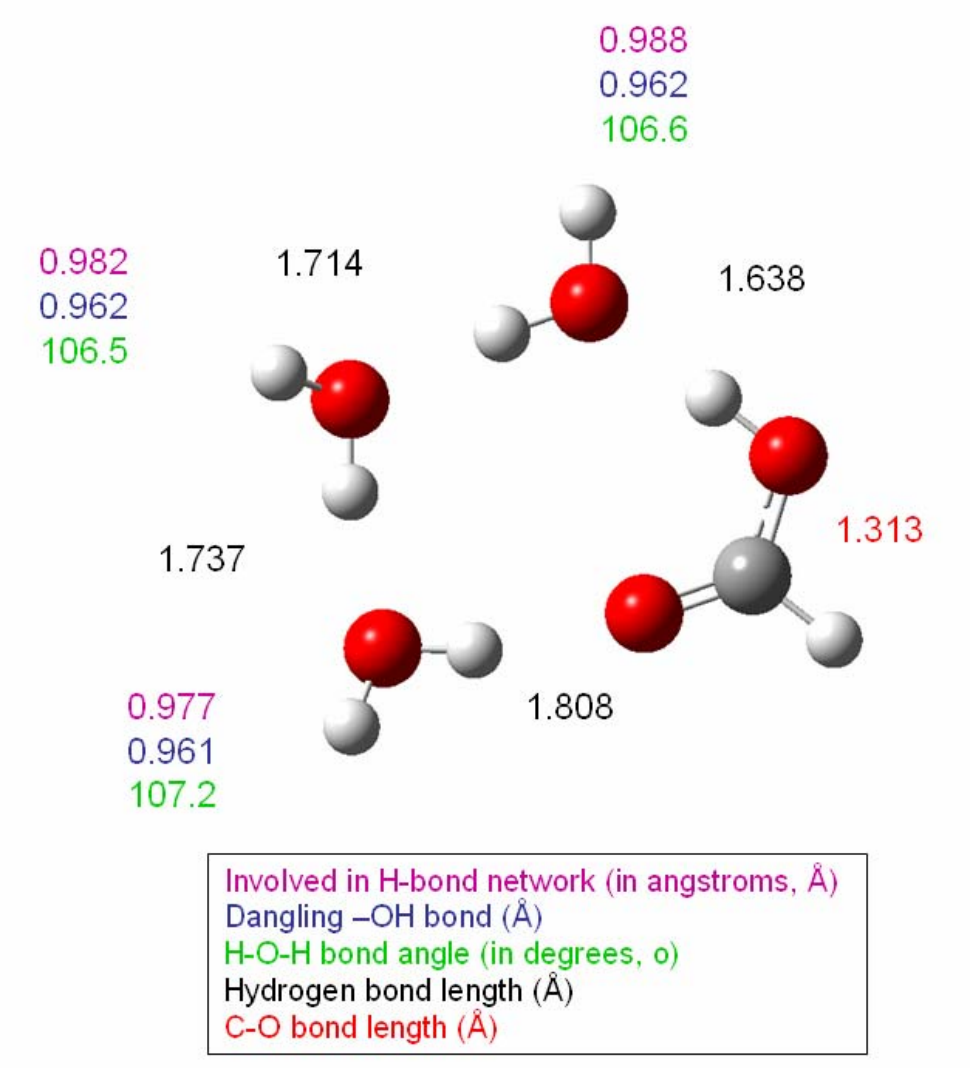

Figure **4.5**: Bond lengths and angles for the neutral $(H_2O)_3HCOOH$ cluster.

In the case of the methanol mixed cluster, the three waters are all equivalent in their ability to form new hydrogen bonds. For the formic acid-mixed cluster, there are two equivalent water molecules and one water molecule that is noticeably different. It is possible that this inequality of the waters produces selective molecules for forming new hydrogen bonds and adding to the cluster hydrogen bonding network. For instance, the water closest to the carbonyl group on the formic acid is donating more hydrogen bonding strength to the two pairs of free electrons on the oxygen and is thus less likely to donate to another hydrogen bond but is more likely to accept hydrogen bonding from another water, meaning it has a slight negative character. The two lone pairs on the carbonyl group could also simply form another hydrogen bond. The third possible selective site arises from the stronger donation of hydrogen bonding by the –OH group of the formic acid to the water closest to it. It can be observed in all of the calculated structures for formic acid that a slight double bonding character forms between the –OH oxygen and the carbon molecules, which results in an extended bond between that oxygen and hydrogen. As a result, the hydrogen is closer to the water molecule than any of the other hydrogen bonds observed, giving that water a slight H_3O^+ character. The donation of positive character has a direct correlation to the slight negative character of the water closest to the carbonyl group, producing a dipole on the neutral water cluster. This dipole produces several additional selective sites for adding waters to the hydrogen bonding network, which could explain why our experimental data shows that formic acid-water mixed clusters selectively form larger cluster sizes. Also, the addition of more than one formic acid would increase the number of selective addition sites, causing further growth of large clusters.

To better compare these calculations to our experimental data, we would need to study the systems on both a larger scale and also for protonated clusters. However, protonated water clusters of small size have a 2-D structure of dangling chains where the neutral clusters form 3-D

cages at sizes of 3 molecules and larger. With increasing sizes the chains observed for protonated clusters begin to form cyclic structures, but a full 3-D cage does not form until the 21 molecule cluster; IR experiments have shown these distinct differences in the hydrogen bonding network of the neutral and ionic clusters at sizes as small as three molecules and as large as 100 molecules [*Miyazaki et al.*, 2004; *Mizuse et al*., 2007; *Shin et al.*, 2004]. An example of the 2-D chain structures for the ionic clusters and the 3-D cage structures of the neutral clusters is shown in Figure **4.6**. The 2-D structures can not be used to compare the difference in water-water hydrogen bonds in a cage structure for small ionic clusters; in order to gain more insight into structural changes in the ionic clusters, ReaxFF calculations were performed on the ionic clusters of 20-28 molecules as this method is much less computationally expensive than DFT calculations.

4.3.2 Force Field Optimization

The structures of all the complexes between formic acid and water molecules that were used in the training set can be found in Aloisio et al. [2002; *Rablen et al.*, 1998]. The force field predicts that the Z conformation of formic acid is more stable than E conformation of formic acid by 4.007 kcal mol^{-1} which is in excellent agreement with the experimental result of 4.0 kcal mol^{-1} [*Hurtmans et al.*, 2000]. Figures **4.7.a** and **4.7.b** show that the trained force field parameters reproduce the QM results adequately for the energies of the complexes between formic acid and water molecule. The worst agreement is for the FAZ3 complex for which the force field overestimates the stability. Given the relative instability of the FAZ3 complex we believe that this discrepancy will not significantly affect the ReaxFF results.

With this optimized force field, we computed the binding energies of formic acid complexes with three water molecules. It should be noted that these data points ($HCOOH\text{-}(H_2O)_3$ complexes) were not used for optimizing the force field, but instead they are used here to test the

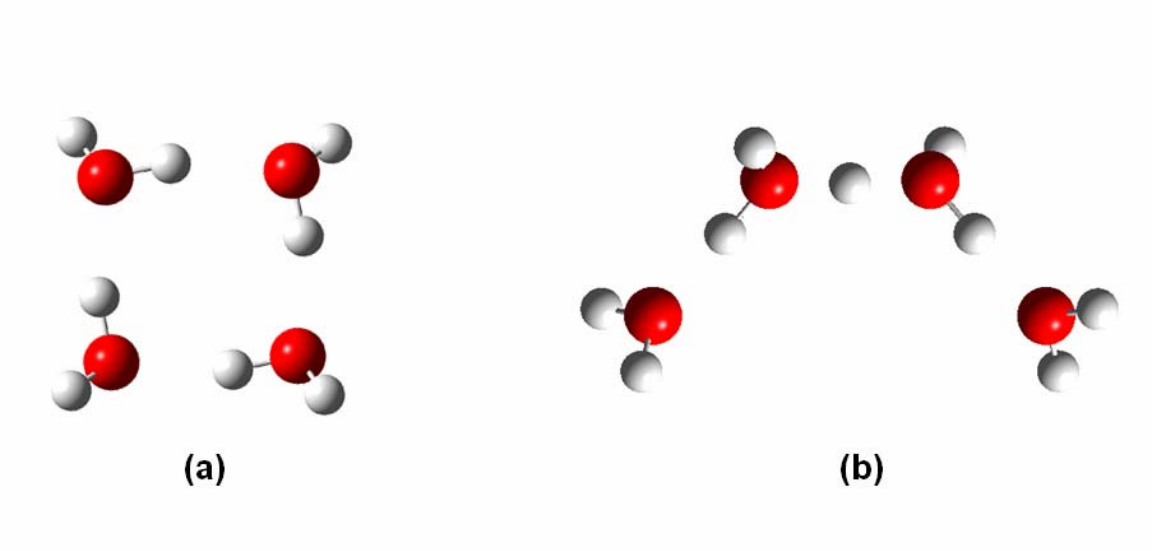

Figure **4.6**: Comparison of the neutral water 4 cluster (a) to the protonated water 4 cluster (b). The neutral clusters form a closed cage structure at sizes as small as three water molecules, while protonated clusters form a structure that consists of dangling chains instead of a closed 3-D structure.

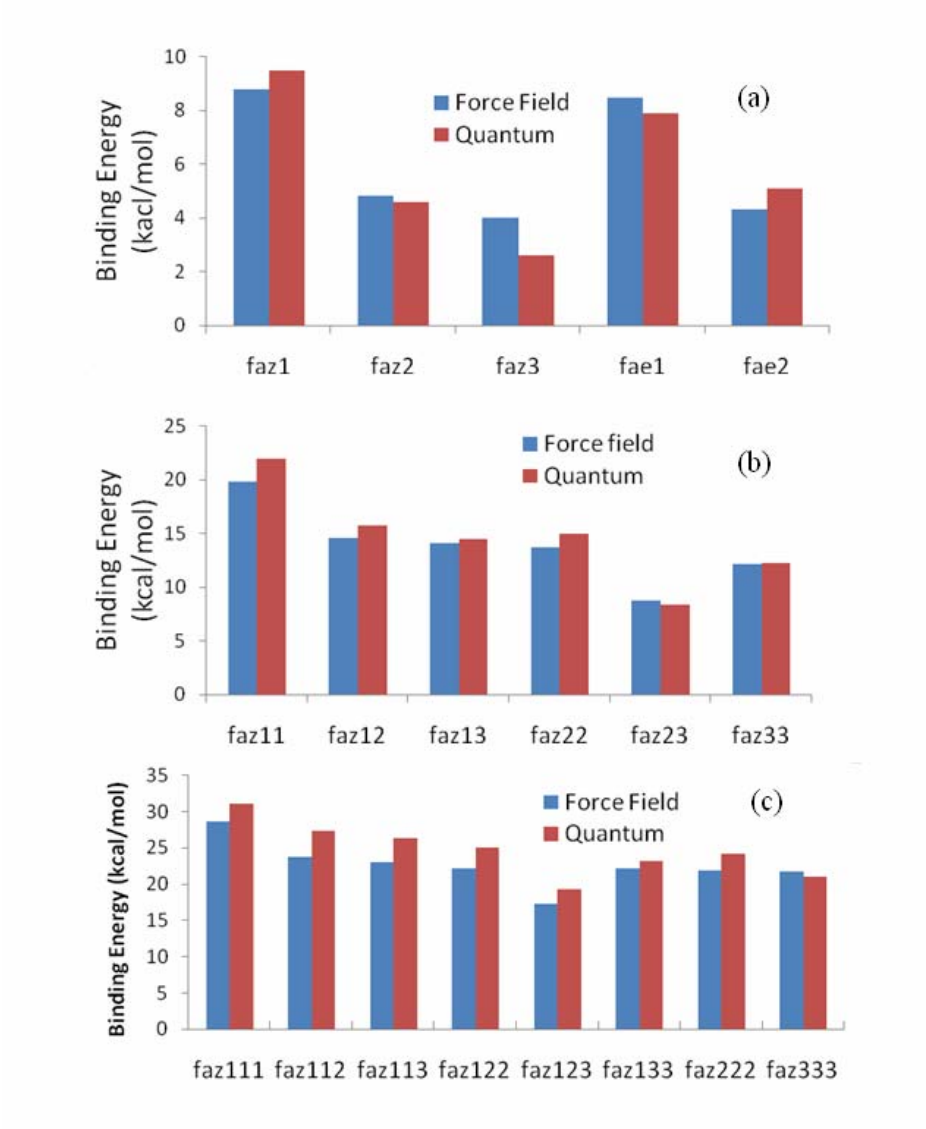

Figure **4.7**: Binding energies of formic acid-water complexes (a) HCOOH-H_2O, (b) HCOOH-$(H2O)_2$, (c) HCOOH-$(H2O)_3$.

accuracy of the optimized force field. Figure **4.7.c** shows that the force field predictions of binding energies are in excellent agreement with the QM calculations.

4.3.3 Molecular Dynamics Simulations

Figure **4.8** shows the calculated binding energies of the protonated clusters as a function of cluster size for pure water, methanol-water, and formic acid-water clusters. For all the three types of clusters, the binding energy per molecule decreases as the cluster size increases. For water clusters $H^+(H_2O)_n$, the binding energy peaks at n=21 indicating the existence of a clathrate-like (3-D cage structure) magic cluster. A similar trend is observed for methanol-water mixed clusters with a peak at n=21 indicating that -CH_3 group of methanol interacts weakly with other water molecules present inside the cluster. However for the formic acid-water mixed clusters, we do not observe any peak at n=21. The overall binding energies of formic acid-water mixed clusters are considerably higher than the other two types of clusters studied. This shows that formic acid strengthens the hydrogen bonding network and makes the clusters more stable. This strengthening is likely related to the higher number of potential hydrogen bonding sites discussed earlier. By increasing the stability of the clusters above the stability of pure water and providing more sites for potential cluster growth, formic acid likely increases the chances of the clusters to nucleate, enhancing the possibility of particle growth.

From the MD anneal simulations the most stable configurations are extracted for each type of water cluster. These stable configurations for the clusters containing 21 molecules are shown in Figure **4.9**. The structure of the methanol-water mixed cluster shows that the -CH_3 group replaces the dangling hydrogen and remains on the outside of the cluster. On the contrary, formic acid becomes incorporated into the hydrogen bonding network by forming multiple hydrogen bonds with the surrounding waters and moves inside the cluster. This disrupts the

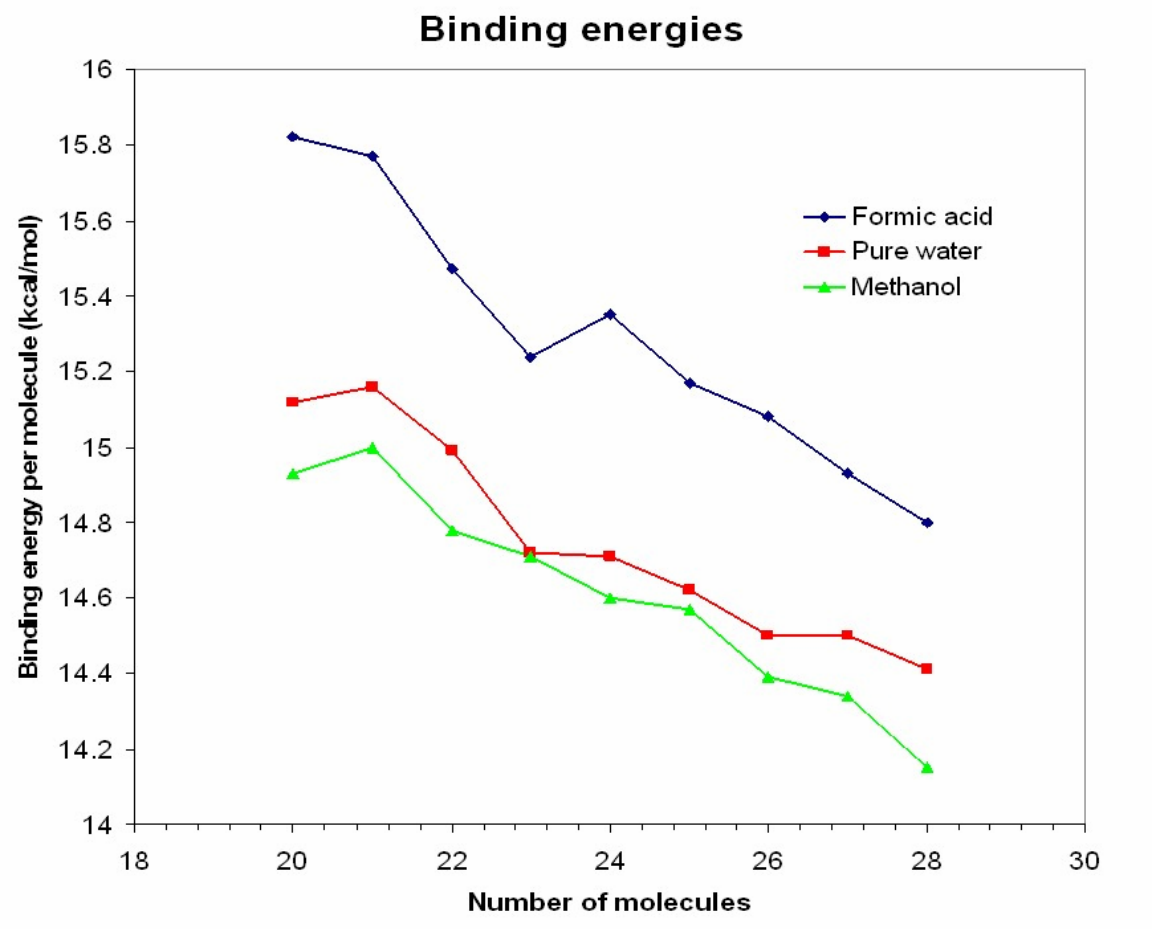

Figure **4.8**: Binding energies per molecule of protonated clusters for pure water, formic acid-water mixed clusters and methanol-water mixed clusters.

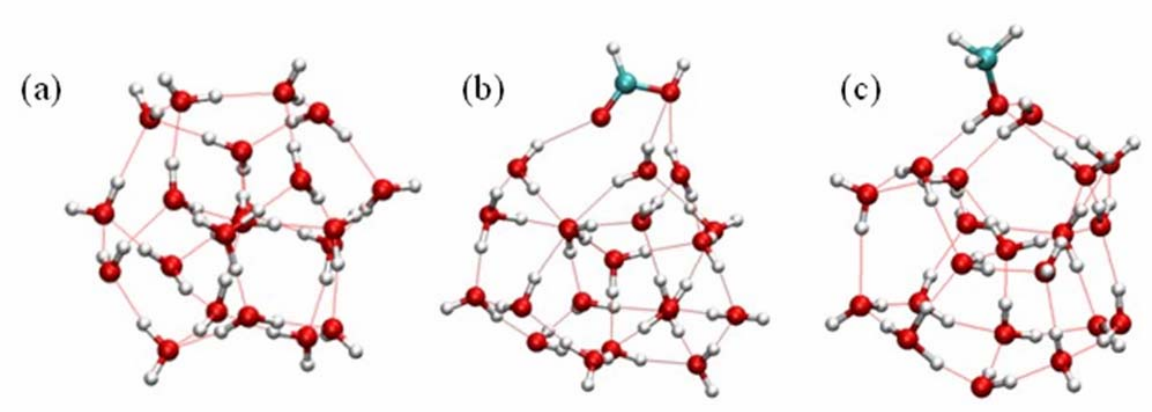

Figure **4.9**: Most stable structures found for the 21-molecule protonated clusters (a) $H^+(H_2O)_{21}$, (b) $H^+(H_2O)_{20}$-HCOOH, (c) $H^+(H_2O)_{20}$-CH_3OH.

shape and configuration of the cluster thereby affecting its stability.

To further compare the large protonated cluster structures to the hypothesis presented by Aloisio et al. that formic acid shortens the water-water hydrogen bonds, the radial distribution function (RDF) of the 21 molecule clusters of pure water and formic acid-water were examined [2002]. Figure **4.10.a** shows the full RDF of the clusters while Figure **4.10.b** shows a closer view of the RDF, zoomed-in on the peaks that represent hydrogen bonding. The first peak in Figure **4.10.a** represents the hydrogens bonded to the oxygen molecule for which the radial distribution function has been calculated. The second peak represents the first shell of hydrogen bonds. The third peak is another shell of hydrogen bonding; this peak is much less resolved due to the varied distances of the water molecules within the second shell of hydrogen bonds and cannot be used for conclusions. Figure **4.10.b** shows a slight reduction in the average hydrogen bond length, 5.48%, in the water cluster with a single formic acid molecule. This reduction in the hydrogen bond length does support the cooperative bonding effect proposed by Aloisio et al. [2002].

When the larger clusters are examined closely, it is clear that the pure water-21 cluster has ten dangling hydrogen bonds. These dangling hydrogen molecules along with the ADD water molecules with the lone pairs of the oxygen pointing toward the outside of the cluster mean that this water cluster has a set number of sites for additional hydrogen bonds to form through accepting or donating hydrogen bonding character. The methanol replaces the dangling hydrogen molecules with a methyl group that is unlikely to form additional hydrogen bonds, acting as a capping molecule and decreasing the number of available sites for water molecules to add to the cluster. The formic acid however adds two additional sites for potential hydrogen bond formation increasing the potential of the cluster for adding water molecules and growth.

Given the different nature of the formic acid and methanol interactions with the water cluster, we thought it interesting enough to examine the evaporation of molecules off of the protonated clusters of 21 molecules. MD simulations were able to give an estimated temperature

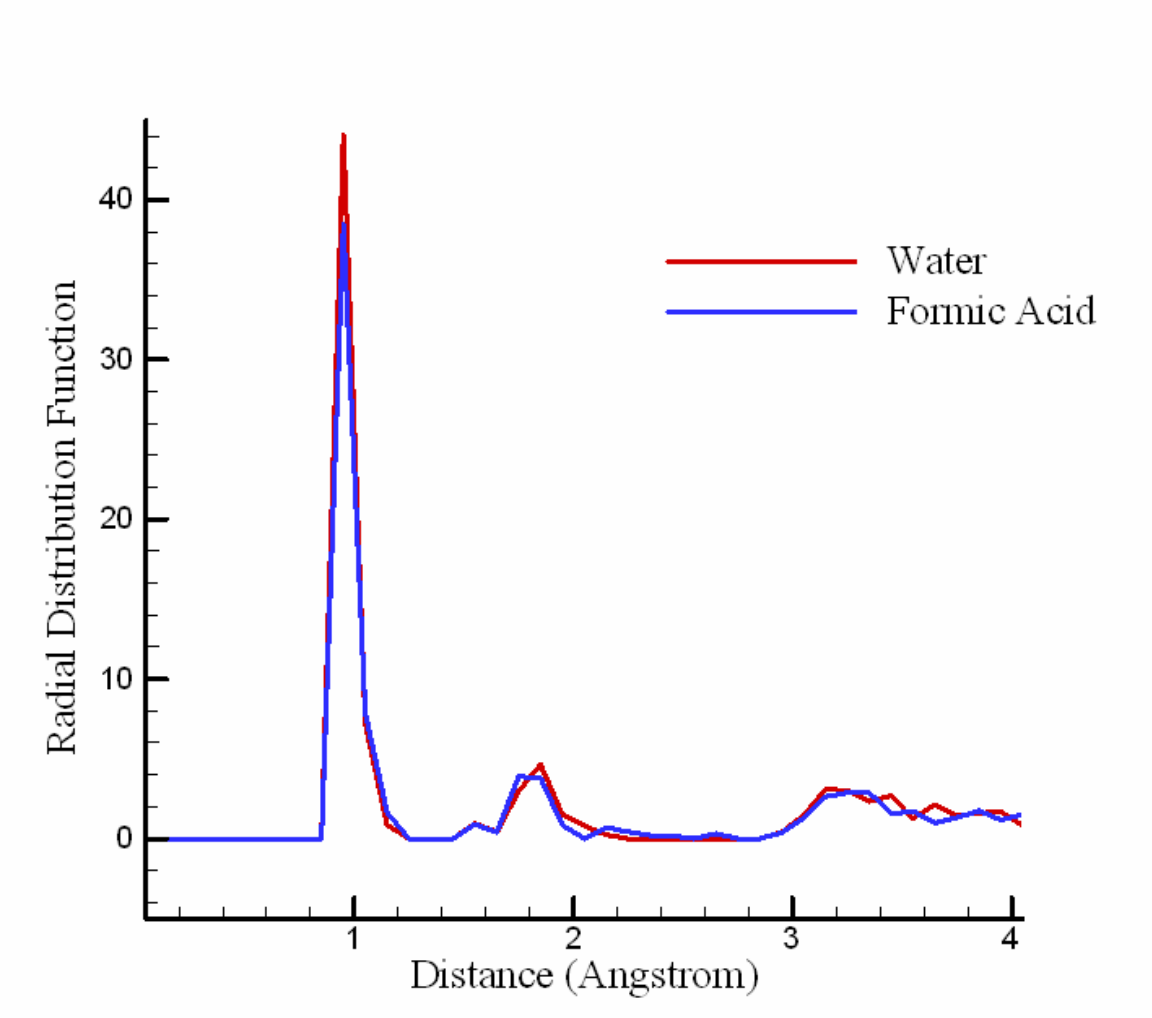

Figure **4.10.a**: Radial Distribution Functions of pure water (red) and formic acid-water (blue) 21 molecule clusters. The first peak represents the hydrogen molecules bound to the central oxygen. The second peak represents the first layer of hydrogen bonds, while the third peak represents the second layer of hydrogen bonds.

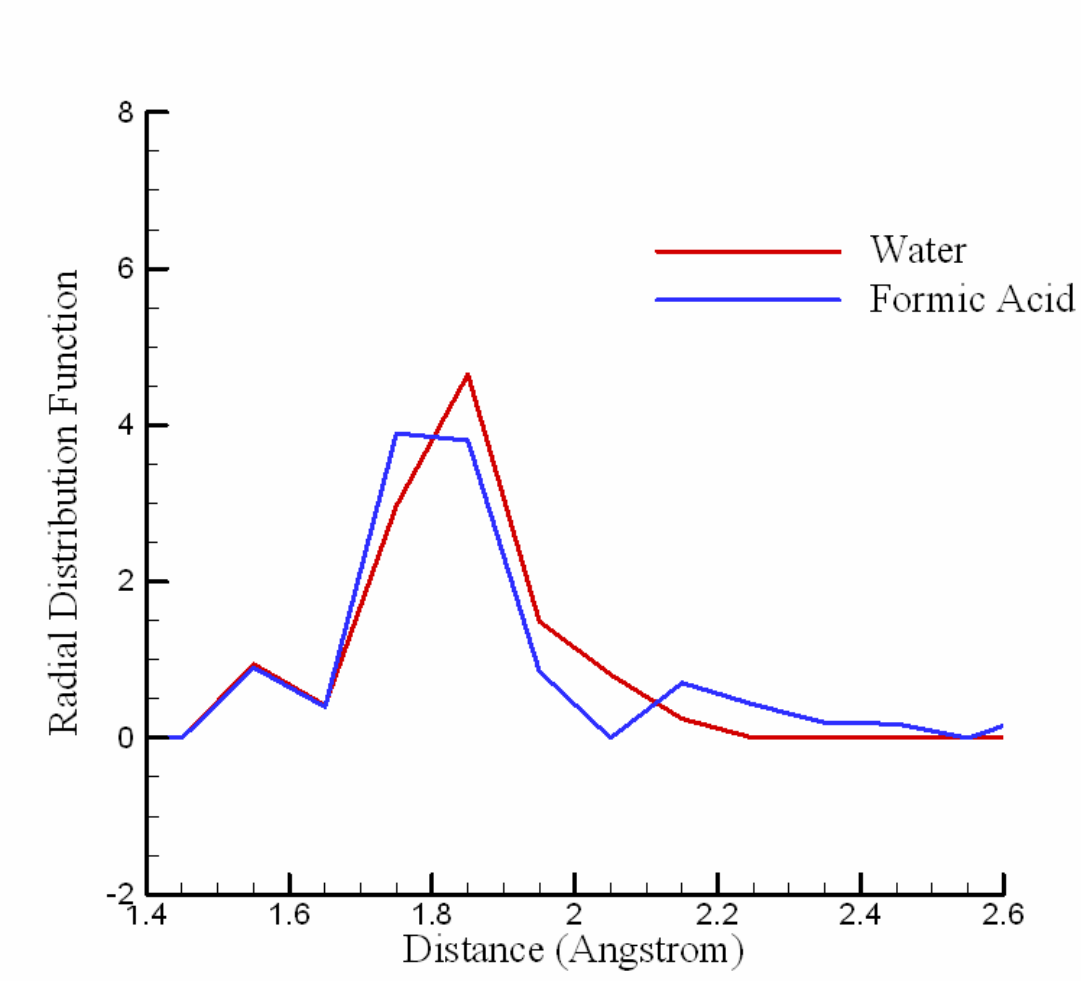

Figure **4.10.b**: Zoomed-in view of RDF near hydrogen bonding region.

that a molecule would evaporate off of the clusters. Methanol evaporated off of the methanol-water molecule at ~160 K. A water molecule evaporated off of the pure water cluster at ~270K. A water molecule evaporated off of the formic acid-water cluster at ~278K. The methanol is clearly more weakly bound to the cluster as it evaporates off at a temperature range of 100K lower than the other two clusters. This weak interaction could explain why methanol-water clusters maintain the hydrogen bonding network of pure water with little structural change. The difference in evaporation temperature between the pure water and the formic acid-water clusters is within the uncertainty of the MD-simulation. However, the fact that a water molecule evaporates off of the formic acid-water mixed cluster rather than the formic acid is a significant finding and shows that formic acid interacts more strongly with the hydrogen bonding network of the cluster than is the case for pure water.

In light of these evaporation studies, we would like to present a potential theory for the magic character of the water-21 cluster. It is possible, based on the literature of the cluster structure [*Miyazaki et al.*, 2004; *Mizuse et al*., 2007; *Shin et al.*, 2004] which shows a 3-D cage being completed at the 21 molecule cluster, that all smaller water clusters build up to the preferred 3-D structure of the 21 cluster. It is also possible that addition of a single water to the 21-molecule 3-D cage could result in a slightly more weakly-bound water molecule that may easily evaporate off. A second magic cluster is seen at water-28 that is of a much lower intensity; the clusters ranging from 22-27 molecules may undergo both growth and evaporation processes. This would cause the clusters in this size range to both grow up to the 28 molecule cluster and evaporate down to the 21 molecule cluster. Having both a growth and an evaporation mechanism competing with one another supports our classic observations of smaller clusters dominating at higher temperatures, while large clusters dominate at lower temperatures; the lower temperatures would cause the growth mechanism to dominate over the evaporation. In this way, formic acid likely causes the growth mechanism to dominate at higher temperatures by making it easier to

add water molecules to the hydrogen bonding network and expanding the stability of the 3-D cage. It is also possible that formic acid-water mixed clusters have a magic cluster at a size that is too large for us to observe in our flow tube. Additionally, if this magic cluster size is above the critical radius for nucleation and particle growth, it might not be observed at all.

4.4 Conclusions

Presented in this chapter are computational results that are compared to experimental results from a flow tube apparatus that demonstrate a distinct difference in the reaction of formic acid with water when compared to the reaction of methanol with water. Formic acid is a chemical species of interest in the atmosphere and was compared to methanol as the interaction between methanol and water clusters has been well studied. Because the formic acid-water mixed cluster species had very different spectral characteristics, particularly the loss of the magic 21 molecule cluster, DFT and ReaxFF calculations were performed to determine the structural changes caused by the integration of either a methanol molecule or a formic acid molecule into the water cluster.

We performed DFT calculations which were compared to those in the prior literature. Our calculations for pure water clusters of up to four molecules as well as water clusters with one formic acid of sizes up to four molecules matched those reported in the literature. We also performed calculations on clusters of the same size with methanol incorporated into the cluster cage. It was determined that while methanol affected the water-water hydrogen bond lengths in these small neutral clusters to a small degree, this change was not to the same extent as seen in the formic acid case. Additionally it was hypothesized that formic acid can induce a slight dipole in the neutral clusters, causing them to have a slightly positive side and a slightly negative side—both of which could act as selective sites for further addition of water molecules to the cluster. In

addition to these selective sites, formic acid has more potential sites for new hydrogen bonds than either water or methanol. Methanol can form hydrogen bonds at the two lone pairs of electrons on the oxygen and at the hydrogen of the O-H group, a total of three potential hydrogen bonds. A water molecule has two O-H groups as well as the two lone pairs, a total of four potential hydrogen bonds. Formic acid, however, has two oxygen molecules and thus four lone pairs of electrons to act as hydrogen bond acceptors and one O-H group to act as a hydrogen bond donor, for a total of five potential hydrogen bonds. The increased number of hydrogen bonding sites as well as the selective sites caused by the induced dipole contribute to the increased growth observed in the flow tube reactions of formic-acid mixed clusters over pure water and methanol.

ReaxFF calculations were used to determine the most stable structure for the pure water, methanol, and formic acid cluster systems for the range in cluster sizes encompassing the magic 21 cluster. The optimized structures show that formic acid interacts with the hydrogen bonding network of the water cluster in multiple places, thus causing a structural change that is not observed with methanol. The ReaxFF calculations showed that while pure water clusters and methanol-water mixed clusters exhibit a peak in binding energy per molecule at 21 molecules, formic acid does not. In addition, the formic acid-water mixed clusters had a higher overall binding energy per molecule, indicating that they are more stable than the other two systems. We conclude that the change to the hydrogen bonding network caused by the formic acid molecule stabilizes the water clusters as indicated by the increased binding energy. This increased stability based on binding energy, the increase in the number of potential sites for hydrogen bonding by adding a formic acid to the cluster, and the strength of the association of formic acid with the hydrogen bonding network are all likely to lead to enhanced growth of the water clusters resulting in nucleation of water molecules at higher temperatures than seen for pure water and increased potential for particle growth in the atmosphere.

4.5 References

Aloisio, S., P. Hintze, and V. Vaida (2002), The Hydration of Formic Acid, *J. Phys. Chem.*, *106*, 363-370, doi:10.1021/jp0121901.

Castleman, A.W. Jr., P. Holland, and R. Keesee (1978), The properties of ion clusters and their relationship to heteromolecular nucleation, *J. Chem. Phys., 68*, 1760-1764, doi:10.1063/1.435946.

Chenoweth, K., A.C.T. van Duin, and W.A. Goddard III (2008), ReaxFF Reactive Force Field for Molecular Dynamics Simulations of Hydrocarbon Oxidation, *J. Phys Chem. A*, *112*, 1040-1053, doi:10.1021/jp709896w.

Chenoweth, K., A.C.T. van Duin, P. Persson, M.J. Cheng, J. Oxgaard, and W.A. Goddard III (2008), Development and Application of a ReaxFF Reactive Force Field for Oxidative Dehydrogenation on Vanadium Oxide Catalysts, *J. Phys. Chem. C*, *112*, 14645-14654, doi:10.1021/jp802134x.

Cheung, S., W. Deng, A.C.T. van Duin, and W.A. Goddard III (2005), $ReaxFF_{MgH}$ Reactive Force Field for Magnesium Hydride Systems, *J. Phys. Chem. A*, *109*, 851-859, doi:10.1021/jp0460184.

Gaussian 03, Revision C.02, Frisch, M. J.; Trucks, G. W.; Schlegel, H. B.; Scuseria, G. E.; Robb, M. A.; Cheeseman, J. R.; Montgomery, Jr., J. A.; Vreven, T.; Kudin, K. N.; Burant, J. C.; Millam, J. M.; Iyengar, S. S.; Tomasi, J.; Barone, V.; Mennucci, B.; Cossi, M.; Scalmani, G.; Rega, N.; Petersson, G. A.; Nakatsuji, H.; Hada, M.; Ehara, M.; Toyota, K.; Fukuda, R.; Hasegawa, J.; Ishida, M.; Nakajima, T.; Honda, Y.; Kitao, O.; Nakai, H.; Klene, M.; Li, X.; Knox, J. E.; Hratchian, H. P.; Cross, J. B.; Bakken, V.; Adamo, C.; Jaramillo, J.; Gomperts, R.; Stratmann, R. E.; Yazyev, O.; Austin, A. J.; Cammi, R.; Pomelli, C.; Ochterski, J. W.; Ayala, P. Y.; Morokuma, K.; Voth, G. A.; Salvador, P.; Dannenberg, J. J.; Zakrzewski, V. G.; Dapprich, S.; Daniels, A. D.; Strain, M. C.; Farkas, O.; Malick, D. K.; Rabuck, A. D.; Raghavachari, K.; Foresman, J. B.; Ortiz, J. V.; Cui, Q.; Baboul, A. G.; Clifford, S.; Cioslowski, J.; Stefanov, B. B.; Liu, G.; Liashenko, A.; Piskorz, P.; Komaromi, I.; Martin, R. L.; Fox, D. J.; Keith, T.; Al-Laham, M. A.; Peng, C. Y.; Nanayakkara, A.; Challacombe, M.; Gill, P. M. W.; Johnson, B.; Chen, W.; Wong, M. W.; Gonzalez, C.; and Pople, J. A.; Gaussian, Inc., Wallingford CT, 2004.

Gilligan, J. and A.W. Castleman, Jr. (2001), Acid Dissolution by Aqueous Surfaces and Ice: Insights from a Study of Water Cluster Ions, *J. Phys. Chem. A.*, *105*, 5601-5605, doi:10.1021/jp003480p.

Goken, E.G. and A.W. Castleman, Jr. (2010) Reactions of formic acid with protonated water clusters: Implications of cluster growth in the atmosphere, *J. Geophys. Res.-Atmos.* (in press).

Hurtmans, D., F. Herregodts, M. Herman, J. Lievin, A. Campargue, A. Garnache, and A.A. Kachanov (2000), Spectroscopic and ab initio investigation of the vOH overtone excitation in trans-formic acid, *J.Chem.Phys.*, *113*, 1535-1545, doi:10/1063/1.481939.

Järvi, T.T., A. Kuronen, M. Hakala, K. Nordlund, A.C.T. van Duin, W.A. Goddard III, and T. Jacob (2008), Development of a ReaxFF description for gold, *Eur. J. Phys. B*, *66*(1), 75-79, doi:10.1140/epjb/e2008-00378-3.

Miyazaki, M., A. Fujii, T. Ebata, and N. Mikami (2004), Infrared Spectroscopic Evidence for Protonated Water Clusters Forming Nanoscale Cages, *Science*, *304*, 1134-1137, doi:10.1126/science.1096037.

Mizuse, K., A. Fujii, and N. Mikami (2007), Long range influence of an excess proton on the architecture of the hydrogen bond network in large-sized water clusters, *J. Chem. Phys.*, *126*, 231101, doi:10.1063/1.2750669.

Nadykto, A., and F. Yu (2007), Strong hydrogen bonding between atmospheric nucleation precursors and common organics, *Chem. Phys. Let.*, *435*, 14-18, doi:10.1016/j.cplett.2006.12.050.

Nagashima, U., H. Shinohara, N. Nishi, and H. Tanaka (1986), Enhanced stability of ion-clathrate structures for magic number water clusters, *J. Chem. Phys.*, *84*, 209-214, doi:10.1063/1.450172.

Nielson, K.D, A.C.T. van Duin, J. Oxgaard, W.Q. Deng, and W.A. Goddard III (2005), Development of the ReaxFF Reactive Force Field for Describing Transition Metal Catalyzed Reactions, with Application to the Initial Stages of the Catalytic Formation of Carbon Nanotubes, *J. Phys. Chem. A*, *109*, 493-499, doi:10/1021/jp046244d.

Ojwang, J.G.O., R. van Santen, G.J. Kramer, A.C.T. van Duin, and W.A. Goddard III (2008), Predictions of melting, crystallization, and local atomic arrangements of aluminum clusters using a reactive force field, *J. Chem. Phys.*, *129*, 244506, doi:10.1063/1.3050278.

Rablen, P.R., J.W. Lockman, and W.L. Jorgensen (1998), Ab Initio Study of Hydrogen-Bonded Complexes of Small Organic Molecules with Water, *J. Phys. Chem. A*, *102*, 3782-3797, doi:10.1021/jp980708o.

Searcy, J.Q., and J.B. Fenn (1974), Clustering of water on hydrated protons in a supersonic free jet expansion, *J. Chem. Phys.*, *61*, 5282-5288, doi:10.1063/1.1681876.

Shin, J.-W., N. Hammer, E. Diken, M. Johnson, R. Walters, T. Jaeger, M. Duncan, R. Christie, and K. Jordan (2004), Infrared signature of structures associated with the $H^+(H_2O)_n$, n=6-27, clusters, *Science*, *304*, 1137-1140, doi:10.1002/chin.200431007.

Suhara, K., A. Fujii, K. Mizuse, N. Mikami, and J. Kuo (2007), Compatibility between methanol and water in the three-dimensional cage formation of large-sized protonated methanol-water mixed clusters, *J. Chem. Phys.*, *126*, 194306, doi:10.1063/1.2734969.

van Duin, A.C.T., S. Dasgupta, F. Lorant, and W.A. Goddard III (2001) ReaxFF: A Reactive Force Field for Hydrocarbons, *J. Phys. Chem. A*, *105*, 9396-9409, doi:10.1021/jp004368u.

van Duin, A.C.T., A. Strachen, S. Stewman, Q. Zhang, X. Xu, and W.A. Goddard III (2003), $ReaxFF_{SiO}$ Reactive Force Field for Silicon and Silicon Oxide Systems, *J. Phys. Chem. A, 107*, 3803-3811, doi:10.1021/jp0276303.

Zhang, X. and A.W. Castleman, Jr. (1994), Evidence for the formation of clathrate structures of protonated water-methanol clusters at thermal energy, *J. Chem. Phys.*, *101*, 1157-1164, doi:10.1063/1.467809.

Zhang, X., E. Mereand, and A.W. Castleman, Jr. (1994), Reactions of Water Cluster Ions with Nitric Acid, *J. Phys. Chem.*, *98*, 3554-3557, doi:10.1021/j100064a044.

Chapter 5

The products of bromoform degradation and their solvation in water

5.1 Introduction

Halogens are of particular interest in the study of atmospheric chemistry because of their high reactivity. Chlorofluorocarbons as well as other halogen-containing species have been shown to destroy ozone in the upper stratosphere, and have been strongly linked to destruction of the ozone layer [*Finlayson-Pitts and Pitts*, 2000]. While the use of CFCs in such products as refrigerants has been restricted, the levels of halogen species in the atmosphere remain high [*Salawitch*, 2006]. The determination of other sources of these halogen species, and the mechanisms involved in atmospheric halogen chemistry, remains a critical scientific need.

Release of halogens from sea salt aerosols is one hypothesized source contributing to halogens in both the troposphere and potentially the stratosphere [*Quack et al.*, 2004; *Sinnhuber and Folkins*, 2006]. Ocean water contains many ionic species which include chlorine, bromine, and iodine in various forms. While the concentration of chlorine is significantly higher in ocean water, bromine and iodine released from sea salt aerosols are both highly active in the atmosphere [*von Glasow*, 2008]. Halogens in the atmospheric layer just above the oceans, called the marine boundary layer, come not only from the release of ionic species from ocean water but also from organic products released by marine algae [*Herrmann et al.*, 2003; *Read et al.*, 2008; *Salawitch*, 2006]. While these sources of halogens are known, current methods of studying the atmosphere are unable to directly attribute how halogens released in the marine boundary layer affect other layers of the atmosphere.

Flow tube studies of water clusters reacting with chemicals of atmospheric significance

have been shown to provide an accurate method for determining reactions of importance in the atmosphere [*Gilligan and Castleman*, 2001a; *Gilligan and Castleman*, 2001b; *Goken and Castleman*, in press; *Zhang et al*., 1994]. Water clusters can be used as a model system for how a specific chemical might react with water in the atmosphere under varying conditions. The flow-tube method employed in this chapter permits detailed study of a chemical species of interest at specific temperatures and specific pressures. The pressures in the flow-tube can be equated to chemical concentrations in order to better mimic various locations in the atmosphere of Earth. In this way, we can study how a chemical would interact with water at levels of the atmosphere ranging from ocean level to the upper stratosphere. These experimental results help to paint a more complete picture of how a molecule might react at varying points in the atmosphere and provide a basis for determining how molecule migration may occur.

Bromoform, $CHBr_3$, is one of many bromocarbon species that are produced by algae in tropical oceans. It is known to decompose in the troposphere before reaching the upper regions of the troposphere and the lower regions of the stratosphere [*Quack and Wallace*, 2003; *Sinnhuber and Folkins*, 2006; *Yokouchi et al.*, 2005]. Because it easily decomposes at lower atmospheric levels, it is a constant source of bromine ions in the global troposphere. In this chapter we present experimental results that describe the decomposition of bromoform into both the anionic and cationic states. Additionally, we obtain important information about the solvation of the gaseous decomposition products by water clusters at various temperatures and pressures of bromoform. Understanding solvation processes of chemicals in the atmosphere leads us to a description of how some molecules can move throughout the atmosphere intact while others decompose rapidly. We seek to interpret our results in terms of the larger picture of the atmosphere, namely how this organic source of halogens creates active halogen species in the troposphere as well as in other atmospheric regions.

5.2 Experimental Methods

The basic instrumental methods used to obtain the data presented in this chapter are outlined in Chapter 2 of this dissertation. However, one major change was made. The bromoform liquid was placed in the specialized glass bubbler described in Figure 2.3, but instead of being connected to the RGI, bromoform vapor (seeded in helium) was added through the source inlet. In this way, the halogens released during the breakdown of $CHBr_3$ were ionized and an adequate amount of OH^- ions were created. These conditions better mimic how halogens are released and react in the troposphere and specifically the marine boundary layer, namely a free halogen ion that has been released from a sea salt aerosol will encounter single water molecules or very small clusters. In this way the solvation shell forms around the ionic halogen core rather than associating with a large water cluster.

5.3 Results and Discussion

These flow tube studies of bromoform found that the organic source of halogens readily formed the anions of BrO^-, $HBrO^-$, and Br_2^-. (As BrO^- and $BrOH^-$ are in equilibrium with one another through a reaction with water and OH^- and because they only differ in mass by one atomic mass unit, it is impossible to refer to one species without also including the other. For ease of explanation we will refer only to BrO^- species [*Finlayson-Pitts and Pitts*, 2000].) Br_2O^- was also observed, but only at very low temperatures, below 140 K. Very small amounts of BrO_2^- are also observed [*Lee*, 1995; *Lee et al.*, 1995]. The appearance of these anions indicates that the breakdown of the anionic bromoform molecules occurs quickly and that the reactivity of the released inorganic halogen species is extremely high.

Under room temperature conditions with no water present in the flow tube, we observed

the breakdown of $CHBr_3$ into the following cationic species: $CHBr_2^+$, $CHBr^+$, and Br_2^+. Based on these flow tube results, the ionic organic molecules are shown to be stable upon the release of Br and Br_2 radicals and/or ions that were observed in the anionic experiments. Br ions are known to react readily with OH^- ions and water molecules in the atmosphere to form inorganic bromine, BrO^- and BrOH, explaining the presence of these molecules in the anionic spectra [*McKinney et al.*, 1997; *Martinez-Aviles et al.*, 2007]. These molecules are highly soluble in water, in contrast to bromoform, which is only slightly soluble [*Lide*, 1997]. Reactions 5.1 – 5.5 below show a few typical reactions by which such halogen ions form under atmospheric conditions. The measured rates of formation are all sufficiently fast enough that we would see these ions in our flow-tube experiments [*Finlayson-Pitts and Pitts*, 2000]. BrO and BrOH and their ions are of particular interest as atmospheric species because of their roles in chlorine chemistry for the release of halogens in the atmosphere as shown in the example reactions 5.6 and 5.7 as well as ozone chemistry [*McKinney et al.*, 1997; *Wahner and Schiller*, 1992].

$$Br^- + O_3 \rightarrow BrO^- + O_2 \quad (5.1)$$

$$BrO^- + H^+ \leftrightarrow HOBr \quad (5.2)$$

$$Br^- + OH \rightarrow HOBr^- \quad (5.3)$$

$$Br + H_2O \rightarrow HOBr^- + H^+ \quad (5.4)$$

$$Br + Br^- \rightarrow Br_2^- \quad (5.5)$$

$$BrO + ClO \rightarrow BrCl + O_2 \quad (5.6)$$

$$HOBr + HCl \rightarrow BrCl + H_2O \quad (5.7)$$

5.3.1 Temperature Study

Flow tube measurements were evaluated at various temperatures to determine the effect of temperature on the solvation of two halogen-containing species that were created upon

breakdown of $CHBr_3$: $BrO(H_2O)_n^-$ and $Br_2(H_2O)_n^-$. The study was performed at a range of temperatures from 143 to 186 K (-129 to -87 °C). At lower temperatures, both species exhibit the formation of larger mass clusters, but the large clusters were not detected at higher temperatures. At temperatures above ~150 K (-125 °C), water molecules tend to form smaller clusters due to the instability of the hydrogen bonding network, so it is reasonable that larger solvated clusters would not be seen under these conditions as seen in Figures **5.1** and **5.2**.

An interesting pattern emerges in the cluster formation in the low temperature data sets, below 150 K (-125 °C). For $Br_2(H_2O)_n^-$ a distinct decrease is seen in the cluster intensity for clusters after the $n = 4$ cluster, and again for intensities of clusters after the $n = 10$ cluster. These features can be seen in Figure **5.2** and more clearly in Figure **5.3** where the intensity ratios are compared. Intensity ratios were obtained using Equation 3.1, described in Chapter 3. Figure **5.3** appears to also display a peak in intensity ratio at the $n = 7$ cluster; however this peak does not have the same pattern across all of the temperatures studied. Also, the spectral intensities do not suggest that this cluster stands out based on mass spectral abundance. Figure **5.4** shows a sample mass spectrum of the bromoform-water reaction; it is clear in this spectrum that only the $n = 4$ and 10 clusters display a distinct discontinuity in the otherwise smoothly varying distribution. Therefore, the $n = 7$ cluster will not be considered to be magic for these experiments because it does not fit both the requirements of spectral abundance and intensity ratio as described in Chapter 3. However, the peaks observed with addition of three waters, from 4 to 7 to 10, for Br_2^- does warrant further examination.

The consistency of the pattern of mass spectral abundance and a peak in the intensity ratios for the clusters of $n = 4$ and $n = 10$ across all temperatures where clusters of these sizes are observed, along with the intensity ratios seen here, indicate that $Br_2(H_2O)_4^-$ and $Br_2(H_2O)_{10}^-$ are of particular interest and possible magic character. The most likely explanation for the magic character is the complete filling of solvation shells of the Br_2^- molecule. The first solvation shell

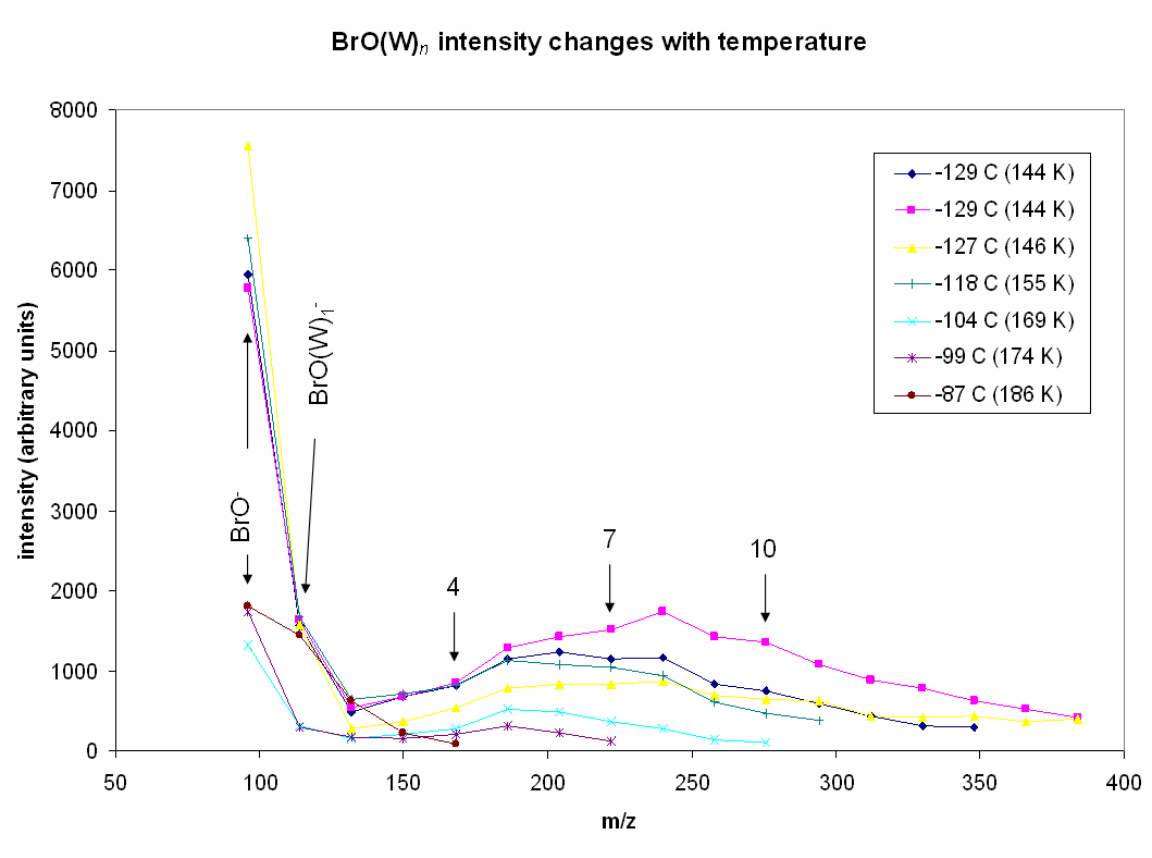

Figure **5.1**: The intensities of $BrO(W)_n^-$ clusters from temperatures ranging from -87 °C to -129 °C . Larger clusters are observed only at lower temperatures. Duplicate runs were performed at -129 °C. The first species, BrO^-, and the first species with one water, $BrO(W)_1^-$ are labeled. The subsequent labels (4, 7, and 10) refer to the number of waters surrounding BrO^-.

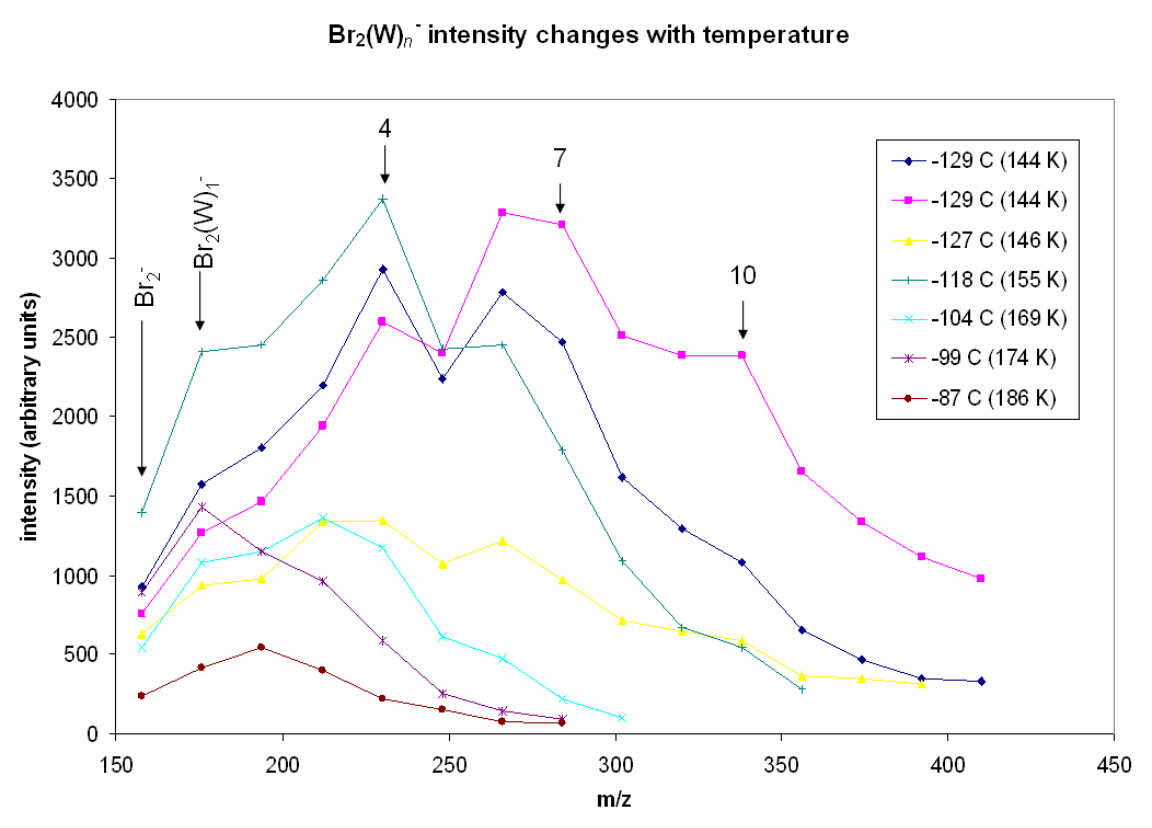

Figure **5.2**: Changes in cluster intensity for $Br_2(W)_n^-$ clusters over the temperature range of -87 °C to -129 °C. Duplicate runs were performed at -129 °C. The first species, Br_2^-, and the species with one water, $Br_2(W)_1^-$, are labeled. The subsequent labels (4, 7, and 10) refer to the number of waters surrounding Br_2^-.

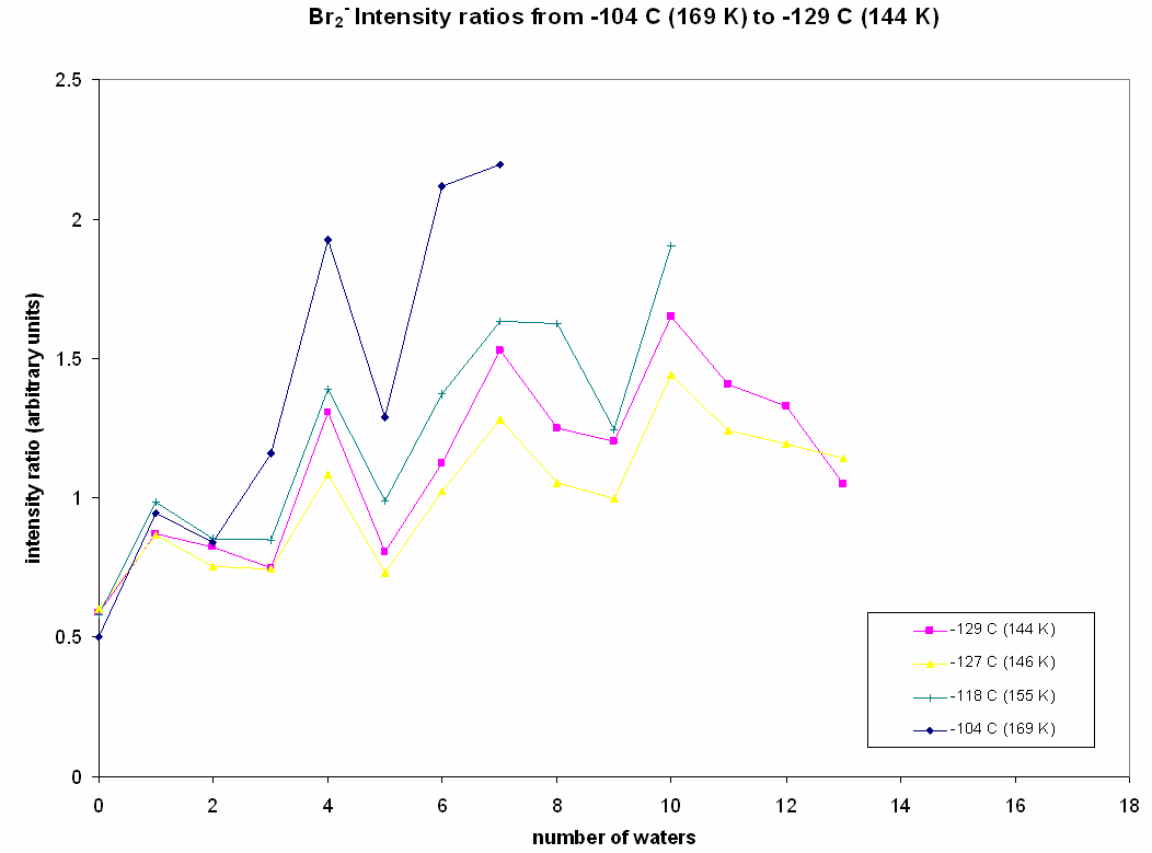

Figure **5.3**: $Br_2(W)_n^-$ intensity ratios are shown for the lower temperature range. A distinct peak for both n = 4 and n = 10 cluster is observed, indicating magic character. Because the pattern for the n = 7 cluster is not consistent it is not considered magic for these experiments.

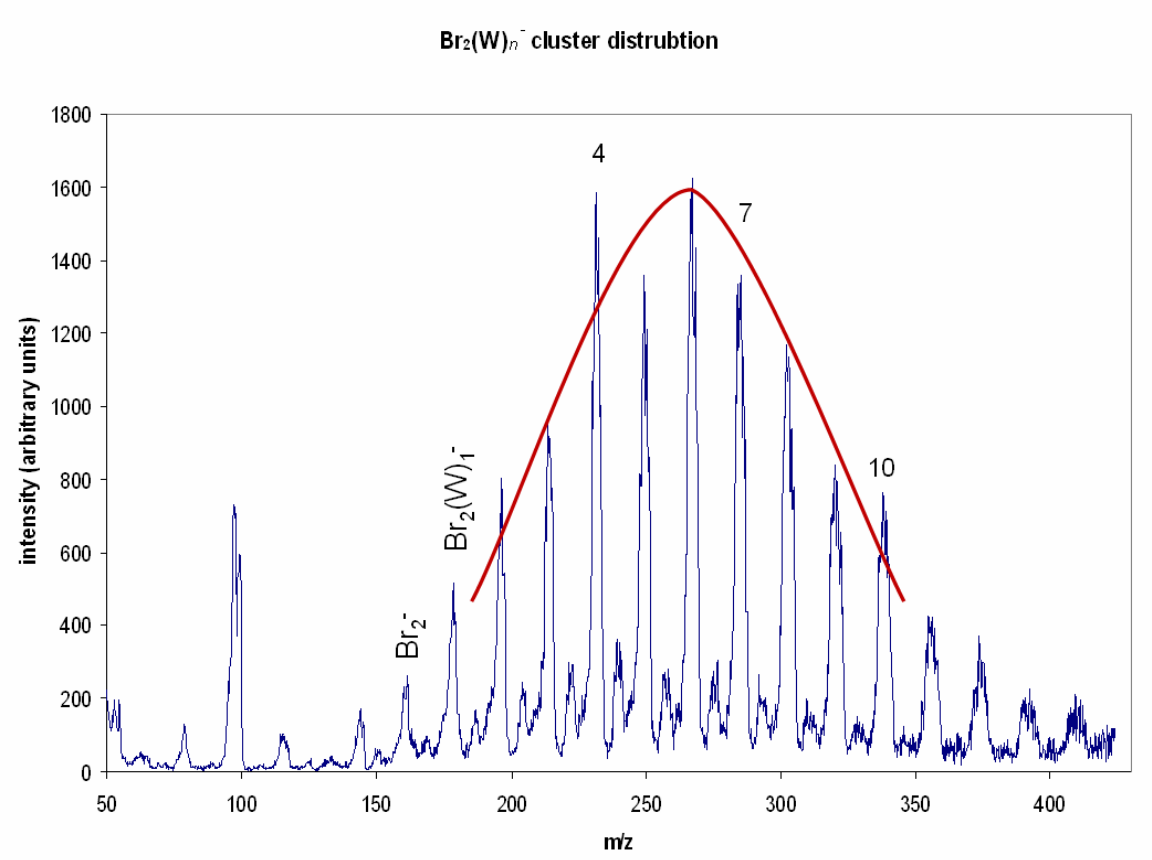

Figure **5.4**: Mass spectrum of the solvated products of the reaction of bromoform with water at -117 ^{o}C (156 K). The curve on the spectrum is a rough estimate of what the shape of a smoothly varying distribution would look like; it is clear that the clusters $Br_2(H_2O)_4^-$ and $Br_2(H_2O)_{10}^-$ stand out from the distribution. The initial species Br_2^- and the species with one water, $Br_2(W)_1^-$, are labeled. The subsequent labels (4, 8, and 10) refer to the number of waters surrounding Br_2^-.

contains four waters and the second contains six waters. This is consistent with prior work on hydration of halide ions, for which data suggests that four water molecules form a pyramidal structure with three waters forming a ring on one side of the ion and a fourth water sitting on the opposite side of the ion [*Ayotte et al.*, 1999; *Cabarcos et al.*, 1999]. It has also been suggested that the uneven solvation cage could arise from the polarizability of the halogen ions [*Cabarcos et al*., 1999]. Based on these previous structural studies and other solvation shell studies, we hypothesize that the four-water solvation shell of Br_2^- would resemble that found for the superoxide tetrahydrate: the Br_2^- molecule would sit between two hydrogen bonded pairs of water [*Weber et al.*, 2000]. In addition, this provides an explanation for the abrupt dip in intensity and intensity ratio at $n = 5$; if the fifth water attached to the cluster is the first water of a new solvation shell it is likely to either evaporate from the cluster to return to the structure of a full solvation shell or the sixth water quickly adds to the cluster. Again, it is hypothesized that the solvation mechanism is addition of a loosely bound water pair, meaning that the $n = 6$ cluster would me much more likely than the $n = 5$, which is observed in Figure **5.2**.

5.3.2 Pressure Study

A study to determine the effect of varying bromoform pressure was also conducted on the anionic products of bromoform deterioration. BrO^-, Br_2^-, and Br_2O^- were all examined at varying bromoform pressures. Two comparative pressure studies were performed, where a spectrum was taken at an initial bromoform pressures and then a subsequent spectrum at a respectively lower bromoform pressure. The total pressure of the flow tube was 0.2935 Torr and 0.2913 Torr for the initial higher bromoform pressure reactions; the pressure of bromoform was then decreased until the total flow tube pressure dropped to 0.2925 Torr and 0.2900 Torr respectively. It was expected that higher flow tube pressures would result in the formation of larger cluster species, which is a

typical result when pressure is increased. However, for all three species, solvated clusters form at higher intensities for lower experimental bromoform pressures as seen in Figures **5.5**, **5.6**, and **5.7**. Clusters of larger mass form more readily for the spectra containing lower pressures of bromoform. The primary explanation for such an occurrence is that the higher relative pressure of water, caused by the decrease in the bromoform pressure, causes water to solvate on the clusters more readily.

In addition, this pressure study demonstrates a unique pattern created by the pressure dependence of the cluster formation. The $BrO(H_2O)_n^-$ clusters represented in Figure **5.5** show that the formation of the clusters where n = 1-7 have roughly the same intensity levels at both low and high pressures of bromoform. However, as the relative water pressure is increased, a divergence of intensity for larger clusters is observed at 8 waters. This divergence is consistent in the data sets for both $Br_2(H_2O)_n^-$ and for $Br_2O(H_2O)_n^-$ shown in Figures **5.6** and **5.7**, indicating a common and important trend. A cluster of this size is particularly interesting as previous studies in our group have shown the uptake of an HBr by protonated water clusters occurs at 7 water molecules [*Gilligan and Castleman*, 2001a]. At higher relative water pressures, the clusters show a propensity to add additional waters. This is likely caused by the ions being completely solvated by water, meaning that additional waters add more readily to the existing hydrogen bonding network and are less affected by the ionic core of the cluster [*Kropman and Bakker*, 2001; *Laage and Hynes*, 2007].

Additional studies were performed on the cationic clusters of the degradation products of bromoform with water. However, these products were found to be primarily hydrocarbon variations of CHBr, which have low relevance to active atmospheric processes. The data from the cationic studies will be presented along with a brief discussion in the Appendix.

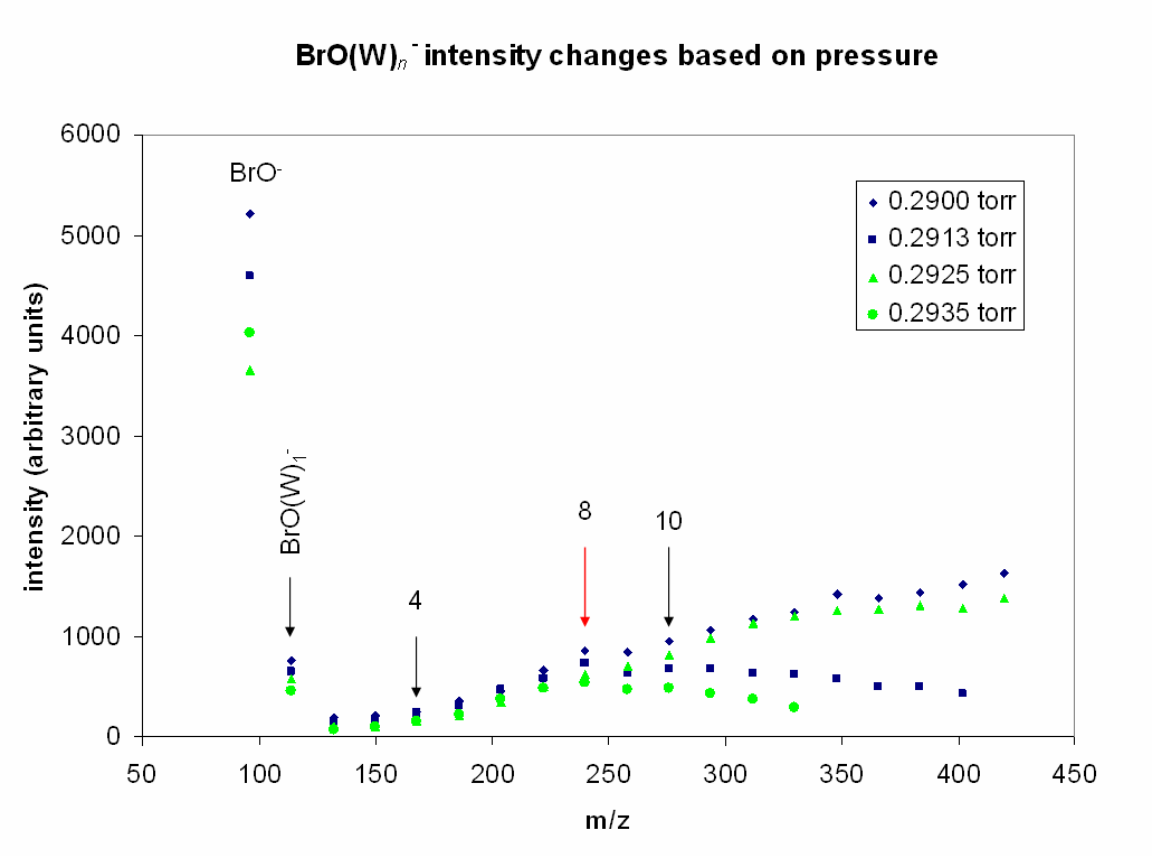

Figure **5.5**: Intensity changes resulting from changes in relative bromoform and water pressures for $BrO(W)_n^-$. A divergence of cluster growth appears in all cases at the addition of 8 water molecules at a higher relative pressure of water. The initial species BrO^- and the species with one water, $BrO(W)_1^-$, are labeled. The subsequent labels (4, 8, and 10) refer to the number of waters surrounding BrO^-.

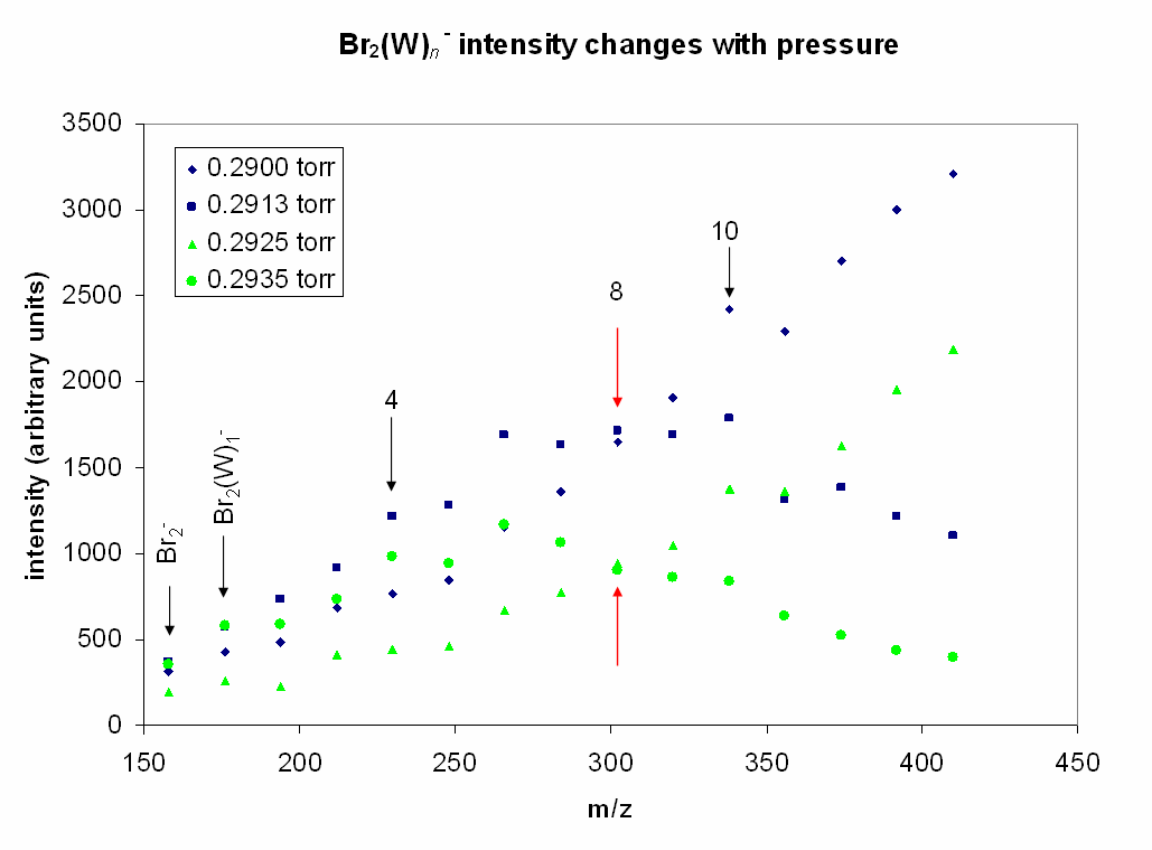

Figure **5.6**: Intensity changes resulting from changes in relative bromoform and water pressures for $Br_2(W)_n^-$. A divergence of cluster growth appears in all cases at the addition of 8 water molecules at a higher relative pressure of water. The initial species Br_2^- and the species with one water, $Br_2(W)_1^-$, are labeled. The subsequent labels (4, 8, and 10) refer to the number of waters surrounding Br_2^-.

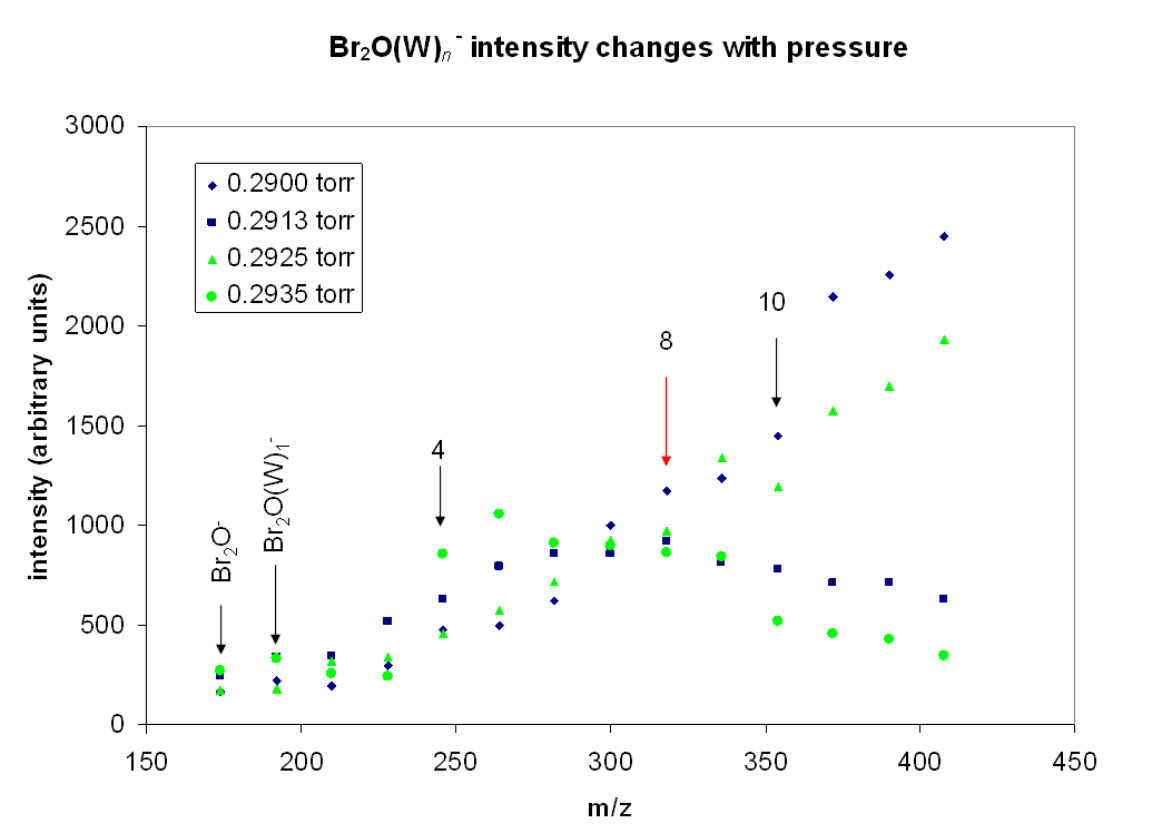

Figure **5.7**: Intensity changes resulting from changes in relative bromoform and water pressures for $Br_2O(W)_n^-$. A divergence of cluster growth appears in all cases at the addition of 8 water molecules at a higher relative pressure of water. The initial species Br_2O^- and the species with one water, $Br_2O(W)_1^-$, are labeled. The subsequent labels (4, 8, and 10) refer to the number of waters surrounding Br_2O^-.

5.4 Conclusions

The experimental results presented in this chapter provide insight into the ways by which bromoform and its derivatives can affect the global concentrations of halogens in the atmosphere. $CHBr_3$ breaks down easily into smaller anionic and cationic fragments which are of varying stability. The main cationic species are direct fragmentations of the organic molecule with the release of bromine ions: $CHBr_2^+$, $CHBr^+$, and much smaller amounts of Br_2^+ and Br^+. The anionic species created during the ionization of bromoform in the presence of water are predominately Br_2^- and BrO^- /$BrOH^-$ (which is the product of Br_2 and H_2O). Very small amounts of BrO_2^- are observed solvated with water, but this was not observed to solvate to larger cluster sizes. In addition, Br_2O^- is observed at lesser intensities for particular pressures of bromoform.

As stated earlier, the cationic species react with water in the flow tube to produce chemical species that are not of great atmospheric interest; therefore we will focus on the discussion of the anionic products. Solvated cluster distributions of $BrO(H_2O)_n^-$ and $Br_2(H_2O)_n^-$ were observed at temperatures ranging from -87^o C to -129^o C. Clusters of large mass were only observed at the lower end of the temperature range; this matches the typical characteristics of formation of water clusters, which form in large sizes only at low temperatures, as shown previously in Figure 3.1 of this dissertation. Such a cluster formation process indicates that the water has a stronger contribution than the specific ion species to the solvation process of these ions at varying temperatures. However, as only small solvated clusters are observed at temperatures above -100^o C, it is unlikely that these ions would survive long enough in the atmosphere to reach the temperatures necessary to form the highly solvated ion clusters.

The pressure study of $BrO(H_2O)_n^-$, $Br_2(H_2O)_n^-$, and $Br_2O(H_2O)_n^-$ reveals a divergence in cluster growth at a particular cluster size based on the relative pressures of bromoform and water. At n = 8 the clusters formed under a higher relative bromoform pressure tend to produce fewer

large clusters. However, as the relative pressure of water is increased, the larger clusters ($n = \leq 8$) are observed at significantly higher intensities. From an atmospheric standpoint, this indicates that the solvation of the halogen ions occurs more readily in regions of the atmosphere with higher levels of water vapor. This could include the marine boundary layer, particularly in the more humid parts of the globe.

The temperature study of $Br_2(H_2O)_n^-$ revealed an interesting aspect of the solvation of Br_2^-. Distinct magic peaks were observed for the $n = 4$ and 10 clusters with a drop in intensity for the $n = 5$ and 11 clusters. Such a pattern suggests that four water molecules form the first solvation shell of the Br_2^- with an additional six water molecules completing the second solvation shell of the anion. The drop in intensities observed after these magic clusters can be explained by the addition of the first water molecule of the next solvation shell being less structurally or energetically favorable. As a result, the cluster will either evaporate off the water molecule or quickly add the next water in the solvation shell. Adding two water molecules at a time may be more favorable if the initial solvation shell resembles that of the superoxide tetrahydrate, which contains two sets of two water molecules hydrogen bonded to one another on either side of the anion. A cluster structure of this type for $n = 4$ could easily support the addition of three further sets of two water molecules, to create the $n = 10$ solvation shell. It is important to note that in the intensity chart for $Br_2(H_2O)_n^-$ in Figure 5.5, the $n = 12$ cluster is shown to be at a higher intensity than the $n = 11$ cluster, which is not the case in Figure 5.2. This can be explained due to the fact that the relative pressure of bromoform to water was too high in the temperature studies to support the growth of the larger clusters.

Both the temperature and the pressure study of the halogen ions produced by degradation of bromoform indicate that the ability to solvate the ions depends heavily on the water concentration. These halogen ions might be transported throughout the troposphere and lower regions of the stratosphere as solvated ions. As mentioned earlier, once the ion is surrounded by

solvation shells, additional water molecules are more likely to react to the hydrogen bonding network present around the ionic core than to the ionic core itself. Therefore, the likelihood of these solvated ions migrating from the marine boundary layer over the ocean into the stratosphere depends more on the amount of water present in the atmosphere. For instance, the halogen ions are more likely to encounter a favorable pressure of water necessary for solvation in warmer, more humid areas. However, as they are not observed to solvate at high temperatures, the high pressure of water present in the marine boundary layer could be negated. Therefore we conclude that solvation of halogen ions is not the dominate process that causes migration of free halogens released from sea salt aerosols into the stratosphere. Rather, these halogens are more likely transported into upper regions of the atmosphere through deep convection and as other halogenated complexes.

The flow tube studies presented in this chapter have produced a big picture of how the ions released from the degradation of an organic source of halogens in the atmosphere could react under various atmospheric conditions including varying temperatures and relative pressures. Studies performed using a flow-tube apparatus are faster, simpler to implement, and much less expensive than large-scale direct measurement of chemicals in the atmosphere; thus flow tube studies can be used to mimic atmospheric reactions and to inspire direct measurements of specific chemical species in the atmosphere.

5.5 References

Ayotte, P.; Weddle, G. H.; Johnson, M. A.; (1999) An infrared study of the competition between hydrogen-bond networking and ionic solvation: Halide-dependent distortions of the water trimer in the $X^-(H_2O)_3$, (X = Cl, Br, I) systems. *J. Chem. Phys.* **110**, 7129-7132.

Cabarcos, O. M.; Weinheimer, C. J.; Lisy, J. M.; Xantheas, S. S.; (1999) Microscopic hydration of the fluoride anion. *J. Chem. Phys.* **110**, 5-8.

Castleman, A.W. Jr., and I. Tang (1972), Role of Small Clusters in Nucleation about Ions, *J. Chem. Phys.*, *57*, 3629-3638, doi:10.1063/1.1678819.

Lide, D.R. (1997) *CRC Handbook of Chemistry and Physics, 77th Edition*, Chemical Rubber Company Press: Boca Raton, Florida.

Finlayson-Pitts, B. and J. Pitts, Jr. (2000), *Chemistry of the Upper and Lower Atmosphere,* Academic Press, New York.

Gilligan, J. J.; Castleman, Jr. A. W.; (2001a) Acid Dissolution by Aqueous Surfaces and Ice: Insights from a Study of Water Cluster Ions. *J. Phys. Chem. A* **105**, 5601-5605.

Gilligan, J.J.; Castleman, Jr. A.W.; (2001b) Direct Experimental Evidence for Reactions between Dissolved Acid Halide and Chlorine Nitrate, *J. Phys. Chem. A*, **105**, 1028-1032.

Goken, E.G. and A.W. Castleman, Jr. (2010) Reactions of formic acid with protonated water clusters: Implications of cluster growth in the atmosphere, *J. Geophys. Res. Atmos.* (in press).

Herrmann, H.; Majdik, Z.; Ervens, B.; Weise, D.; (2003) Halogen production from aqueous tropospheric particles, *Chemosphere*, **52**, 485-502.

Kropman, M. F.; Bakker. H. J.; (2001) Dynamics of water molecules in aqueous solvation shells, *Science*, **291**, 2118-2120. DOI:10.1126/science.1058190

Laage, D.; Hynes, J.T.; (2007) Reorientational dynamics of water molecules in anionic hydration shells, *PNAS*, **104**, 11167-11172. DOI: 10.1073/pnas.0701699104

Lee, T.J.; (1995) *Ab Initio* Characterization of Triatomic Bromine Molecules of Potential Interest in Stratospheric Chemistry, *J. Phys. Chem.*, **99**, 15074-15080.

Lee, T.J.; Mejia, C.N.; Beran, G.J.O.; Head-Gordon, M.; (2005) Search for Stratospheric Bromine Reservoir Species: Theoretical Study of the Photostability of Mono-, Tri-, and Pentacoordinated Bromine Compounds, *J. Phys. Chem. A*, **109**, 8133-8139.

McKinney, K.A.; Pierson, J.M.; Toohey, D.W., (1997), A wintertime *in situ* profile of BrO between 17 and 27 km in the arctic vortex, *Geophys. Res. Lett.* **24** 853.

Martinez-Aviles, M.; Rosado-Reyes, C.M.; Fransisco, J.S., (2007) Atmospheric Oxidation Mechanism of Bromoethane, *J. Phys. Chem. A*, **111** (45), 11652–11660. **DOI:** 10.1021/jp073862w

Quack, B.; Wallace, D.W.R.; (2003) Air-sea flux of bromoform: Controls, rates, and implications, *Global Biogeochemical Cycles*, **17**, 1023. DOI: 10.1029/2002GB001890 *Correction published 7 January 2004.

Quack, B.; Atlas, E.; Petrick, G.; Stroud, V.; Schauffler, S.; Wallace, D.W.R.; (2004) Oceanic bromoform sources for the tropical atmosphere, *Geophys. Res. Lett.*, **31**, L23S05. DOI: 10.1029/2004GL020597

Read, K. A. et al. (2008) Extensive halogen-mediated ozone destruction over the tropical Atlantic Ocean, *Nature*, **453**, 1232-1235. DOI: 10.1038/nature07035

Salawitch, R. J. (2006) Biogenic bromine, *Nature,* 439, 275-277.

Sinnhuber, B.-M.; Folkins, I.; (2006) Estimating the contribution of bromoform to stratospheric bromine and its relation to dehydration in the tropical tropopause layer, *Atmos. Chem. Phys.*, **6**, 4755-4761.

von Glasow, R.; (2008) Sun, sea and ozone destruction, *Nature*, **453**, 1195-1196.

Wahner, A.; Schiller, J.; (1992), Twilight variation of vertical column abundances of OclO and BrO in the North polar region, *J. Geophys. Res.* **97(D8)** 8047-8055.

Weber, J. M.; Kelley, J. A.; Nielsen, S. B.; Ayotte, P.; Johnson, M. A.; (2000) Isolating the Spectroscopic Signature of a Hydration Shell With the Use of Clusters: Superoxide Tetrahydrate. *Science*, **287**, 2461. DOI: 10.1126/science.287.5462.2461

Yokouchi, Y. et al.; (2005) Correlations and emission ratios among bromoform, dibromochloromethane, and dibromomethane in the atmosphere, *J. Geophys. Res.*, **110**, D23309. DOI: 10.1029/2005JD006303.

Zhang, X., E. Mereand, and A.W. Castleman, Jr. (1994), Reactions of Water Cluster Ions with Nitric Acid, *J. Phys. Chem.*, *98*, 3554-3557, doi:10.1021/j100064a044.

Chapter 6

Conclusions

6.1 Concluding Remarks

Flow tube studies of organic molecules and their reactions with water clusters have proven to be a productive method for studying molecules of interest in the atmosphere. Cluster research has been useful in many areas of chemistry, and its utility in terms of atmospheric chemistry is highlighted in this dissertation. In particular, examining the reactions of molecules with water clusters helps to enhance the understanding of how gas-phase reactions are related to solvated and liquid-phase chemical reactions.

A description of the experimental apparatus was presented in Chapter 2 of this dissertation. The flow tube instrument was described in detail to serve as a guide for future experimentalists as to how the water clusters are formed and studied. Both cationic and anionic reactions can be examined to gain knowledge about the varying role of a single molecule of interest in the atmosphere. Another advantage of this method is the ability to manipulate pressure, temperature, and chemical species to study reactions under the various conditions that can exist in the atmosphere.

The flow tube experiments on formic acid that are presented in Chapter 3 of this dissertation have shown that formic acid reacts with water clusters in a way that disrupts the existing hydrogen bonding network. The disappearance of the magic 21-molecule cluster in the formic acid-water clusters was in direct contrast with methanol-water mixed clusters which exhibit the magic cluster character. The shape of the experimental distribution was observed to closely resemble the theoretical distribution for a nucleation process. These findings indicate that

while methanol can interact with the hydrogen bonding network with little change to the cluster structure, formic acid significantly alters the structure of the clusters. This structural change leads to a growth in cluster size that is not observed for pure water, meaning formic acid enhances the growth of water clusters and could possibly lead to nucleation of particles in the atmosphere.

Theoretical calculations were performed with our collaborators in order to gain more knowledge on how formic acid affects the structure of water clusters. Chapter 4 demonstrated that formic acid affects the cluster in several ways that promote cluster growth in the mixed clusters over the growth of pure water clusters. First, formic acid interacts more strongly with the hydrogen bonding network by forming multiple hydrogen bonds with the cluster structure; this affects the 3-D structure of the cluster causing the disappearance of the magic 21-molecule cluster. Second, formic acid provides additional potential hydrogen bonding sites on the cluster, increasing the chances of cluster growth. Formic acid has five potential sites for hydrogen bonding compared with water which has four and methanol which has three. In addition, the formic acid causes a slight dipole in the cluster which adds potentially selective sites for hydrogen bond addition to the cluster. Chapters 3 and 4 provide the first direct evidence that formic acid is a chemical species of interest in atmospheric particle growth processes.

Bromoform is a chemical that is believed to be a major source of halogens in the atmosphere, particularly in the marine boundary layer. Results presented in Chapter 5 show that it readily degrades to form halogen ions and oxohalides. These degradation species have been shown to solvate with water; the solvation of the ions has been shown to be more dependent on the pressure of water in the system than the specific ions being solvated. The influence of the ionic core decreases as the amount of solvation increases, meaning the ion only affects the addition of the first few waters while any additional waters attach to the cluster as though it were a pure water cluster. Because of this, the solvation of the ions follows the typical cluster growth patterns shown by pure water clusters after the initial solvation shells form: larger clusters form at

both lower temperatures and at higher pressures of water vapor. While solvated halogen ion clusters do form, they are not shown to be highly stable in sufficient numbers at the conditions of temperature and pressures that would allow such solvated clusters to move from the marine boundary layer in the troposphere into the stratosphere. It is possible that a certain percentage of the ions migrate through the atmosphere as solvated ions, but we do not believe this to be the dominate process that brings halogens released from sea salt aerosols into the stratosphere.

Our instrumental technique allows us to obtain detailed chemical information about such pre-nucleation clusters. With the experimental technique presented, we are able to observe the mechanisms of possible atmospheric reactions with highly specific chemical detail. We believe our instrumental laboratory studies, which gain information on the chemical composition of small clustering species, serve as an excellent companion to direct measurement of atmospheric events by providing more chemical specific detail of the initial (small particle) stages of particle formation events. As we are able to limit our experiments to a few select species and water, we would be able to tell if certain chemicals could or definitely could not contribute to particle growth; this could help focus direct measurement studies since we are able to isolate reactions to gain more detail about the possible particles that are formed. We hope that the data presented in this dissertation will call more attention to small organic acids in the atmosphere and how they can affect atmospheric chemistry, particle growth, nucleation, and cloud formation. As such, further studies of larger carboxylic acids and other organic species that are present in the atmosphere will aid in the understanding of the contribution of organic acids to nucleation and particle formation.

6.2 Future studies

To further compare calculations to the experimental data of formic acid-water mixed clusters, the most stable structures and the binding energies should be determined for the clusters containing multiple formic acid molecules. It is known that methanol can replace up to ten water molecules in the 21 molecule cluster without significant structural change. Also, the experimental data show that addition of 2, 3, 4, and 5 formic acid molecules into the cluster system at higher concentrations of formic acid cause an increase in the proportion of larger water clusters formed. Future studies using ReaxFF calculations could examine if and to what extent the addition of more formic acid molecules increases the stability of the cluster over the pure and the methanol systems. Another interesting calculation that has been proposed to be performed using ReaxFF is to simulate the actual formation of the formic acid-water mixed clusters by simulating the environment inside the flow tube, i.e. cluster growth and collisional stabilization in the presence of the helium carrier gas.

Another set of experiments that could be carried out using ReaxFF and MD simulations would be an extension of the evaporation studies on formic acid, methanol, and water clusters. While we determined at what temperature the first molecule would evaporate off of the 21-molecule clusters, it is likely that there is also a time dependence necessary for release of a molecule. It would be interesting to see how much time is required at the necessary temperatures for a molecule to be removed from the cluster.

Studies of the solvation of Br_2^- should be performed to further probe the magic clusters to determine the solvation shells of the ion. Experimental studies presented in Chapter 5 showed that Br_2^- surrounded by 4 and by 10 waters exhibited magic character. However, there was a potential peak in the intensity ratios for the cluster containing 7 water molecules. Further experiments could help determine if the $n = 7$ cluster plays an important role in the solvation of

the Br_2^- ion. Theoretical calculations could be performed to determine the likely structures of the solvated ion clusters. These calculations could be performed using DFT methods for the smaller clusters and expanded to less computationally expensive methods, like ReaxFF, for the larger clusters.

Experimental flow tube studies of organic molecules could easily be continued by studying new chemical species. To expand on the nucleation studies of small chain organic acids, flow tube studies of acetic acid could be performed. Acetic acid is slightly larger than formic acid and has a polar and a non-polar end. It would be interesting to see if acetic acid also contributes to particle growth, and if it does so to a greater or lesser extent than formic acid. Organic halide studies could be expanded with the study of iodine and chlorine containing organic molecules. Iodine is of particular interest for its role in the halogen chemistry in the marine boundary layer.

Appendix

Cationic bromoform reaction with water: growth of hydrocarbon clusters

Flow tube studies of the cations that result from the degradation of bromoform yielded surprising and interesting results. Bromoform was contained in a glass bubbler that is diagramed in Figure 2.3. Helium was passed over the liquid to obtain bromoform vapor seeded in helium. This mixture was then leaked into the high pressure source of the flow tube apparatus through a secondary port. Water was also passed through the source to mimic the reaction of the halogen containing organic molecule in the marine boundary layer. In order to obtain only the degradation products, the concentration of bromoform was controlled by placing the glass bubbler in an ice bath; this lowered the vapor pressure of the organic liquid. This method allowed us to obtain spectra with clear isotopic splitting of the chemical species.

Figure A.1 shows that the bromoform breaks down into $CHBr_3^+$, $CHBr_2^+$, Br_2^+, and $CHBr^+$. $CHBr_2^+$ and Br_2^+ are clearly the dominant degradation products in this spectrum. A peak for Br^+ is not observed, due to both the high reactivity of lone bromine ions as well as the high probability that lone bromines are anions.

Upon performing a pressure dependent study of bromoform at room temperature, we find that four distinct distribution series form: clusters containing Br, Br_2, Br_3, and Br_4. It can be seen in Figure A.2 that at lower relative pressures of bromoform, the Br_2 series dominates with the Br_3 series being the second most abundant. The Br series again has a lesser intensity due to a higher reactivity. What is surprising about these distributions is that a Br_4 series also forms. The Br_4 series actually begin to dominate the spectra at higher relative pressures of bromoform. It was initially surprising to see growth of such large cluster sizes, as this distribution is not common

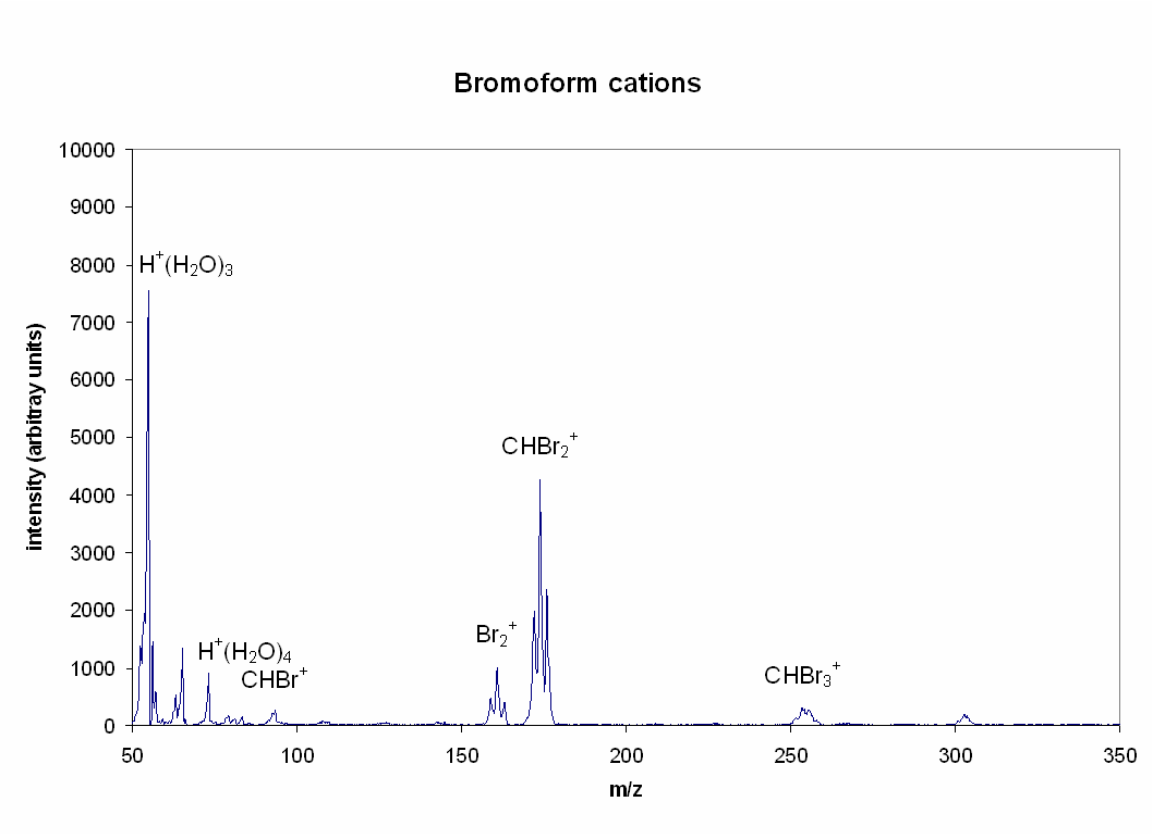

Figure **A.1**: The cationic degradation products of $CHBr_3$ are shown.

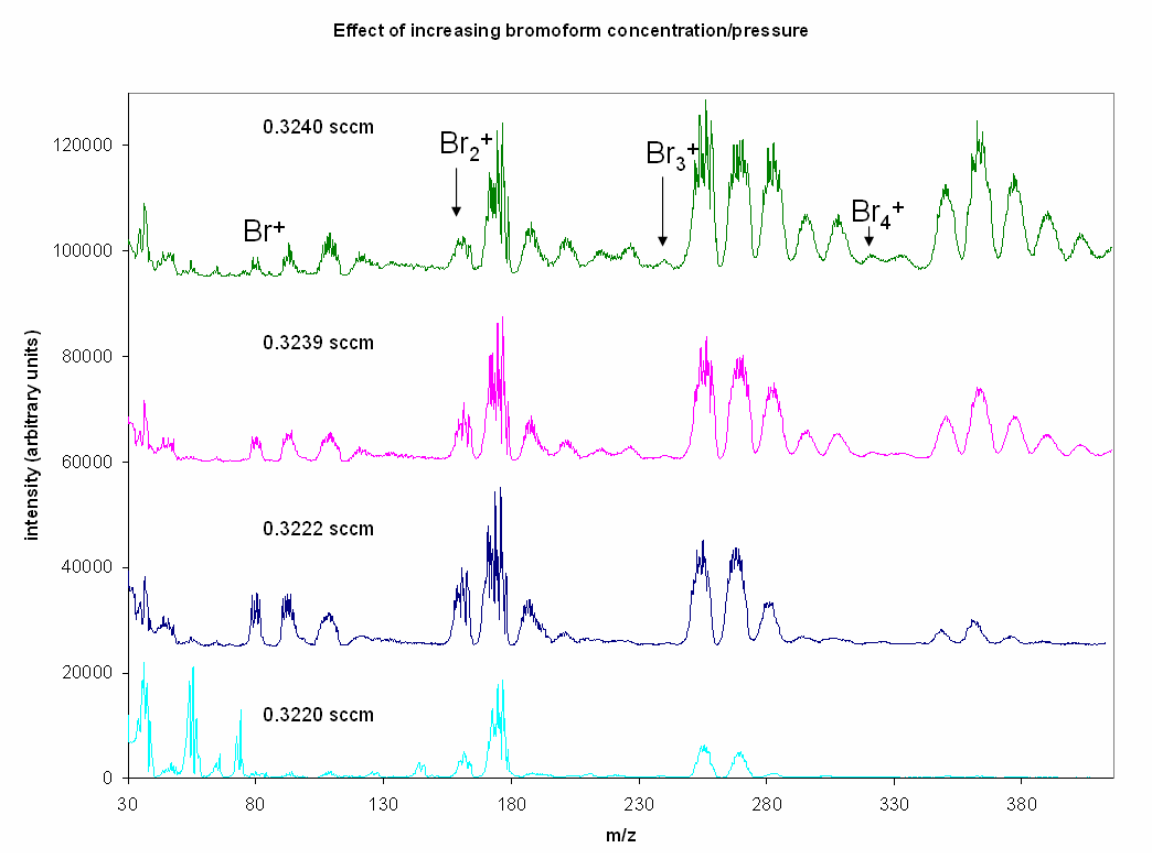

Figure **A.2**: Increasing the pressure/concentration of bromoform results in the formation of cluster series containing 1-4 bromine atoms.

for water clusters at room temperature, or in fact at any temperature above ~150 K.

Upon analysis of the data, it becomes clear that the cluster series are separated by spacings of 13 amu, which can only represent addition of hydrocarbons (CH) to the clusters. These results are unique relative to our other studies, as clusters in all the other studies presented in this dissertation are composed predominantly of water molecules. Here, the series represent the formation of hydrocarbon clusters.

Figure A.3 shows that while the Br_4 series exists, the clusters do not appear at high intensity until the $C_2H_2Br_4^+$ cluster. This is likely due to the very low stability of a cluster containing four bromine molecules which are all relatively large atoms with high reactivity. Additional atoms such as carbon are necessary to begin to stabilize such a cluster, and the cluster only appears at high intensities at very high pressures of bromoform.

Figure A.4 is a zoomed view of Figure A.3 in the mass range of 150 to 240 amu, which is the range of the Br_2^+ series. The zoomed view shows that there are resolved isotopic peaks for Br_2^+ (158, 160, 162), HBr_2^+ (159, 161, 163), and $H_2Br_2^+$ (160, 162, 164). The next set of peaks is the $CHBr_2^+$ group, with the following sets of peaks representing a further addition of a CH group. We hypothesize that the peaks from 171 to 179 amu represent the following clusters: $CHBr_2^+$ (171, 173, 175), $CH_2Br_2^+$ (172, 174, 176), Br_2O (174, 176, 178), and Br_2OH^+ (175, 177, 179). We believe the Br_2O species to be slightly more likely than further addition of hydrogen molecules ($CH_3Br_2^+$ and $CH_4Br_2^+$) but cannot be certain without further study of the clustering reaction. The next set of peaks from 184 to 194 amu is assigned as the following: $C_2H_2Br_2^+$ (184, 186, 188), $C_2H_3Br_2^+$ (185, 187, 189), $COBr_2^+$ (186, 188, 190), $HCOBr_2^+$ (187, 189, 191), $H_2COBr_2^+$ (188, 190, 192), $H_3COBr_2^+$ (189, 191, 193), and $Br_2O_2^+$ (190, 192, 194). The pattern of cluster growth is similar for the Br, Br_3, and Br_4 series as well. However, the relevance of such clusters and likelihood of formation in the atmosphere is not clear at the moment. A solid

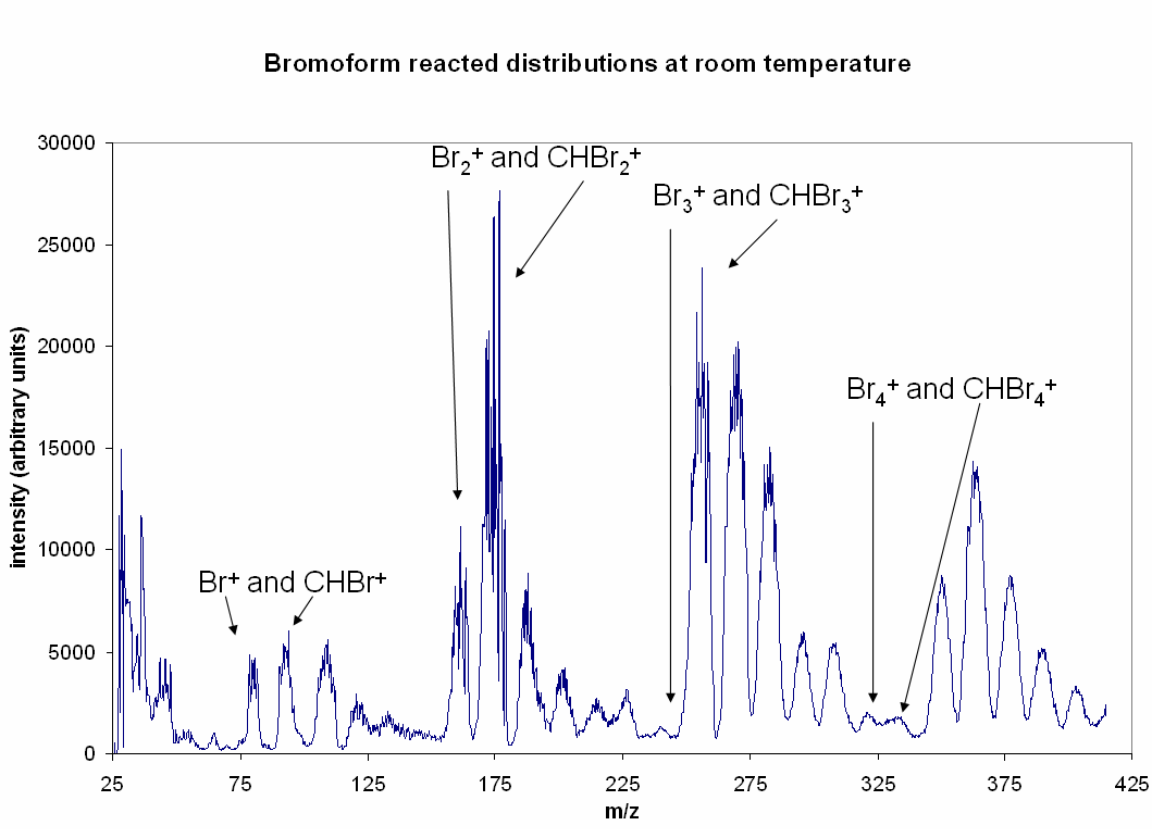

Figure **A.3**: Result of a high bromoform pressure in the flow tube. The peak spacings in each series is 13 amu, or a CH group.

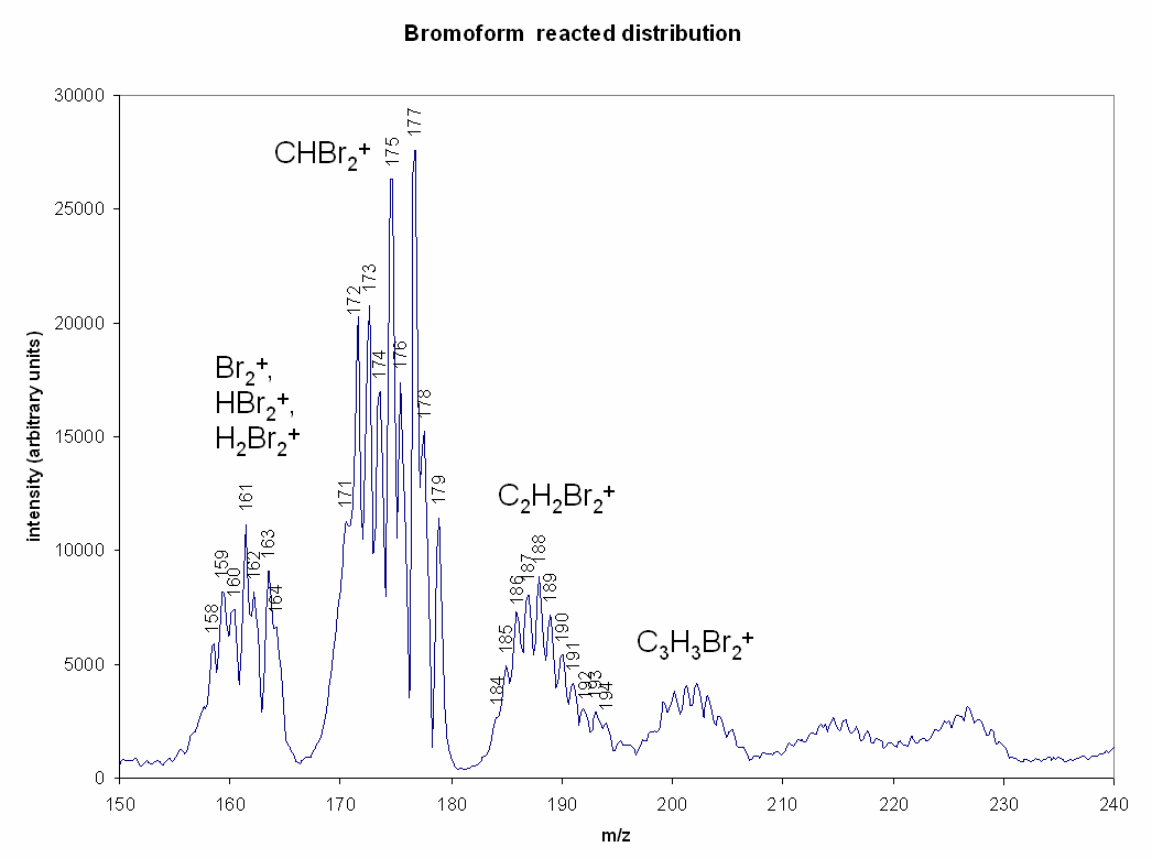

Figure **A.4**: A zoomed view on the mass region of 150-240 amu. Resolved peaks suggesting addition of CH groups as well as hydrogen addition are labeled. Not all labels are included; masses are discussed in detail in the text.

conclusion from these data is that bromoform reacts to form halogenated organic molecules as well as inorganic sources of bromine (Br_2O, etc.) in the lower regions of the atmosphere under conditions of high pressure of bromoform and in the presence of water.

Cold temperature studies were performed as well. However, while pure water distributions were obtained, no signal was obtained when bromoform was present. We conclude that the clusters that were formed by the reaction at cold temperature were too large for detection in our system. The hypothesis that the clusters formed were too large to detect is supported by the fact that signal returned upon removal of bromoform from the source. When the bromoform valve was shut, the signal would gradually return in the form of very large water clusters and over time it would return to the typical cluster size distribution observed for water at temperatures below ~ 150 K.

VITA

Erin Gabrielle Goken

Education

Ph. D. Chemistry, The Pennsylvania State University, University Park, PA, December, 2010
B.S. Biochemistry, Northern Illinois University, DeKalb, IL, May, 2005

Awards

2009 Second Place Poster at Environmental Chemistry Student Symposium
2005 New Graduate Student Award

Publications

1. Goken, E. G.; Joshi, K; Russo, M; Van Duin, A.; Castleman, A.W., Jr., The Effect of Formic Acid Addition on Water Cluster Structure and Stability. (*in preparation*).

2. Goken, E. G.; Castleman, A.W., Jr., Reactions of Formic Acid with Protonated Water Clusters: Implications of Cluster Growth in the Atmosphere. *J. Geophys. Res.-Atmos.* (In Press).

Presentations

1. Goken, E. G.; Castleman, A.W., Jr., A Study of Weak Acids in the Atmosphere Using a Flow Tube, poster presentation at the Environmental Chemistry Student Symposium at Pennsylvania State University; March 2009.

2. Goken, E. G.; Jones, C.; Castleman, A. W., Jr., Formic Acid Addition to Water Cluster Systems, poster presentation at the Gordon Research Conference on Clusters, Nanosystems and Nanostructures at Mount Holyoke College; July/Aug 2007.

Other publications

1. Goken, E. G., "A few moments with Tom Mallouk," Penn State Department of Chemistry 2008 Newsletter.

2. Goken, E. G., "The Artist in Residence," Penn State Department of Chemistry 2008 Newsletter.